AD_____

Award Number: W81XWH-04-1-0493

TITLE: Functional Analysis of the Beclin-1 Tumor Suppressor Interaction with hVps34 (Type-III PI3'-kinase) in Breast Cancer Cells

PRINCIPAL INVESTIGATOR: William A. Maltese, Ph.D.

CONTRACTING ORGANIZATION: Medical College of Ohio
Toledo, OH 43614-5804

REPORT DATE: June 2006

TYPE OF REPORT: Annual

PREPARED FOR: U.S. Army Medical Research and Materiel Command
Fort Detrick, Maryland 21702-5012

REPORT DOCUMENTATION PAGE

Form Approved
OMB No. 0704-0188

1. REPORT DATE *(DD-MM-YYYY)*	**2. REPORT TYPE**	**3. DATES COVERED** *(From - To)*
01-06-2006	Annual	7 May 2005 - 6 May 2006

4. TITLE AND SUBTITLE
Functional Analysis of the Beclin-1 Tumor Suppressor Interaction with hVps34 (Type-III PI3'-kinase) in Breast Cancer Cells

5a. CONTRACT NUMBER

5b. GRANT NUMBER
W81XWH-04-1-0493

5c. PROGRAM ELEMENT NUMBER

6. AUTHOR(S)
William A. Maltese, Ph.D.

E-Mail: wmaltese@meduohio.edu

5d. PROJECT NUMBER

5e. TASK NUMBER

5f. WORK UNIT NUMBER

7. PERFORMING ORGANIZATION NAME(S) AND ADDRESS(ES)
Medical College of Ohio
Toledo, OH 43614-5804

8. PERFORMING ORGANIZATION REPORT NUMBER

9. SPONSORING / MONITORING AGENCY NAME(S) AND ADDRESS(ES)
U.S. Army Medical Research and Materiel Command
Fort Detrick, Maryland 21702-5012

10. SPONSOR/MONITOR'S ACRONYM(S)

11. SPONSOR/MONITOR'S REPORT NUMBER(S)

12. DISTRIBUTION / AVAILABILITY STATEMENT
Approved for Public Release; Distribution Unlimited

13. SUPPLEMENTARY NOTES

14. ABSTRACT: Macroautophagy plays a pivotal role in type II programmed cell death. Beclin 1 regulates macroautophagy. Overexpression of Beclin promotes autophagy and inhibits tumorigenesis in breast carcinoma cells, and conversely, heterozygous disruption of the Beclin gene can promote tumorigenesis in mice. In Year-1 we established that Beclin associates with the human type-III phosphatidylinositol 3-kinase (PI3K), hVps34, but not with another putative partner, Bcl-2. The lipid product of Vps34, PI(3)P, is required not only for autophagy, but also for assembly of proteins involved in endocytosis and trafficking of enzymes from the trans-Golgi network to the lysosomes. Our studies indicated that Beclin is required for hVps34 to function in autophagy, but is dispensable for hVps34 to function in endocytosis. In Year-2 we have generated a stable MCF7 breast cancer cell line with expression of FLAG-tagged Beclin under the control of an inducible promoter. Using this cell line, we purified the FLAG-Beclin-Vps34 complex and performed mass spectrometry to identify other protein components present in the complex. We established for the first time that p150, a regulatory subunit of type-III PI3K, associates with Beclin. We generated a Beclin mutant that fails to associate with p150, but remains competent to interact with Vps34. We are currently developing stable MCF7 cells in which p150 and Beclin are individually and jointly suppressed by RNAi. Using these resources, we will determine how Beclin and p150 contribute to the regulation of Vps34 kinase activity and downstream signaling to the mTOR pathway. These studies will provide important insights into how Beclin controls type II cell death in breast cancer.

15. SUBJECT TERMS

16. SECURITY CLASSIFICATION OF:			**17. LIMITATION OF ABSTRACT**	**18. NUMBER OF PAGES**	**19a. NAME OF RESPONSIBLE PERSON**
a. REPORT	**b. ABSTRACT**	**c. THIS PAGE**			USAMRMC
U	U	U	UU	39	**19b. TELEPHONE NUMBER** *(include area code)*

Table of Contents

Introduction

The general goal of this study is to define at the molecular level the basis for the tumor suppressor function of Beclin-1 in breast cancer. We hypothesize that the primary intracellular partner for Beclin in human cells is a class-III phosphatidylinositol 3'-kinase termed hVps34 [1]. We further hypothesize that Beclin, through its interaction with hVps34 and perhaps other proteins in a larger complex, plays a key role in regulating macroautophagy. Macroautophagy is a process whereby cytoplasmic proteins and organelles are incorporated into vacuoles termed autophagosomes, and subsequently are degraded when these structures fuse with lysosomes [2;3]. Some types of cells use macroautophagy as a short-term survival strategy in response to stress or nutrient deprivation. However, autophagy is also a major feature of a non-apoptotic form of cell death, often referred to as type-II programmed cell death [4]. Type-II cell death has been reported to occur during the regression of hormone-dependent breast cancer cells treated with tamoxifen and related compounds [5;6]. By understanding the molecular details of how Beclin regulates macroautophagy, we hope to identify components of the pathway that can be manipulated to enhance type-II cell death in malignant cells.

Body

This progress report will follow the outline of the Objectives listed in the Statement of Work described in the original grant proposal. For each objective I will indicate what has been done, what is planned for the next year, and where we may wish to adopt a modified research strategy.

Objective 1: Test the hypothesis that Beclin-1 acts through Vps34 to mediate autophagic cell death in cultured breast carcinoma cells.

Task 1. Suppression of Beclin-1 expression in MCF7 cells by siRNA-mediated gene silencing and evaluation of the effects of this manipulation on the development of autophagosomes and autophagic cell death in response to tamoxifen or nutritional deprivation. (In Progress)

Progress: Year-1: In the first year of the project we used siRNA-mediated gene silencing to deplete Beclin in cultured cells and determine whether or not Beclin selectively affects the function of hVps34 in autophagy *versus* normal trafficking. The results indicated that Beclin is important for regulating the function of hVps34 in autophagy, but that Beclin is dispensable for the function of hVps34 in endocytosis and trafficking of proteins to the lysosomal compartment [7] (Included in APPENDIX). In contrast, knocking down the expression of hVps34 caused significant perturbation of trafficking in the late endosome compartment [8] (Included in APPENDIX). Year 2- During the past year others have reported that unlike wild-type Beclin-1, a Beclin mutant that cannot bind to hVps34 lacks tumor suppressor function in MCF7 cells [9]. These studies strongly suggest that autophagic events regulated by Beclin are important for determining breast cancer cell survival. In recent months we have re-initiated our attempts to generate a Beclin knockdown in MCF7 cells using the AMAXA nucleofection system, hoping to achieve a greater depletion of Beclin than the 60% obtained previously using the pSuper RNAi retroviral infection. Once we have achieved the goal of >90% knockdown (similar to what we obtained in glioblastoma cells), we will complete Task-1 by comparing the responses of wt and Beclin knockdown MCF7 cells to tamoxifen.

Task 2. Over-expression of wild-type Beclin or Vps34-interaction-deficient Beclin (Δ80-107) and evaluation of the effects of this manipulation on the development of autophagosomes in other estrogen receptor positive (T47D, ZR-75) and negative (MDA-MB231) breast cancer cell lines. (In Progress)

Progress: Year-1: As described in the previous progress report, we have generated a stable MCF7 breast cancer cell line that over-expresses FLAG-tagged wild-type Beclin under control of a tetracycline-responsive promoter (tet-off). Year-2: During the past year we made excellent use of the inducible MCF7 cell line to isolate proteins associated with FLAG-Beclin (Objective 3). These studies required considerable time and effort, necessitating that we defer the planned experiments on the tamoxifen responsiveness of cells overexpressing Beclin until Year-3. As described under Objective 3, we have now completed the identification of the components of the Beclin-Vps34 protein complex and are beginning to explore the function of these proteins in the control of the mTOR pathway essential for autophagy. With this information in hand, we plan to return to Task-2 this year, and determine how expression levels of Beclin and the Vps34 adapter, p150, affect the response of MCF7 and other breast cancer lines to tamoxifen.

Task 3. Examination of the effects of Beclin gene-silencing on autophagy in other estrogen receptor positive (T47D, ZR-75) and negative (MDA-MB231) breast cancer cell lines with higher (compared to MCF7) Beclin expression. (In Progress).

Progress: Year-1: While the studies on the basic cell biology of Beclin in protein trafficking were being conducted, we continued to experiment with siRNA-mediated suppression of Beclin in estrogen receptor-positive breast cancer cell lines, so that we could come back to the question of how Beclin depletion might affect the response of these cells to anti-estrogens. In T47D cells we were able to obtain a 60-65% suppression of Beclin expression similar to what we observed in MCF7. However, as shown in last-year's progress report, the siRNA was much more effective in ZR-75 breast carcinoma cells, resulting in 90-95% knockdown of Beclin expression. Year-2: A report from Codogno and colleagues [10] suggested that tamoxifen's ability to induce type-II cell death in MCF7 cells is mediated through an accumulation of the intracellular sphingolipid, ceramide, which is known to be a potent inducer of autophagy. Based on these observations, we decided to begin our assessment of the effects of Beclin knockdown by examining the responsiveness of wild-type and Beclin knockdown ZR-75 breast cancer cells to C2-ceramide. The results (**Fig. 1**) showed that suppression of Beclin expression in ZR-75 breast cancer cells blunts the induction of autophagy that normally occurs when these cells take up C2-ceramide. In these studies, autophagy was measured by quantifying the expression of the autophagosome-associated marker protein, LC3-II [11]. There have been some suggestions that autophagy may be increased as a pro-survival response in cells that incur damage to organelles (e.g., mitochondria), to enable cells to degrade these organelles before they can trigger apoptosis. With this in mind, we hypothesized that ZR-75 cells treated with ceramide, but lacking Beclin necessary to initiate autophagy, might accumulate increased numbers of mitochondria with membrane damage, compared with cells that can mount an autophagic response. This was tested by measuring mitochondrial membrane potential with the dye, JC-1. In healthy cells the dye is sequestered in the mitochondria and emits red fluorescence, but collapse of the membrane potential causes the dye to leak into the cytoplasm, where it fluoresces green [12]. Thus, a decrease in the ratio of red/green fluorescence signifies accumulation of damaged mitochondria. As shown in **Fig. 2,** ceramide caused a decline in the red/green ratio indicative of mitochondrial damage (permeability transition) in ZR-75 cells after 24 h, but

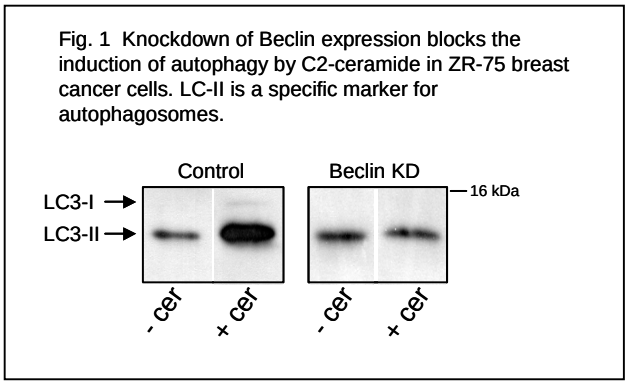

Fig. 1 Knockdown of Beclin expression blocks the induction of autophagy by C2-ceramide in ZR-75 breast cancer cells. LC-II is a specific marker for autophagosomes.

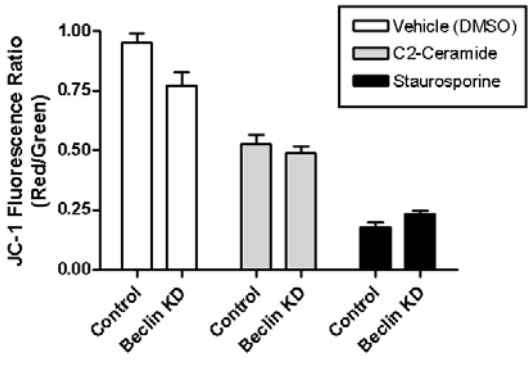

Fig. 2 Beclin knockdown does not affect ceramide-induced mitochondrial damage in ZR-75 breast cancer cells

there was no significant difference between the Beclin knockdown cells and the controls. This suggests that although ceramide stimulates autophagy, at least in this case the autophagic activity does not play a major role in eliminating mitochondrial damage. Further studies in Year-3 will determine whether the presence of an intact Beclin-mediated autophagy pathway renders the ZR-75 cells more or less sensitive to the effects of tamoxifen on cell growth and viability.

Objective 2. Define the mechanism of Beclin action by determining whether Beclin regulates the catalytic activity or membrane recruitment of hVps34 PI-3'-kinase.

*Task 1. S*tudies of the effects of recombinant Beclin on the activity of hVps34 *in vitro*. (This task is no longer necessary. The goal can be achieved by methods described under Task-2)

Progress: Year –1: Efforts to produce sufficient quantities of recombinant Beclin in *E. coli* were hampered by the tendency of this protein to form insoluble aggregates when overexpressed in bacterial systems.
Year-2: In light of the difficulties in purifying recombinant Beclin and hVps34 for Task-1, we explored the alternative of refining our ability to pull-down the FLAG-Beclin/Vps34 complex from stable MCF7 breast cancer cells. This technique has now succeeded to the point where we can address the central question posed under Objective 2 by working with cell extracts instead of recombinant proteins. Since completion of Task-1 in its original form is no longer essential to completing Objective 2, *we request permission to delete Task-1* from the experimental plan. Instead we propose to focus attention on the more productive approach of working with the immunoprecipitated proteins isolated from MCF7 cells (Task-2).

Task 2. Assess the effects of Beclin on the activity of hVps34 in cultured cells (In Progress).

Progress: Year-1: We generated an inducible (Tet-off) MCF7 breast cancer cell line that expresses a moderate amount of Beclin in the presence of doxycycline (Dox) and a robust over-expression of Beclin when Dox is removed. The parental MCF7 cell line exhibits very low levels of Beclin expression due to monoallelic deletion of the Beclin gene.
Year-2: We have used the Beclin Tet-off cell line and wild-type MCF7 cells to test the hypothesis that Beclin may function as a molecular chaperone that regulates the subcellular partitioning of Vps34 between soluble and membrane compartments. When cells with graded levels of Beclin expression were fractionated into soluble and particulate components, we found no major differences in the distribution of Vps34 (**Fig. 3B**), despite huge differences in Beclin expression (**Fig. 3A**). We are continuing to work on obtaining a more complete knockdown of Beclin in MCF7 cells, so that we can definitively determine if a complete absence of Beclin may have any effect on Vps34 membrane targeting. Instead of using retroviral vectors to introduce RNAi constructs, we have started working with the AMAXA nucleofection system and are currently optimizing conditions for high-efficiency transfer of RNAi into MCF7 cells. In the meantime, we have tentatively concluded that Beclin must affect the function of Vps34 in autophagy by some mechanism other than directing its membrane targeting. This leaves us with the alternative possibility that Beclin can affect the enzymatic activity of the Vps34 complex or its interaction with specific downstream molecular effectors. We have set up the thin-layer chromatography system to separate the product of Vps34, phosphatidylinositol 3'-phosphate (PI3P), from the substrate phosphatidylinositol (PI), and other

Fig. 3 Overexpression of Beclin does not cause a major shift in the subcellular distribution of hVps34 between soluble and membrane compartments. Equal portions of soluble (100,000 x g supernatant) and particulate (100,000 pellet) fractions were loaded.

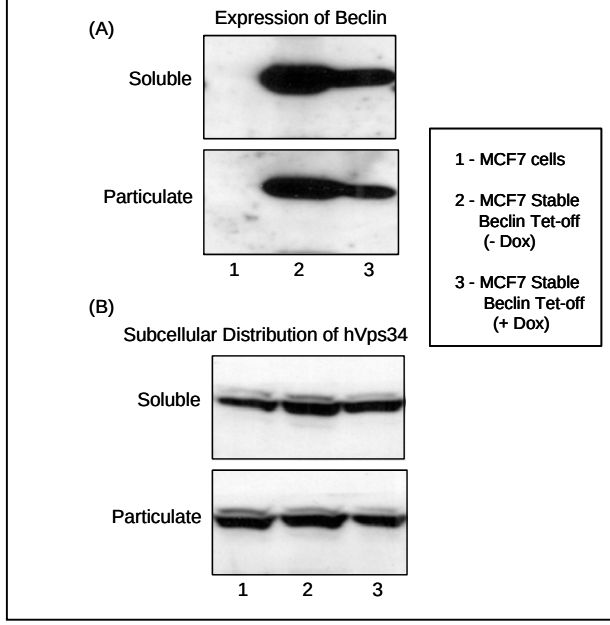

related lipids (e.g., PI4P). Using this system in conjunction with MCF7 or ZR-75 Beclin knockdown cell lines, we should be able to perform PI3K kinase activity assays by standard techniques [13] to determine if the presence or absence of Beclin affects the catalytic activity of the Vps34 complex. Because of the presence of other classes of PI 3-kinases, these studies cannot be done with whole-cell extracts. Unfortunately, the available antibodies against human Vps34 have proven to be very inefficient as precipitating reagents, delaying our completion of Task-2 (originally scheduled for months 12-16). To remedy the situation, we propose to use the AMAXA nucleofection system to generate stable cell lines expressing Myc-tagged hVps34 in the Control or Beclin KD cells (ZR-75 or MCF7). We know from experience that immunoprecipitation of Myc-tagged proteins generally works well. This should allow us to obtain sufficient quantities of enriched Myc-Vps34 from Beclin + or - backgrounds to determine if the enzymatic activity of the Vps34 is altered by the presence or absence of Beclin. This approach should yield a clear answer to the question posed under Objective 2 regarding the potential ability of Beclin to control the activity of Vps34.

Objective 3: Elucidation of the nature of the Beclin-Vps34 complex by determining whether the interaction between Beclin and hVps34 is direct or indirect (Tasks 1 & 2), and identifying other proteins that may be part of the complex (Tasks 3-5). In particular, we will test the hypothesis that interaction of Beclin with hVps34 is mediated by p150, a known Vps34 partner, or by novel bridging proteins similar to Apg14 in yeast.

Task 1. Complete studies of the physical interaction between recombinant Beclin and hVps34 in vitro (Completed via alternative approach described in Task 3)

Task 2. Assess the effects of recombinant p150 on the interaction between Beclin and hVps34. (Completed via alternative approach described in Task 3)

Progress: Year 1: Size exclusion chromatography analyses of the endogenous cytosolic complexes containing Beclin and Vps34 in MCF7 breast cancer cells and U-251 glioma cells indicated that the protein complexes migrate at a much larger size than predicted by the individual molecular masses of Beclin (60 kDa) and Vps34 (105 kDa). This led us to believe that the regulatory subunit of type-III PI 3-kinase, termed p150, or other unidentified proteins, could be components of the Beclin complex.
Year-2: Because of the aforementioned difficulty of expressing and purifying recombinant Beclin (Objective-2, Task-1), we decided to approach Objective 3 through the use of the FLAG-Beclin MCF7 cell line, which allows us to isolate intact Beclin complexes under native conditions. Essentially, these are the studies discussed in connection with Tasks 3-5, below.

Task 3. Perform FLAG-Beclin affinity isolation to identify other proteins that may be functional components of the Beclin/hVps34 complex. (Completed)

Progress: Year-1: In last-year's progress report we proposed a minor modification of the experimental approach for Task 3, using FLAG-Beclin immunoaffinity interaction instead of GST-Beclin interaction to capture cellular Beclin interacting proteins and characterize them by mass spectrometry.
Year-2: We have made very significant progress on Task-3 this year and have completed it ahead of schedule. Our approach has been to grow large batches of MCF7 cells side-by-side with MCF7 (tet-off) cells expressing low levels of FLAG-Beclin. By keeping the expression levels of FLAG-Beclin low (through the inclusion of low concentration of Doxycycline in the culture medium), we hoped to capture physiologically relevant Beclin protein complexes. Cells collected from 10 large dishes were lysed in non-denaturing buffer and mixed with anti-FLAG affinity beads. FLAG-Beclin was eluted from the beads under mild conditions using an excess of FLAG peptide, and the proteins eluted together with FLAG-Beclin were run on an SDS gel. As a control for non-specific protein interactions with the anti-FLAG beads, the lysates from regular MCF7 cells were treated in an identical manner. After staining the parallel SDS-gels with silver stain or colloidal blue, the control and FLAG-Beclin gels were compared side-by-side to identify any unique bands that were present only in the FLAG-Beclin pull-downs (see **Fig. 4**). These unique bands were excised and subjected to tryptic digestion. The resulting peptides were separated by liquid chromatography and analyzed by tandem mass spectrometry by

our collaborator, Dr. Basrur, in our proteomics core lab. Based on the amino acid sequences, two proteins were identified as specific Beclin partners. The first was the anticipated hVps34. The second was p150 [14], the human homolog of Vps15, and a proposed regulatory adapter subunit for Vps34. These interactions were confirmed independently by immunoblot analysis of the proteins co-eluted with FLAG-Beclin from the FLAG affinity beads (**Fig. 5**). This represents the first demonstration that p150 is present in the complex with Beclin and Vps34. When we repeated the pull-down analysis with MCF7 cells expressing a mutant form of FLAG-Beclin(Δ80-107), we found that the mutant was markedly defective in its interaction with p150, but was still able to pull-down Vps34. This observation favors a tripartite model wherein Beclin makes contact with *both* Vps34 and p150, rather than a tandem model where Beclin interacts only with Vps34, while p150 is captured indirectly, via its association with Vps34. A final surprising observation from these studies is that p150 can be detected in FLAG-Beclin complexes isolated from both the soluble and membrane fractions of MCF7 cells, despite earlier assumptions that p150 (a myristylated protein) is localized exclusively in membranes. Extensive analysis (using gels of various percent acrylamide to resolve different molecular weight ranges), have thus far not revealed any additional proteins specifically associated with the Beclin complex in MCF7 cells.

Fig. 4 Stained gel comparing proteins eluted from Anti-FLAG affinity beads: Right lane: MCF7 cells expressing FLAG-Beclin Left lane: Regular MCF7 cells expressing no FLAG-tagged protein. The unique bands marked with arrows were excised, digested with trypsin, and identified based on the amino acid sequences of individual peptides, determined by tandem mass spectrometry.

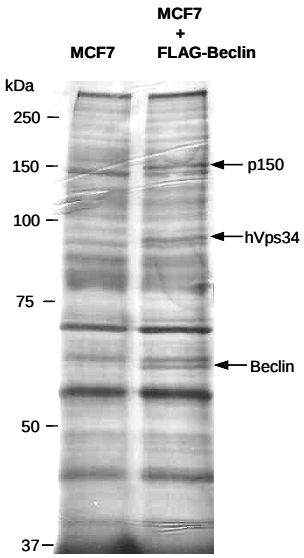

Fig. 5 Immunoblot analysis of proteins associated with FLAG-Beclin in MCF7 cells. Cells were lysed and immunoprecipitation was performed with anti-FLAG beads. Proteins eluted from the beads were subjected to SDS-PAGE and sections of the gel were immunoblotted with anti-p150 (hVps15), anti-hVps34, or anti-FLAG, as indicated. Right lane: MCF7 cells expressing FLAG-Beclin. Left lane: Regular MCF7 cells.

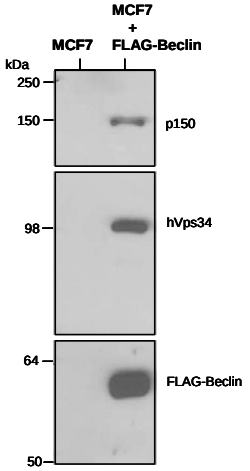

Task 4. Perform yeast two-hybrid screen with Beclin as the bait to identify other proteins that may be functional components of the Beclin/hVps34 complex. (Unnecessary, due to success of Task-3)

Progress: Year-1: Because of the labor-intensive nature of the yeast two-hybrid approach and the high probability of obtaining false positives, we proposed to defer this task until we evaluated the FLAG-pull down + mass spectrometry approach as a means to identify Beclin partners (Task 3). Year-2: Having completed Task-3, we have achieved the goal of identifying key protein components of the Beclin complex. While it remains possible that additional proteins may be present that escaped detection by mass spectrometry, we believe that the time and effort required to perform a confirmatory yeast two-hybrid screen would be far better spent on determining the functional roles of the proteins already identified as Beclin partners (p150 and Vps34); i.e., the studies proposed under Task 5 below.

Task 5. Begin to address the functional significance of any newly identified Beclin interacting proteins for the formation of the Beclin-hVps34 complex and the initiation of autophagy in MCF7 cells. (In Progress).

Progress: Although this task was originally planned for Year-3 of the project, our success in identifying p150 as a component of the Beclin complex in MCF7 cells has allowed us to begin studies aimed at assessing the importance of p150 for the function of Beclin and Vps34 in autophagy. There are two current models for how Beclin may regulate the Vps34 PI 3'-kinase and control autophagy. The first model is based on the concept that Vps34 generates PI(3)P, which is essential for recruitment of regulatory and structural proteins to the

autophagosome membrane [15]. According to this model, induction of autophagy should be accompanied by an *increase* in the activity of Vps34. In this model, the role of Beclin might be to stimulate the activity of Vps34, at least in the specific compartments involved in autophagosome biogenesis. More recently, a very different alternative model has been proposed. In this model *decreasing* the activity of Vps34 triggers autophagy. This model focuses on mTOR, which stimulates protein synthesis via phosphorylation of p70 S6 kinase under nutrient-rich conditions. mTOR is generally considered to inhibit autophagy when it is active. Consistent with this idea, drugs that block mTOR (e.g., rapamycin) stimulate autophagy. Likewise, amino acid deprivation causes a reduction in mTOR activity, leading to an increase in autophagy. An unexpected link between Vps34 and regulation of mTOR was suggested by the recent work of Byfield et al. [16] They showed that knockdown or inhibition of Vps34 suppresses mTOR activity (measured by phosphorylation of its substrates, S6 kinase or eIF4E). This suggests that Vps34 may normally inhibit autophagy by activating mTOR, and that downregulation rather than stimulation of Vps34 is necessary for increased autophagic activity. In this model, the role of Beclin might be to suppress the activity of Vps34. Even more interesting is the possibility that the regulation of mTOR by Vps34 is mediated by the associated p150 , which has been reported to have ser/thr kinase activity [14]. We are currently testing the hypothesis that Beclin functions as an inhibitor of Vps34-mediated regulation of mTOR. Preliminary studies suggest that MCF7 breast cancer cells with increased levels of Beclin expression show reduced phosphorylation of p70 S6 kinase by mTOR. The next step will be to knock down the expression of p150 with RNAi to determine if p150 is required for the effects of Beclin and Vps34 on mTOR. Finally, we will attempt to use chemical cross-linking methods and immunoprecipitation to determine if the Beclin/Vps34/p150 complex associates directly with mTOR under conditions where autophagy is stimulated by nutrient deprivation of treatment with drugs (e.g., tamoxifen). If these studies show that either Vps34 or p150 ser/thr kinase can trigger autophagy by inhibiting mTOR, they would raise the exciting possibility that specific inhibitors of these enzymes could be developed and used to stimulate type-II cell death in breast cancer.

Key Research Accomplishments

Year-1

1. Vps34 PI 3-kinase is an interacting partner for Beclin in human MCF7 and U-251 cells
2. Vps34 co-elutes with Beclin in a broad peak suggestive of a 500-600 kDa complex, indicating that there are other proteins in this complex besides these two proteins.
3. To study the role of Beclin in relation to the function of Vps34, we attempted to suppress the expression of Beclin in MCF7 breast carcinoma cells using siRNA. Although this approach was successful, the extent of Beclin suppression was incomplete. Similar problems were encountered with another breast cancer line (T47D)
4. To facilitate basic cellular studies of Beclin and Vps34, we turned to U-251 glioma cells, where we were able to obtain a much more extreme suppression of Beclin and/or Vps34 expression.
5. In U251-cells the apparent molecular mass of the cytosolic Vps34 complex is reduced to 200-300 kDa when Beclin expression is ablated in the Beclin knockdown cells. This suggests that Beclin is essential for the formation of the cytosolic Vps34 complex.
6. Beclin plays an essential role in Vps34-dependent macroautophagy induced by nutrient deprivation or treatment with C2-ceramide.
7. Knockdown of Vps34 expression demonstrates that this PI 3-kinase plays an important role in maintenance of late endosome morphology and trafficking of proteins to the lysosome.
8. Beclin is not required for Vps34 to function in lysosomal enzyme sorting and endocytic protein trafficking.
9. Beclin's role as a tumor suppressor is most likely related to its specific role in regulating Vps34's function in macroautophagy.
10. A stable ZR-75 breast cancer cell line was established with Beclin expression suppressed by more than 90%. This cell line will be used for future studies to determine whether Beclin plays a role in the induction of autophagic cell death in response to treatment with anti-estrogens.

11. Stable MCF7 breast cancer cell lines expressing FLAG-tagged wild-type and Vps34-binding-deficient forms of Beclin have been established. These will be used to isolate novel Beclin interacting partners that comprise the Vps34 complex.

Year-2

1. In light of the fact that tamoxifen induces type-II cell death in breast cancer cells through an accumulation of the intracellular sphingolipid, ceramide, we evaluated the effects of Beclin knockdown on the responsiveness of ZR-75 breast cancer cells to C2-ceramide. The results showed that suppression of Beclin expression (90%) in ZR-75 cells prevents the induction of autophagy that normally occurs when these cell take up C2-ceramide.
2. JC-1 mitochondrial membrane potential assays showed that elimination of Beclin-mediated autophagy in ZR-75 breast cancer cells did not increase the amount of mitochondrial damage, compared to cells with normal autophagic response.
3. Using Tet-inducible MCF7 cells lines with graded levels of Beclin over-expression, we found that the subcellular distribution of the Beclin partner, Vps34 PI 3'-kinase, does not vary in conjunction with the level of Beclin expression. This suggests that Beclin may affect the function of Vps34 in autophagy by some mechanism other than directing its membrane targeting.
4. Using anti-FLAG affinity beads, we have isolated the Beclin complex from MCF7 cells and have used mass spectrometry to identify two specific proteins that associate with Beclin; hVps34 and the p150 ser/thr kinase. This represents the first identification of p150 as a component of the Beclin complex.
5. Immunoblot methods were used to confirm the identities of the Beclin interacting proteins and to establish that p150 is present in both soluble and membrane-associated Beclin complexes.
6. Using FLAG pull-down assays, we have established that the mutant form of Beclin, (Δ80-107), fails to associate with p150 but remains capable of interacting with Vps34. This supports a model of a trimeric complex wherein Beclin interacts directly with *both* Vps34 and p150.
7. Preliminary studies indicate that increasing levels of Beclin expression may stimulate autophagy by inhibiting mTOR and reducing phosphorylation of p70 S6 kinase in MCF7 breast cancer cells. Studies planned for Year-3 with Beclin and p150 knockdown cells will establish if this effect is dependent on p150, and if Beclin directly affects the catalytic activity of Vps34.
8. We have obtained two siRNA sequences that work well to knockdown expression of p150. Work is underway to use these sequences in conjunction with the pSuper vector and AMAXA nucleofection technology to generate stable MCF7 cell lines with reduced expression of p150.

Reportable Outcomes

Manuscripts Published:

Zeng, X., Overmeyer, J.H., and Maltese, W.A. (2006) Functional specificity of the mammalian Beclin-Vps34 PI 3'-kinase complex in macroautophagy versus endocytosis and lysosomal enzyme sorting. *J. Cell Sci.* **119**, 259-270.

Johnson, E.E. Overmeyer, J. H., Gunning, W.T. and Maltese, W.A. (2006) Specific function of mammalian Vps34 phosphatidylinositol 3-kinase in late *versus* early endosomes revealed by siRNA-mediated gene silencing. *J. Cell Sci.* **119,** 1219-1232.

Presentations:

Xuehuo Zeng and William A. Maltese (2004) Formation of a Beclin complex with Vps34 is required for autophagy but not endocytic trafficking. The American Society for Cell Biology 44th Annual Meeting, Washington, DC.

Johnson, E.E, Gunning, W.T., and Maltese W.A. (2004) Endosomal and lysosomal perturbations caused by siRNA-mediated silencing of Vps34 PI 3'-kinase expression in glioblastoma cells. The American Society for Cell Biology 44th Annual Meeting, Washington, DC.

Johnson, E.E., Gunning, W.T., and Maltese, W.A. (2004) Endosomal and lysosomal perturbations caused by siRNA-mediated silencing of Vps34 PI 3'-*k*inase expression in glioblastoma cells. Michigan Microscopy and Microanalysis Society Fall Meeting, Michigan State University, Lansing, MI

Maltese, W.A., Zeng, X., Johnson, E.E. and Overmeyer, J.H. (2005) Beclin 1 is required for cellular macroautophagy but not endocytic trafficking. Department of Defense "Era of Hope" Breast Cancer Meeting, Philadelphia, PA.

Conclusions

Several lines of evidence support the idea that Beclin is a key component required for the accumulation of autophagosomes in Type II non-apoptotic cell death. The latter type of cell death appears to be particularly important for the demise of estrogen receptor positive breast cancer cells treated with tamoxifen or similar compounds. Therefore, our basic investigations into the details of how Beclin regulates autophagosome biogenesis may lay the groundwork for eventual manipulations of Beclin-dependent pathways to enhance the response of breast tumor cells to anti-estrogens. The work completed during Year-1 provided important new insights into the basic mechanisms whereby two key proteins, Beclin and hVps34, function in autophagy and late endosomal protein trafficking. Whereas Vps34 plays a dual role in both autophagy and endosomal protein trafficking, our findings support the hypothesis that Beclin functions selectively to regulate hVps34 PI 3-kinase in the autophagic pathway. An alternative role for Beclin as an essential chaperone or adapter for hVps34 in normal vesicular trafficking has been ruled out by our work. These findings are important because they shed new light on the molecular mechanism whereby Beclin may function as a tumor suppressor. The studies completed in Year-2 have resulted in the identification of another protein, the p150 serine/threonine kinase, as a component of the Beclin/Vps34 complex. It appears that p150 interacts directly with Beclin in addition to Vps34. Our Beclin overexpression and knockdown studies suggest that Beclin does not play a major role in directing the subcellular localization of Vps34. This raises the likely possibility that Beclin affects the catalytic activity of Vps34 or its interaction with specific downstream molecular targets. The next step in this line of research will be to determine if Beclin is an enhancer or an inhibitor of Vps34 activity by assaying the enzyme immunoprecipitated from control or Beclin knockdown cells. Another important extension of this work will address the question of p150's function in autophagy. We hypothesize that p150 may play a key role in downregulation of mTOR by the Beclin/Vps34 complex, thereby triggering autophagy. If this proves to be true, it will highlight a novel kinase pathway that may be amenable to drug targeting, with the goal of stimulating autophagic Type-II cell death in breast cancers.

List of Cited References

1. S. Volinia et al., *EMBO J.* 14, 3339-3348 (1995).
2. W. A. Jr. Dunn, *Trends Cell Biol.* 4, 139-143 (1994).
3. D. J. Klionsky and S. D. Emr, *Science* 290, 1717-1721 (2000).
4. Z. Zakeri, W. Bursch, M. Tenniswood, R. A. Lockshin, *Cell Death Differentiat.* 2, 87-96 (1995).
5. W. Bursch et al., *Carcinogenesis* 17, 1595-1607 (1996).
6. B. Levine and D. J. Klionsky, *Dev.Cell* 6, 463-477 (2004).
7. X. Zeng, J. H. Overmeyer, W. A. Maltese, *J Cell Sci* 119, 259-270 (2006).
8. E. E. Johnson, J. H. Overmeyer, W. T. Gunning, W. A. Maltese, *J Cell Sci* 119, 1219-1232 (2006).
9. N. Furuya, J. Yu, M. Byfield, S. Pattingre, B. Levine, *Autophagy* 1, 46-52 (2005).
10. F. Scarlatti et al., *J.Biol.Chem.* 279, 18384-18391 (2004).
11. N. Mizushima, *Int.J Biochem.Cell Biol.* 36, 2491-2502 (2004).
12. M. Reers et al., *Methods Enzymol.* 260, 406-417 (1995).
13. A. Tassa, M. P. Roux, D. Attaix, D. M. Bechet, *Biochem.J* 376, 577-586 (2003).
14. C. Panaretou, J. Domin, S. Cockcroft, M. D. Waterfield, *J.Biol.Chem.* 272, 2477-2485 (1997).
15. D. J. Klionsky, *J Cell Sci* 118, 7-18 (2005).
16. M. P. Byfield, J. T. Murray, J. M. Backer, *J Biol.Chem.* 280, 33076-33082 (2005).

APPENDICES

1) Copy of publication:

Zeng, X., Overmeyer, J.H., and Maltese, W.A. (2006) Functional specificity of the mammalian Beclin-Vps34 PI 3'-kinase complex in macroautophagy versus endocytosis and lysosomal enzyme sorting. *J. Cell Sci.* **119**, 259-270.

2) Copy of publication:

Johnson, E.E. Overmeyer, J. H., Gunning, W.T. and Maltese, W.A. (2006) Specific function of mammalian Vps34 phosphatidylinositol 3-kinase in late *versus* early endosomes revealed by siRNA-mediated gene silencing. *J. Cell Sci.* **119,** 1219-1232.

Functional specificity of the mammalian Beclin-Vps34 PI 3-kinase complex in macroautophagy versus endocytosis and lysosomal enzyme trafficking

Xuehuo Zeng, Jean H. Overmeyer and William A. Maltese*

Department of Biochemistry and Cancer Biology, Medical University of Ohio, Toledo, OH 43614, USA

*Author for correspondence: (e-mail: wmaltese@meduohio.edu)

Accepted 7 October 2005
Journal of Cell Science 119, 259-270 Published by The Company of Biologists 2006
doi:10.1242/jcs.02735

Summary

Beclin 1 was originally identified as a novel Bcl-2-interacting protein, but co-immunoprecipitation studies suggest that the major physiological partner for Beclin 1 is the mammalian class III phosphatidylinositol 3-kinase (PI 3-kinase) Vps34. Beclin 1 has been proposed to function as a tumor suppressor by promoting cellular macroautophagy, a process that is known to depend on Vps34. However, an alternative role for Beclin 1 in modulating normal Vps34-dependent protein trafficking pathways has not been ruled out. This possibility was examined in U-251 glioblastoma cells. Immunoprecipitates of endogenous Beclin 1 contained human Vps34 (hVps34), but not Bcl-2. Suppression of Beclin 1 expression by short interfering (si)RNA-mediated gene silencing blunted the autophagic response of the cells to nutrient deprivation or C_2-ceramide. However, other PI 3-kinase-dependent trafficking pathways, such as the post-endocytic sorting of the epidermal growth factor receptor (EGFR) or the proteolytic processing of procathepsin D en route from the trans-Golgi network (TGN) to lysosomes, were not affected. Depletion of Beclin 1 did not reduce endocytic internalization of a fluid phase marker (horseradish peroxidase, HRP) or cause swelling of late endosomal compartments typically seen in cells where the function of hVps34 is impaired. These findings argue against a role for Beclin 1 as an essential chaperone or adaptor for hVps34 in normal vesicular trafficking, and they support the hypothesis that Beclin 1 functions mainly to engage hVps34 in the autophagic pathway.

Key words: Beclin, Autophagy, Vps34, Phosphatidylinositol-3-kinase, Cell death, Endocytosis, Glioblastoma

Introduction

Animal cells utilize macroautophagy as a mechanism for turnover of long-lived proteins, and as a survival strategy under conditions of amino acid deprivation (Dunn, 1994; Klionsky and Emr, 2000). Autophagic vacuoles (autophagosomes) are initially formed from membranes of the endoplasmic reticulum (ER) that surround a region of cytoplasm (Dunn, 1990a; Dunn, 1990b). These structures, bounded by a double membrane, then develop into mature degradative vacuoles (autolysosomes) by progressive fusion with late endosomes and lysosomes (Gordon and Seglen, 1988; Dunn, 1990a; Lawrence and Brown, 1992). Accumulation of autophagosomes and autolysosomes is a hallmark morphological feature of type II programmed cell death, also referred to as autophagic cell death (Lockshin and Zakeri, 2004; Levine and Klionsky, 2004). This type of cell death has been postulated to occur during embryonic development in connection with tissue remodeling (Zakeri et al., 1995). More recently, it has also been described in neurodegenerative diseases (Kegel et al., 2000; Larsen and Sulzer, 2002) and in tumor cells exposed to anti-neoplastic agents (Bursch et al., 1996; Paglin et al., 2001; Kanzawa et al., 2003; Kanzawa et al., 2004). However, it remains unclear whether the accumulation of autophagosomes is a direct cause of cell death or a symptom of an unsuccessful attempt of cells to adapt to metabolic stress.

Beclin 1 (hereafter referred to simply as Beclin) is a 60 kDa protein that has been implicated as an important regulator of macroautophagy. It was originally discovered during the course of a yeast two-hybrid screen of a mouse brain cDNA library using human Bcl-2 as the bait (Liang et al., 1998). The human *beclin* gene has been mapped to a region of chromosome 17q21 that is monoallelically deleted in many breast, ovarian and prostate cancers (Aita et al., 1999). Expression of Beclin in MCF7 mammary carcinoma cells increases their autophagic response to nutrient deprivation (Liang et al., 1999). Consistent with this observation, several additional studies have implicated *beclin* as an essential gene for cell survival under adverse nutritional conditions. Deletion of the gene encoding Vps30 (Atg6), the Beclin ortholog in *Saccharomyces cerevisiae*, hastens cell death induced by starvation (Kametaka et al., 1998). Similarly, suppression of Beclin expression in mammalian cells impairs autophagy and sensitizes the cells to starvation-induced apoptosis (Boya et al., 2005). In addition to its specific role in adaptation to nutrient deprivation, accumulating evidence suggests that Beclin might play a more general role in cell survival during embryonic development. In *Caenorhabditis elegans*, short interfering (si)RNA-mediated suppression of *bec-1* inhibits autophagy and interferes with morphogenesis of the developmental stage known as the dauer diapause. The latter represents a survival strategy that can be triggered by unfavorable environmental conditions (Melendez et al., 2003). In mice with homozygous deletions of *beclin*,

death occurs at an early stage of embryonic development (Qu et al., 2003; Yue et al., 2003). Studies with *beclin*$^{-/-}$ embryonic stem cells have shown that they fail to form normal embryoid bodies in vitro (Yue et al., 2003). Finally, overexpression of Beclin in the brains of adult mice protects neurons from apoptosis induced by Sindbis virus infection (Liang et al., 1998). The specific mechanism of this protective effect and its relationship to autophagy remains to be established.

In contrast to the foregoing indications that Beclin functions to promote cell survival, there is also a growing body of evidence that Beclin might, paradoxically, also function as a tumor suppressor under specific circumstances. For example, augmentation of Beclin expression in MCF7 cells decreases their proliferation, clonigenicity in soft agar, and tumorgenicity in nude or severe combined immunodeficient (*scid*) mice (Liang et al., 1999; Furuya et al., 2005). Heterozygous disruption of *beclin* in mice results in an increased frequency of spontaneous lymphomas, as well as lung and liver carcinomas (Qu et al., 2003; Yue et al., 2003). The possibility that the tumor-suppressing effects of Beclin might be related to a role in regulating autophagic cell death has been raised by two recent studies. In the first, silencing Beclin expression in L929 cells prevented autophagic death triggered by treatment of the cells with a caspase inhibitor (Yu et al., 2004). In the second, interference with Beclin expression blocked non-apoptotic (autophagic) cell death induced by etoposide treatment of Bax/Bak$^{-/-}$ double-knockout mouse cells that are resistant to apoptosis (Shimizu et al., 2004).

Despite the apparent importance of Beclin in the regulation of macroautophagy, cell survival and non-apoptotic cell death, little is known about the molecular mechanisms that are involved. Studies of Vps30 (Atg6), the Beclin ortholog in *S. cerevisiae*, indicate that it is part of two distinct protein complexes that contain the PI 3-kinase Vps34 (Kihara et al., 2001b). One complex functions in post-Golgi sorting of proteases to the vacuole (equivalent to the lysosome), whereas the other complex is essential for macroautophagy and degradation of cytoplasmic proteins under starvation conditions. The importance of Vps34 in protein trafficking is related to the role of its product, phosphatidylinositol 3-phosphate [PtdIns(3)*P*], in the membrane recruitment of proteins involved in the vesicle docking and fusion machinery (Wurmser et al., 1999). These proteins typically contain specific PtdIns(3)*P*-binding domains termed the FYVE finger (Fruman et al., 1999; Stenmark et al., 2002) or the Phox homology domain (Song et al., 2001; Cheever et al., 2001; Xu et al., 2001; Kanai et al., 2001), and their roles in vesicular transport have been reviewed in recent articles (Simonsen et al., 2001; Deneka and van Der, 2002).

Mammalian cells express a homolog of the yeast Vps34 PI 3-kinase (Volinia et al., 1995). Like its yeast counterpart, the mammalian Vps34 appears to be required for the initiation of macroautophagy (Petiot et al., 2000; Eskelinen et al., 2002). However, studies using PI 3-kinase inhibitors, a dominant-negative form of Vps34, or antibody microinjection have also implicated mammalian Vps34 in normal protein trafficking pathways such as the delivery of proteases from the trans-Golgi network (TGN) to the lysosomes (Row et al., 2001), endocytic trafficking and sorting of cell-surface receptors (Siddhanta et al., 1998; Tuma et al., 2001; Petiot et al., 2003), and the formation of internal vesicles in multivesicular endosomes (MVEs) (Futter et al., 2001). Most recently, we have observed that siRNA-mediated knockdown (KD) of human Vps34 (hVps34) expression causes vacuolation of late endosomal compartments, impedes the trafficking of cathepsin D from late endosomes to lysosomes, and slows the lysosomal degradation of activated epidermal growth factor receptor (EGFR) in U-251 glioblastoma cells (E. E. Johnson, J.H.O., W. T. Gunning and W.A.M., unpublished data).

Since hVps34 can be immunoprecipitated together with Beclin (Kihara et al., 2001a), it is important to consider the possibility that Beclin might influence cell growth and tumorgenicity not only by controlling macroautophagy, but also by functioning as a chaperone or adaptor for hVps34 in normal protein trafficking pathways that depend on the production of PtdIns(3)*P*. A recent study suggests that Beclin is not required for post-Golgi trafficking of lysosomal hydrolases in MCF7 cells, based on the observation that maturation of cathepsin D is unaffected in cells overexpressing a mutant form of Beclin that cannot bind hVps34 (Furuya et al., 2005). In the present study, we conducted a more comprehensive assessment of the potential role of Beclin in hVps34-dependent protein trafficking pathways using siRNA-mediated gene silencing to suppress Beclin expression chronically in U-251 glioblastoma cells. Near-complete suppression of Beclin expression markedly attenuated the ability of the cells to initiate macroautophagy but had no effect on cell growth, endosomal morphology, endocytic uptake of a fluid phase marker, internalization and degradation of the EGFR, or delivery of cathepsin D to late endosomes and lysosomes. These studies provide new insight into the biological significance of the interaction between Beclin and hVps34 PI 3-kinase by showing that it is essential for engagement of hVps34 in the process of macroautophagy, but is dispensable for the normal function of hVps34 in endocytic trafficking or lysosomal enzyme sorting.

Results

Generation of stable Beclin KD cell lines

To obtain a cell population in which expression of Beclin was specifically suppressed, cells were infected with a replication-deficient retroviral vector that drives the expression of RNAi sequences and confers puromycin resistance on infected cells (Brummelkamp et al., 2002). Vectors were engineered to contain either an inverted repeat stem-loop sequence matching a unique region of the human *beclin* mRNA, or a 'control' sequence that did not match any known GenBank entry. The newly synthesized hairpin RNA is processed into siRNA, triggering the cellular Dicer-mediated degradation of the target *beclin* RNA (Sui et al., 2002). In preliminary tests with several cell lines infected with a green fluorescent protein (GFP) reporter construct, the human U-251 glioblastoma cell line showed high initial infection efficiency. Therefore, we chose to use this cell line for studies of Beclin. As shown by the immunoblots in Fig. 1, expression of Beclin was almost undetectable in puromycin-resistant cells that received the Beclin KD vector compared with cells that were infected with the control vector. Expression of unrelated soluble and membrane-bound proteins [e.g. lactate dehydrogenase (LDH), LAMP1] was not reduced, indicating that the loss of Beclin expression was not due to a general effect of the siRNA on protein synthesis in the KD cells (Fig. 1). In all of the

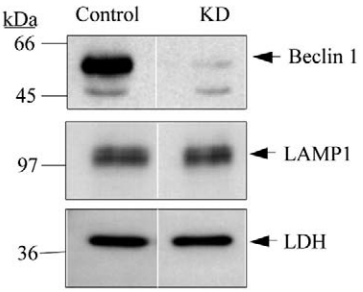

Fig. 1. siRNA-mediated suppression of Beclin expression in U-251 glioma cells. U-251 cells infected with retroviral vectors and surviving after 6 days in medium containing 1 μg/ml puromycin were pooled to generate stable cell lines. Expression levels of Beclin, LAMP1 and LDH were determined in whole-cell lysates from control and Beclin KD cells by immunoblot analysis as described in the Materials and Methods.

experiments described in this paper, similar immunoblot results were obtained, verifying that expression of Beclin was decreased by at least 90-95% relative to the parallel control cultures.

Endogenous Beclin forms a complex with hVps34 in U-251 glioblastoma cells

Previous studies have indicated that Beclin can be co-immunoprecipitated with mVps34 in HeLa cells (Kihara et al., 2001a). However, Beclin has also been described as a Bcl-2- and Bcl-X_L-interacting protein, based on yeast two-hybrid assays and fluorescence resonance energy transfer (FRET) analysis of co-expressed proteins (Liang et al., 1998). To determine if these proteins are normal endogenous binding partners for Beclin in U-251 glioblastoma cells, Beclin was immunoprecipitated from whole-cell lysate and the associated proteins were probed by immunoblot analysis with antibodies against hVps34, Bcl-2 or Bcl-X_L. Although hVps34, Bcl-2 and Bcl-X_L were all readily detected in the cell lysates, only hVps34 was co-precipitated with Beclin (Fig. 2A). In accord with these studies, the converse immunoprecipitation of endogenous Bcl-2 did not pull-down any detectable endogenous Beclin (Fig. 2B). Immunoprecipitation with the antibody against hVps34 was not possible because the latter was not a good precipitating reagent.

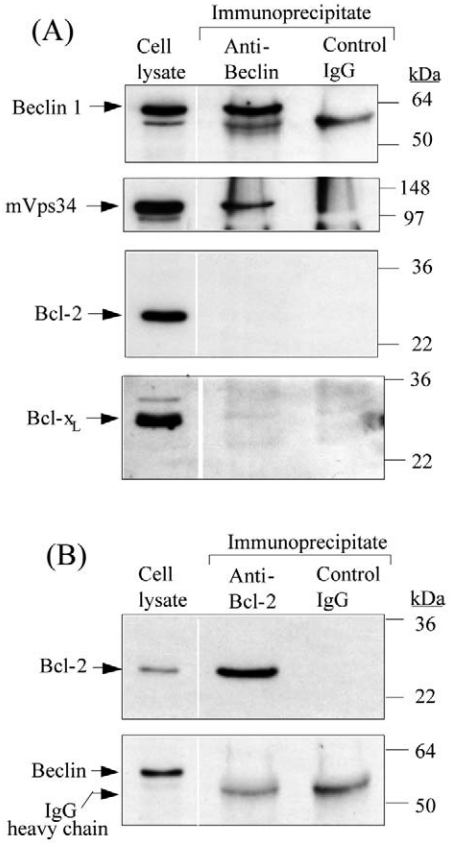

Fig. 2. Immunoprecipitated Beclin complex from U-251 cells contains hVps34 but not Bcl-2 or Bcl-X_L. (A) Cell lysates were prepared from parallel cultures as described in the Materials and Methods and 10% of each lysate was saved for immunoblot analysis. The remainder of each lysate was immunoprecipitated with either IgG against Beclin or a 'control' IgG against an unrelated protein (SPARC, Santa Cruz Biotechnology). Equal aliquots of the immune complexes eluted from protein A Sepharose beads were probed by immunoblot analysis using the antibodies indicated at the left of each panel. The band appearing just below Beclin in the upper panel is a nonspecific crossreacting protein. (B) Immunoprecipitation was performed as described in panel A, except that a rabbit antibody against Bcl-2 was used for the pull-down. The immunoprecipitated protein complexes were probed with the antibodies indicated at the left of each panel.

Suppression of Beclin expression interferes with macroautophagy

To assess the consequences of knocking down Beclin for the induction and progression of macroautophagy in U-251 cells, we subjected the cells to two established pro-autophagic stimuli: treatment with C_2-ceramide (Scarlatti et al., 2004) and nutrient deprivation (Klionsky et al., 2000; Levine et al., 2004). Microtubule-associated protein light-chain 3 (LC3) was used as a molecular marker to monitor autophagosome biogenesis. LC3 is the mammalian homolog of the yeast autophagy protein Atg8. Like Atg8, LC3 exists in a cytosolic form (LC3-I) and a form that is conjugated to phosphatidylethanolamine (PE) on autophagosome membranes (LC3-II) (Kabeya et al., 2000; Tanida et al., 2002). Initially, we attempted to compare autophagosome biogenesis in control versus Beclin KD cells by determining the subcellular localization of ectopically expressed GFP-LC3 by fluorescence microscopy of transiently transfected cells. However, the results of this assay were difficult to interpret, owing to the low transfection efficiency of U-251 cells and the tendency of the overexpressed GFP-LC3 to associate with punctate structures even under normal culture conditions. An alternative approach that avoids overexpression of LC3 entails measuring the ratio of endogenous LC3-II to LC3-I by immunoblot analysis. It is well established that the conversion of LC3-I to LC3-II is closely correlated with the formation of autophagosomes (Kabeya et al., 2000; Tanida et al., 2004). Because LC3-II associates specifically with the nascent autophagosome isolation membrane and remains on the autophagosome until it matures to an autolysosome, accumulation of LC3-II is now viewed as a definitive marker for activation of the autophagic pathway (Mizushima, 2004; Kirkegaard et al., 2004). As shown in Fig. 3A, nutrient

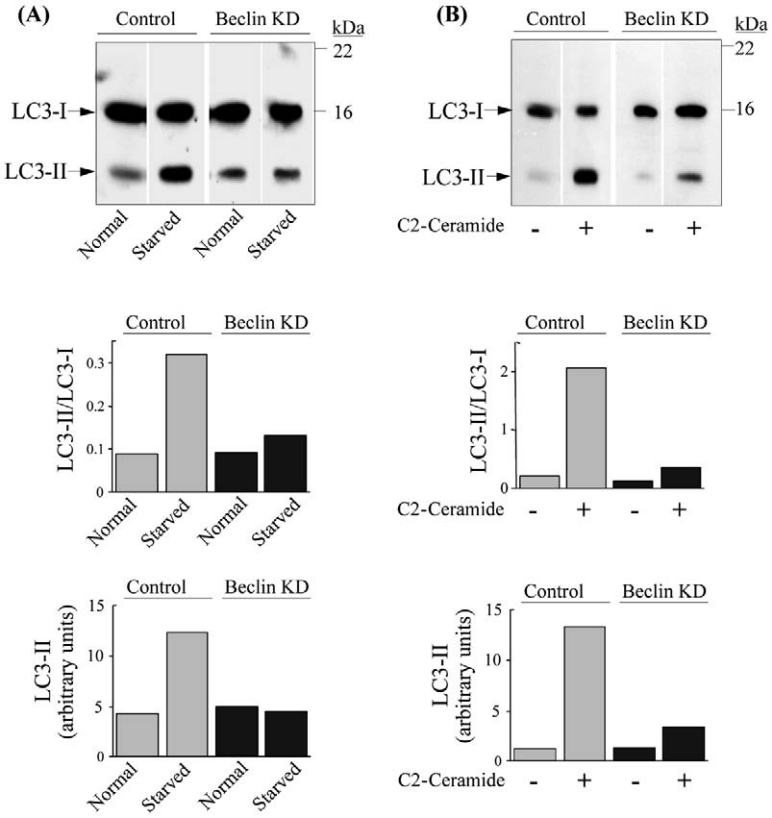

Fig. 3. Suppression of Beclin expression impairs the autophagy-associated post-translational processing of endogenous LC3-I to LC3-II. (A) Cells were incubated in DMEM + 10% FBS (normal) or HBSS (starved) for 4 hours. (B) Cells were treated with vehicle (–) or 10 μM C_2-ceramide (+) for 24 hours. All cells were subjected to SDS-PAGE and immunoblot analysis to detect the endogenous cytosolic LC3-I and the PE-conjugated LC3-II. The total LC3-II and the ratios of LC3-II to LC3-I represented in the bar graphs were determined from scans of the blots performed with a Kodak 440CF Image Station.

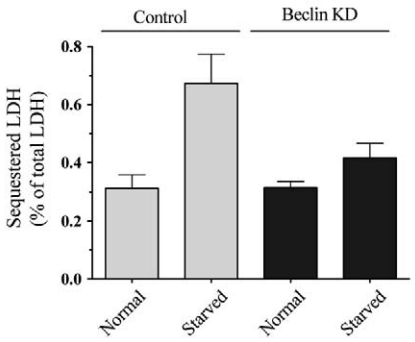

Fig. 4. Suppression of Beclin expression impairs macroautophagy as measured by sequestration of LDH. Control or Beclin KD cells were incubated in DMEM + 10% FBS (normal) or HBSS (starved) for 4 hours. Cells were lysed and fractionated as described in the Materials and Methods. LDH was assayed by immunoblotting aliquots of the cell lysate, and the pellet fraction was recovered after centrifugation through a metrizamide/sucrose cushion. LDH sequestered in the pellet fraction was expressed as a ratio to the total LDH in the cell lysate. The results are derived from separate fractionations of cells from three parallel cultures (mean ± s.e.).

deprivation caused a threefold increase in the total amount of LC3-II and the ratio of LC3-II to LC3-I in the control U-251 cells. However, there was comparatively little change in LC3-II in the Beclin KD cells. Ceramide treatment caused an even greater (sevenfold) increase in LC3-II in the control cells, with a markedly attenuated response again seen in the Beclin KD cells (Fig. 3B).

Previous studies have determined that macroautophagy can be assessed by measuring the sequestration of cytosolic enzymes into membrane-bound compartments (Kopitz et al., 1990; Stromhaug et al., 1998). When the U-251 cells were starved for 4 hours in Hanks balanced salt solution (HBSS), we observed a doubling of the amount of LDH sequestered in membrane compartments (Fig. 4). By contrast, the Beclin KD cells responded to nutrient deprivation with a much smaller change in LDH sequestration (Fig. 4).

The maturation of autophagosomes to autolysosomes is accompanied by a loss of LC3-II and an increase in the acidity of the lumen (Mizushima, 2004). Therefore, to assess the relative number of autolysosomes in control versus Beclin KD cells, we used an assay that measures supravital staining of acidic compartments with the lysosomotropic agent acridine orange (AO). When the dye enters an acidic compartment, the protonated form becomes trapped in aggregates that fluoresce bright red or orange (Traganos and Darzynkiewicz, 1994; Paglin et al., 2001; Kanzawa et al., 2003). Although AO stains lysosomal and late endosomal compartments as well as autolysosomes, extensive studies have established that a substantial increase in AO-positive acidic vesicular organelles (AVOs) occurs in conjunction with the induction of macroautophagy in glioblastoma cells (Kanzawa et al., 2003; Kanzawa et al., 2004; Komata et al., 2004; Takeuchi et al., 2005). As shown in Fig. 5A, a general increase in the intensity of AO-positive structures could be detected in ceramide-treated control cells, but not in the parallel ceramide-treated Beclin KD cells. To obtain a more accurate evaluation of the amount of AO sequestered in acidic compartments, the cells were lysed and the red fluorescence emanating from AO was quantified and normalized to DNA (ethidium bromide fluorescence) (Fig. 5B). The results confirmed that ceramide treatment stimulated a large increase in the amount of AO sequestered into AVOs in control cells, and that the response to ceramide was greatly reduced in the Beclin KD cells.

Protein trafficking from the TGN to the lysosomes in the Beclin KD cells

Previous studies have indicated that treatment of cells with the PI 3-kinase inhibitor wortmannin causes a block in trafficking of procathepsin D from the TGN to the late endosomes and lysosomes (Davidson, 1995; Brown et al., 1995). Similar effects have been reported in cells expressing a kinase-deficient form of rat Vps34 (Row et al., 2001). Most recently, we have determined that siRNA-mediated suppression of hVps34 expression in U-251 cells results in marked accumulation of the late endosomal intermediate form of cathepsin D, with reduced production of the mature lysosomal form (E. E.

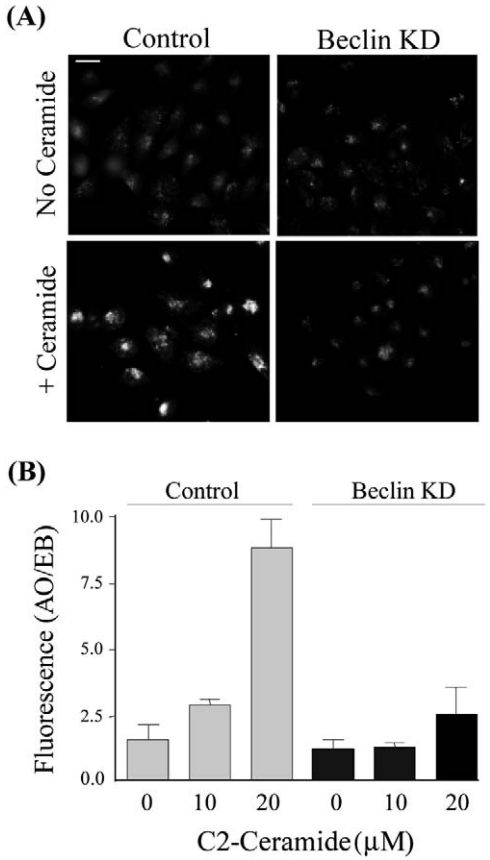

Fig. 5. Accumulation of acidic vesicular organelles (AVOs) induced by ceramide treatment is impaired in Beclin KD cells. (A) Control and Beclin KD cells were maintained for 24 hours in medium with or without 10 μM C2-ceramide, as indicated. Cells were then incubated with acridine orange (AO) and examined by fluorescence microscopy, using a filter combination to detect red fluorescence. All digital micrographs were taken at the same exposure setting. Bar, 50 μm. (B) Control and Beclin KD cells were treated with 0, 10 or 20 μM C2-ceramide for 24 hours and incubated with AO. The relative amount of AO trapped in vesicular compartments (red fluorescence; excitation at 488 nm, emission at 655 nm) was measured by fluorimetry and normalized to cellular DNA detected with ethidium bromide (EB). The data represent the mean ± s.e. of three determinations from parallel cultures.

Johnson, J.H.O., W. T. Gunning and W.A.M., unpublished data). In light of the association between Beclin and hVps34, we wished to determine if cells lacking normal amounts of Beclin would exhibit any defects in this PI 3-kinase-dependent trafficking pathway. Newly synthesized procathepsin D (51-53 kDa) associates with the cation-independent mannose 6-phosphate receptor (M6PR) in the TGN and is delivered to the endosomal compartment, where it is activated by removal of the pro-peptide to generate an intermediate form that migrates at 47-48 kDa on SDS gels. The final step in cathepsin D processing is completed in the lysosomes, where the intermediate form is cleaved to the mature form, which contains two non-covalently linked chains of 31 kDa and 14 kDa (Rijnboutt et al., 1992; Delbruck et al., 1994). As shown by the immunoblots in Fig. 6A, the steady-state levels of the 53 kDa procathepsin D, the 47 kDa intermediate and the 31 kDa mature cathepsin D were similar in the control and Beclin KD cells. In cells depleted of hVps34, this method readily detects a 3-4-fold increase in the steady-state level of the 47 kDa intermediate (E. E. Johnson, J.H.O., W. T. Gunning and W.A.M., unpublished data). In cells treated with ammonium chloride to raise the pH of the endosomal and lysosomal compartments, a substantial increase in 53 kDa procathepsin D can be observed (Fig. 6A).

To obtain a more direct assessment of the kinetics of processing of newly synthesized procathepsin D, we performed a pulse-chase analysis (Fig. 6B). When [^{35}S]methionine-labeled cathepsin D was immunoprecipitated after a 30 minute pulse, nearly all of the radiolabeled protein was in the 53 kDa pro form in both control and KD cells. After a 4 hour chase, the mature 31 kDa cathepsin D was the predominant form detected, with no significant difference in the percentage of total procathepsin D processed to the mature form in the control and Beclin KD cells (Fig. 6C). After 4 hours, there was no residual 53 kDa procathepsin D and only a small amount of the 47 kDa endosomal intermediate. By comparison, cells treated with ammonium chloride generated almost no mature cathepsin D during the same time period (Fig. 6B,C). Immunoprecipitation of the culture medium revealed that, in the latter cultures, most of the radiolabeled procathepsin D (approx. 80%) was secreted during the 4 hour chase. However, prolonged film exposure revealed only small amounts of secreted procathepsin D (<7% of total) in the control and Beclin KD cultures (not shown). These results indicate that Beclin is not required for normal PI 3-kinase-dependent trafficking of procathepsin D from the TGN to the endosomal and lysosomal compartments in U-251 cells.

Endocytic trafficking in the Beclin KD cells

In addition to disrupting trafficking between the TGN and lysosome, wortmannin causes marked swelling of late endosome compartments (Reaves et al., 1996; Fernandez-Borja et al., 1999). This appears to be a result of failure of inward vesiculation of multivesicular endosomes, without a compensatory decrease in endocytic membrane influx (Futter et al., 2001). We have recently observed a similar enlargement of vesicular compartments containing the late endosome/lysosome membrane marker LAMP1 when hVps34 expression was silenced in U-251 cells (E. E. Johnson, J.H.O., W. T. Gunning and W.A.M., unpublished data). In contrast to these findings, immunofluorescence microscopy of the Beclin KD cells revealed no detectable changes in the morphology or distribution of molecular markers for late endosomes/lysosomes (LAMP1), early endosomes (EEA1) or Golgi membranes (GM130) (Fig. 7).

To assess directly the endocytic transport pathway, we measured the cellular uptake of the fluid-phase marker horseradish peroxidase (HRP) (Fig. 8). The results did not reveal any consistent perturbation of HRP endocytosis in cells lacking Beclin. To explore the endocytic pathway further, we followed the fate of activated EGFR. In serum-deprived cells grown in the absence of EGF, degradation of EGFR is minimal and receptors accumulate on the cell surface. However, upon addition of EGF, the receptors are rapidly activated by tyrosine phosphorylation in the C-terminal cytoplasmic domain and the EGF-EGFR complexes are internalized into clathrin-coated

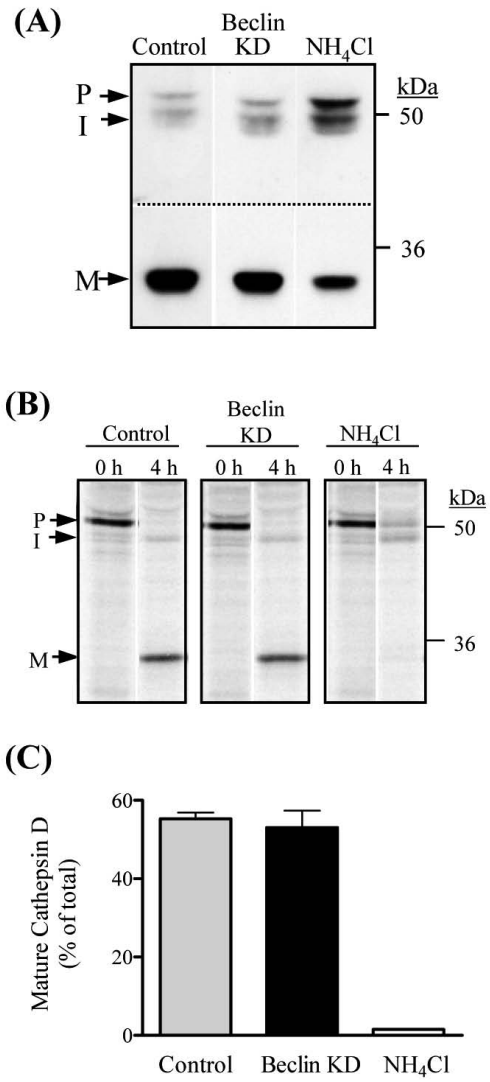

Fig. 6. Suppression of Beclin expression does not impede lysosomal enzyme sorting as measured by cathepsin D processing. (A) Immunoblot analysis was performed on endogenous cathepsin D in whole-cell lysates from control and Beclin KD cells. To demonstrate inhibition of cathepsin D processing, a separate control culture was incubated with 10 mM NH_4Cl for 24 hours prior to harvest. Equal amounts of protein were loaded in each lane. The part of the blot above the dashed line was exposed seven times longer than the lower portion, to permit detection of the precursor forms of cathepsin D. The forms of cathepsin D are labeled as follows: P, proenzyme; I, endosomal intermediate; M, mature lysosomal enzyme. (B) Cells were labeled with 100 μCi/ml [^{35}S]methionine, then harvested immediately or chased in medium with unlabeled methionine for 4 hours. A separate control culture was incubated with 15 mM NH_4Cl during the 4 hour chase. Cathepsin D was immunoprecipitated and subjected to SDS-PAGE and fluorography. (C) Immunoprecipitations were performed on control and Beclin KD cells from three parallel cultures immediately after the pulse and after a 4 hour chase, and the total radioactivity recovered in the mature form of cathepsin D at 4 hours was expressed as a ratio to the total radiolabeled procathepsin D at 0 hours (mean ± s.e.). Quantification of radioactivity was performed with a Molecular Dynamics Storm Phosphorimager.

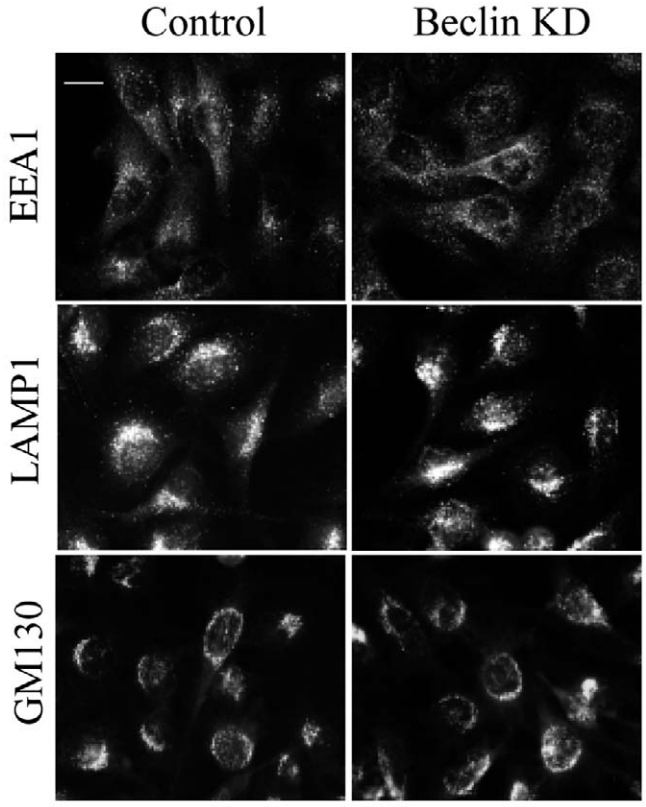

Fig. 7. Morphology of endosomes, lysosomes and Golgi membranes is similar in Beclin KD cells compared with controls. Control or Beclin KD cells were seeded in parallel dishes at the same density and examined by immunofluorescence microscopy after two days, using the primary antibodies indicated at the left of the figure. Bar, 20 μm.

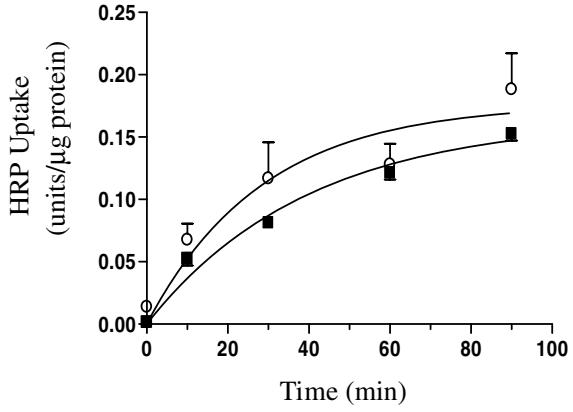

Fig. 8. Suppression of Beclin expression does not interfere with endocytosis of the fluid phase marker horseradish peroxidase (HRP). Control (■) and Beclin KD (○) cells were seeded at the same density, grown for two days and then incubated for the indicated periods of time with 2 mg/ml HRP in DMEM + 1% BSA. Washed cells were lysed and HRP activity was determined as described in the Materials and Methods. Each point represents the mean ± s.e. from three determinations on parallel cultures. Similar results were obtained when the experiment was repeated with different batches of control and Beclin KD cells derived from separate retroviral infections and puromycin selections.

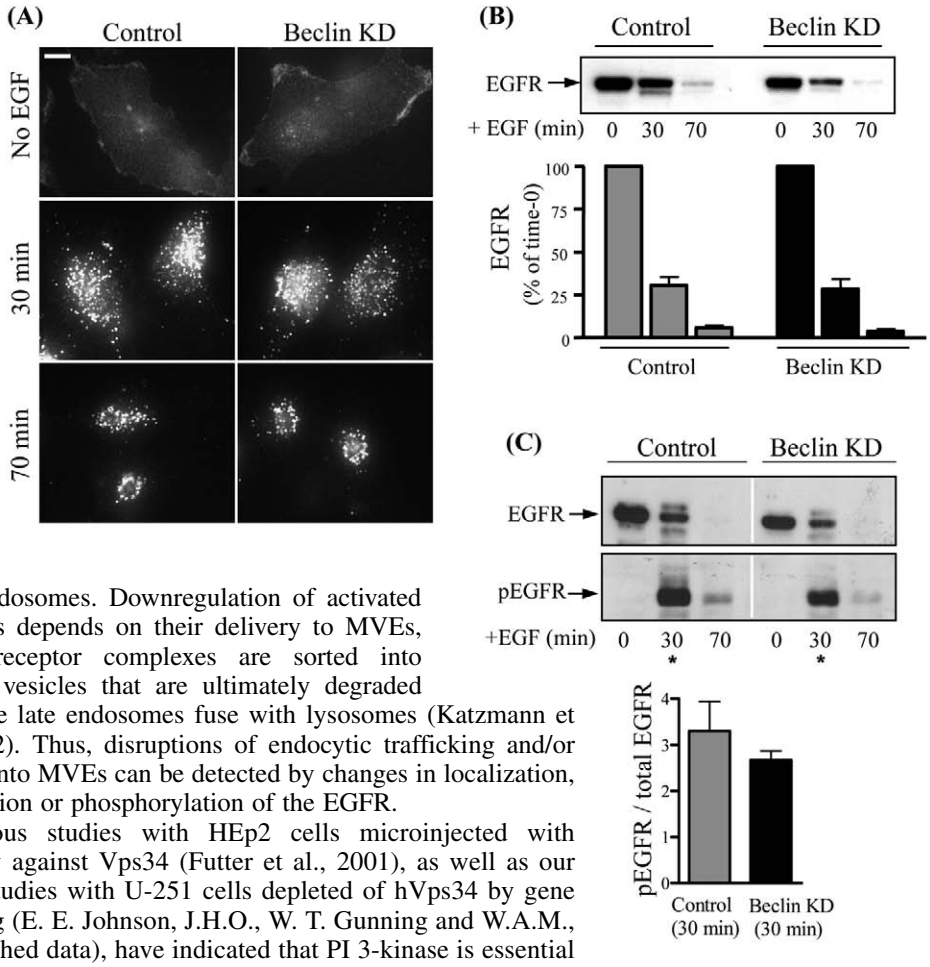

Fig. 9. Suppression of Beclin expression does not disrupt EGF-stimulated endocytosis or post-endocytic degradation of the EGFR. (A) Control or Beclin KD cells were fixed and processed for immunofluorescence detection of EGFR after overnight growth in serum-free medium (No EGF), and after 30 minutes or 70 minutes incubation with 200 ng/ml EGF. Bar, 10 μm. (B) Cells were harvested at the indicated times after addition of EGF and subjected to immunoblot analysis for total EGFR (upper panel). The bar graph (lower panel) shows the data derived from Kodak 440CF Imager scans performed on blots from three cultures harvested at each time point. (C) Cells were harvested at the indicated times after addition of EGF and subjected to immunoblot analysis for total EGFR (upper panel) or EGFR phosphorylated on Tyr1068 (pEGFR). The bar graph depicts the ratio of pEGFR to total EGFR determined in three parallel control or Beclin KD cultures at 30 minutes after EGF stimulation (mean ± s.e.).

early endosomes. Downregulation of activated receptors depends on their delivery to MVEs, where receptor complexes are sorted into internal vesicles that are ultimately degraded when the late endosomes fuse with lysosomes (Katzmann et al., 2002). Thus, disruptions of endocytic trafficking and/or sorting into MVEs can be detected by changes in localization, degradation or phosphorylation of the EGFR.

Previous studies with HEp2 cells microinjected with antibody against Vps34 (Futter et al., 2001), as well as our recent studies with U-251 cells depleted of hVps34 by gene silencing (E. E. Johnson, J.H.O., W. T. Gunning and W.A.M., unpublished data), have indicated that PI 3-kinase is essential for the inward vesiculation of MVEs. In hVps34 KD cells, EGFR is internalized but remains on limiting membranes of enlarged vesicular structures that appear to be derived from late endosomes (E. E. Johnson, J.H.O., W. T. Gunning and W.A.M., unpublished data). In the latter situation, the rate of degradation of the EGFR is reduced, and there is a marked attenuation of receptor dephosphorylation, manifested as a doubling of the ratio of phosphorylated receptor (pEGFR) to total receptor at 30 minutes after EGF stimulation. In contrast to the results with hVps34 KD cells, immunofluorescence localization studies revealed no discernable differences in EGFR distribution before or after EGF stimulation in Beclin KD cells compared with controls (Fig. 9A). Before addition of EGF, most of the receptors were present in the peripheral cell membrane (Fig. 9A). Within 30 minutes after addition of EGF, most of the receptors had moved into internal vesicles arrayed throughout the cytoplasm, with some concentration around the nucleus (Fig. 9A). This pattern is typical of early and late endosomes (Fig. 7). By 70 minutes, most of the EGFR-positive structures were clustered in the juxtanuclear region (Fig. 9A) in a pattern typical of lysosomes (Fig. 7). Of particular note, there was no evidence of localization of EGFR to enlarged vesicular structures at any of these stages. In contrast to our observations with hVps34 KD cells, the time course of receptor degradation after addition of EGF was nearly identical in the Beclin KD cells compared with the controls (Fig. 9B), and there was no significant impairment of EGFR dephosphorylation in the Beclin KD cells (Fig. 9C).

Growth properties of Beclin KD cells

Disruption of endocytic trafficking might be expected to have negative consequences for cell proliferation by impeding internalization of nutrient carriers (e.g. transferrin or LDL receptors) or growth factor receptors (e.g. insulin). Alternatively, alterations at later stages, such as the internalization of receptors into MVEs, might prolong proliferative signals propagated by phosphorylated growth factor receptors. Thus, as a final indirect means to detect such changes in the Beclin KD cells, we compared their rate of cell proliferation to control cells with normal levels of Beclin (Fig. 10A). Consistent with the normal morphology (Fig. 7) and endocytic internalization of HRP or EGFR (Figs 8, 9), the suppression of Beclin expression had no detectable effect on the rate of proliferation of U-251 cells (Fig. 10A). Moreover, the Beclin KD cells were indistinguishable from controls with respect to their ability to form colonies in soft agar (Fig. 10B).

Discussion

Beclin is an interacting partner for the mammalian class III PI 3-kinase mVps34. Previous studies have established that this PI 3-kinase is required for macroautophagy in nutrient-starved cells (Petiot et al., 2000; Eskelinen et al., 2002), for normal lysosomal enzyme sorting and protein trafficking in the endocytic pathway (Row et al., 2001; Futter et al., 2001; Petiot et al., 2003), and for cell cycling (Siddhanta et al., 1998). In contrast with its documented role in macroautophagy, the

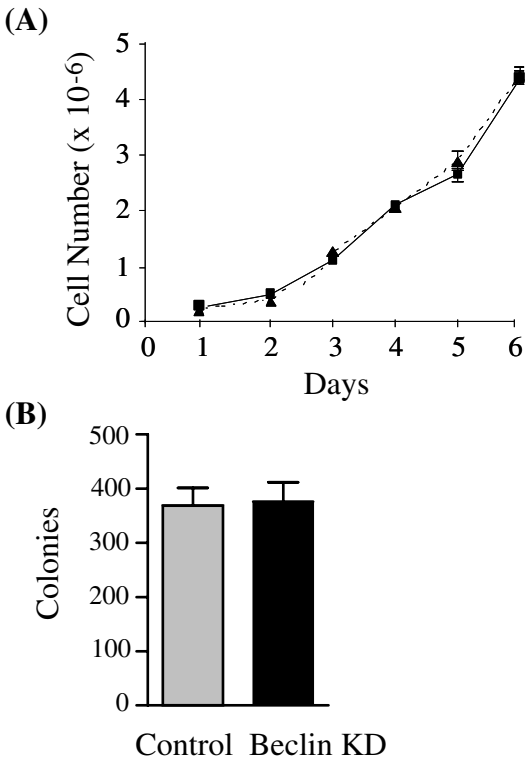

Fig. 10. Suppression of Beclin expression does not affect the growth rate or clonogenicity of U-251 cells. (A) Control (solid line) and Beclin KD (dashed line) cells were seeded in 60 mm dishes on day 0 at an initial density of 200,000 cells per dish. On each of the indicated days, cells were harvested from three dishes in each group and counted with a Coulter Z1 particle counter (mean ± s.e.). (B) Control or Beclin KD cells were seeded in soft agar and assayed for colony formation after 14 days as described in the Materials and Methods. Results are means (± s.e.) of colony counts performed on three dishes.

possible role of Beclin as an essential chaperone or adaptor for hVps34 in normal trafficking pathways has received little attention. Furuya et al. (Furuya et al., 2005) recently reported that overexpression of a Beclin mutant lacking the conserved Vps34-binding domain does not alter cathepsin D maturation in MCF7 cells, compared with cells expressing high or low levels of wild-type Beclin. In the present studies, we used a different approach (siRNA-mediated gene silencing) to show that Beclin is required specifically for the function of hVps34 in the macroautophagy pathway, but not for the normal functions of this PI 3-kinase in trafficking from the TGN to the lysosome in U-251 glioblastoma cells. Moreover, we extend this line of investigation by showing that Beclin is also not required for the proposed functions of hVps34 in endocytic trafficking and inward vesiculation of multivesicular endosomes.

The current findings contrast with previous studies of the Beclin homolog Vps30 (Atg6) in *S. cerevisiae.* In those studies, Vps30 interaction with Vps34 was found to be required both for starvation-induced autophagy (Seaman et al., 1997; Kametaka et al., 1998) and vesicular transport of carboxypeptidase Y (CPY) from the Golgi compartment to the vacuole (Klionsky et al., 1990). The dual role of Vps30 in yeast can be attributed to its assembly into two distinct protein complexes (Kihara et al., 2001b). In the autophagy pathway, Vps30 is linked to Vps34 through an interaction with a novel bridging protein, Atg14, whereas, in the Golgi-to-vacuole pathway, a different linker protein, Vps38, mediates this interaction. Several lines of evidence suggest that the mammalian Beclin-Vps34 complex might be different from these yeast Vps30-Vps34 complexes. First, in *vps30*-defective yeast, Beclin can complement Vps30 in the autophagy pathway, but not in the vacuolar protein-sorting pathway (Liang et al., 1999). This would be consistent with the evidence indicating that Beclin does not function in post-Golgi sorting of cathepsin D in mammalian cells. Second, homologs of the bridging proteins Atg14 and Vps38 have not yet been identified in mammalian cells. Finally, whereas Vps30 (Atg6) and Beclin share substantial amino acid sequence similarity in their central coiled-coil and evolutionarily conserved Vps34-binding domains (Liang et al., 1998; Furuya et al., 2005), Vps30 (Atg6) is significantly larger (557 amino acids) than human Beclin (450 amino acids), with several regions of sequence divergence. For example, Vps30 (Atg6) contains 22 unique N-terminal amino acids and 17 unique C-terminal amino acids, compared with human Beclin. In addition, several internal regions of Vps30 (Atg6) (e.g. residues 38-48, 147-157, 403-416, 499-514) generate notable gaps when aligned against human Beclin. Although the specific functions of these domains remain to be defined, one could speculate that structural features conferred by the unique sequences in Vps30 (Atg6) might account for its broader role in promoting Vps34 interaction with both normal trafficking and autophagy pathways, compared with the more-restricted role of Beclin in macroautophagy.

PtdIns(3)*P* is distributed throughout cellular endomembranes, where it serves to recruit a variety of proteins implicated in the regulation of vesicular transport and intracellular protein sorting (Simonsen et al., 2001; Corvera, 2001). Some of these proteins contain a Phox-homology phosphoinositide-binding domain (Song et al., 2001; Cheever et al., 2001; Xu et al., 2001; Kanai et al., 2001), whereas others contain a structural motif termed the FYVE finger, which binds to PtdIns(3)*P* with high affinity (Wurmser et al., 1999; Fruman et al., 1999; Corvera et al., 1999). Little is known about the molecular events that direct the targeting of the hVps34 PI 3-kinase to specific subcellular compartments. Like its yeast counterpart, hVps34 appears to associate with intracellular membranes through interaction with a myristoylated adaptor, p150 (hVps15) (Volinia et al., 1995; Panaretou et al., 1997). There is some evidence that recruitment of mVps34 to endosomal membranes is facilitated by specific Rab GTPases (e.g. Rab5, Rab7) that can bind to p150 (Murray et al., 2002; Stein et al., 2003). Once it is associated with the membrane, hVps34 presumably generates the PtdIns(3)*P* required for membrane association of FYVE-domain proteins such as the Rab effectors EEA1 and Rabenosyn-5 (Simonsen et al., 1998; De Renzis et al., 2002), and the PtdIns(3)*P* 5-kinase PIKfyve (Ikonomov et al., 2003). Our finding that Beclin can be substantially depleted from mammalian cells without any detectable consequences for endosome morphology, EEA1 distribution, or endocytic trafficking strongly suggests that Beclin is not required for targeting or recruitment of hVps34 to endosomal membranes. However, because Beclin expression

was not entirely eliminated in the KD cells, we cannot definitively rule out the possibility that very low residual levels of Beclin are sufficient to mediate these processes. By contrast, our studies clearly implicate Beclin in one or more key steps required for generating a central component of the pre-autophagosome protein complex.

Several reviews have summarized the recent advances in understanding the pre-autophagosomal protein assemblies involved in initiating the formation of the isolation membrane (Klionsky, 2005; Kirkegaard et al., 2004; Marino and Lopez-Otin, 2004). The conjugation of LC3 (Atg8) to PE, generating LC3-II, occupies a central position in this scheme. LC3 is first cleaved by a cysteine protease (Atg4/autophagin) to expose a C-terminal glycine. The protein is then conjugated sequentially, first to Atg7, then to Atg3, before the final conjugation to PE on the pre-autophagosome membrane (Tanida et al., 2004). An oligomeric protein complex containing Atg12-Atg5 and Atg16 plays a key role in recruiting LC-II to the pre-autophagosome membrane (Mizushima et al., 2001; Yoshimori, 2004). Therefore, our observation that Beclin is required for the formation of LC3-II implies that Beclin functions in the earliest steps required for autophagosome biogenesis, rather than in the later maturation events involving fusion with endosomes or lysosomes. Since inhibitors of PI 3-kinase have been reported to cause a reduction in LC3-II production (Aki et al., 2003), we believe that the attenuated production of LC3-II observed in starved or ceramide-treated Beclin KD cells is related to an impaired ability of hVps34 to function in the autophagy pathway without Beclin. The molecular basis for the apparent requirement for PtdIns(3)*P* in the autophagic process in mammalian cells remains to be determined. However, recent studies have described an autophagy-linked FYVE-domain protein, Alfy (Simonsen et al., 2004), and a Rab GTPase, Rab24 (Munafo and Colombo, 2002), associated with autophagosomes. These findings raise the intriguing possibility that PtdIns(3)*P*-dependent molecular assemblies not unlike those described on early endosomes (De Renzis et al., 2002) might also play a role in the formation and/or maturation of autophagosomes.

As mentioned in the introduction, ectopic overexpression of Beclin in breast cancer cells with monoallelic deletions of the *beclin* gene can inhibit cell proliferation, colony formation in soft agar and tumorigenesis in nude or *scid* mice (Liang et al., 1999; Furuya et al., 2005). These observations, coupled with the increased frequency of spontaneous tumors detected in *beclin*$^{-/+}$ mice (Qu et al., 2003; Yue et al., 2003), indicate that Beclin can function as a tumor suppressor. The exact mechanisms underlying the effects of Beclin on tumorigenesis remain to be defined, but the apparent requirement for Beclin for the accumulation of autophagosomes in the initial stages of type II programmed cell death (Scarlatti et al., 2004; Yu et al., 2004; Shimizu et al., 2004) suggests that its role as a tumor suppressor is most probably related to regulation of macroautophagy. Nevertheless, without knowing if Beclin interaction with hVps34 is also required for the function of this PI 3-kinase in normal vesicular trafficking pathways, some question has remained as to whether or not the loss of Beclin could contribute to tumor formation by alternative mechanisms, such as the disruption of hVps34-dependent endocytic pathways and consequential potentiation of growth factor signaling. The results of the present studies argue against this possibility by showing that normal levels of Beclin are not required for the function of hVps34 in endocytosis, the biogenesis of multivesicular endosomes, or EGFR degradation.

Although our stable Beclin KD glioblastoma cells were unable to mount a typical autophagic response when challenged by nutrient deprivation or ceramide treatment, the loss of Beclin had no detectable effect on their basal growth rate or ability to form colonies in soft agar. Unlike MCF7 breast cancer cells, U-251 cells harbor deletions in the *PTEN* gene, which encodes a protein/lipid phosphatase that dephosphorylates phosphatidylinositol (3,4,5)-trisphosphate [PtdIns(3,4,5)P_3], which is the product of class I p110/p85 PI 3-kinases (Vazquez and Sellers, 2000). Consequently, these cells exhibit high levels of constitutive Akt activation. There is some evidence that increasing the intracellular concentration of PtdIns(3,4,5)P_3 by stimulating the activity of class I PI 3-kinase inhibits macroautophagy, which is the opposite effect of stimulating the mVps34 class III PI 3-kinase (Petiot et al., 2000). Along the same line, inhibiting Akt/protein kinase B, a major downstream target in the class I PI 3-kinase signaling pathway, synergistically enhances macroautophagy in glioblastoma cells treated with rapamycin (Takeuchi et al., 2005). Therefore, one possible explanation for the absence of an effect of Beclin depletion on glioblastoma cell proliferation is that high basal levels of PtdIns(3,4,5)P_3 and constitutive activation of Akt suppress hVps34-dependent macroautophagy and supercede any regulatory effects of Beclin, unless the cells are exposed to a strong pro-autophagic stimulus (e.g. starvation, rapamycin, C_2-ceramide). Definition of the relationship between Beclin-Vps34-mediated macroautophagy and the activity of the p110/p85 PI 3-kinase signaling pathways in malignancies with different genetic backgrounds promises to be an important area for further investigation.

In conclusion, we propose that a primary function of Beclin is to facilitate the interaction of hVps34 PI 3-kinase with specific effectors on the pre-autophagosomal isolation membrane in response to pro-autophagic conditions or death signals. However, a major unsolved puzzle concerning Beclin is the biological significance of its reported interaction with the anti-apoptotic proteins Bcl-2 and Bcl-X_L, which have no known connection to mVps34-mediated protein trafficking or the pre-autophagosomal Atg protein complexes. Interest in this question has intensified with the recent observation that etoposide treatment induces autophagic cell death instead of classical apoptosis in wild-type or Bax/Bak$^{-/-}$ double-knockout mouse embryonic fibroblasts overexpressing Bcl-2 or Bcl-X_L (Shimizu et al., 2004). The interaction between Beclin and Bcl-2 was first observed in yeast two-hybrid assays and then confirmed by FRET analysis of the two proteins overexpressed in COS cells (Aita et al., 1999). In a more recent study, Pattingre et al. (Pattingre et al., 2005) showed that overexpression of wild-type Bcl-2, but not Beclin-binding-defective Bcl-2 mutants, can suppress Beclin-dependent autophagy in yeast and mammalian cells. In accord with published observations (Pattingre et al., 2005), we have found it easy to observe an interaction between FLAG-Beclin and Bcl-2 in pull-down assays using transfected 293 cells overexpressing both proteins. However, as shown in Fig. 2, we have been unable to detect an interaction between endogenous Beclin and Bcl-2 or Bcl-X_L under conditions that allow co-

immunoprecipitation of Beclin with hVps34. Our findings are consistent with those of Kihara et al. (Kihara et al., 2001a), who demonstrated that all of the endogenous Beclin in Hela cells could be co-immunoprecipitated together with hVps34, using an antibody against the latter protein. Nevertheless, these studies do not completely rule out the possibility that low-affinity interactions might occur between membrane-bound Bcl-2 or Bcl-X_L and the Beclin-mVps34 complex. Indeed, there is some evidence that overexpression of Bcl-2 reduces the amount of Beclin in the hVps34 complex (Pattingre et al., 2005). Transient interactions might be lost in the detergent-containing buffers typically used for immunoprecipitation. Alternatively, the interactions between Beclin and Bcl-2 might be more prominent in specific cell types or under certain metabolic conditions. This will be an important topic for future study.

Materials and Methods

siRNA-mediated silencing of Beclin

U-251 human glioblastoma cells were obtained from the National Cancer Institute Frederick Cancer DCT Tumor Repository and were maintained in Dulbecco's modified Eagle medium (DMEM), supplemented with 10% fetal bovine serum (FBS). The pSUPER.retro.puro vector was obtained from OligoEngine. The oligonucleotide sequence used for siRNA interference with Beclin expression corresponded to nucleotides 1201-1219 (5′-GGCAAGAUUGAAGACACAG-3′) downstream of the transcription start site of *beclin* (GenBank accession number: AF077301), followed by a 9-nucleotide non-complementary spacer (TATCTTGAC) and the reverse complement of the initial 19-nucleotide sequence. A control vector was constructed with a similar insert where the 19-nucleotide sequence had no homology to any known human gene sequence. Retrovirus was produced in 293-GPG packaging cells (Ory et al., 1996) maintained in DMEM + 10% heat-inactivated FBS with 1 μg/ml puromycin, 300 μg/ml G418 and 2 μg/ml doxycycline. For transfection, the 293-GPG cells were seeded at 1.2×10^7 cells per dish in 100 mm dishes in DMEM containing 10% heat-inactivated FBS. After 24 hours. the cells were transfected with the pSuper.retro.puro constructs using Lipofectamine-Plus reagent (Invitrogen). At 48 and 72 hours after transfection, the virus-enriched medium was collected and passed through a 0.22 μm filter. Infections of the U-251 cells were performed on two sequential days in the presence of 4.0 μg/ml hexadimethrine bromide (Sigma). At 24 hours after the second infection, the cells were trypsinized and re-plated in selection medium containing 1 μg/ml puromycin. After a selection period of six days, the surviving cells were pooled and used for studies described in the following sections.

Immunoprecipitation of endogenous Beclin protein complexes

U-251 cells were grown to 80% confluence in 100 mm dishes in DMEM with 10% FBS. The cells were washed three times with Hanks balanced salt solution (HBSS), scraped from the dish and homogenized in IP buffer: 50 mM Tris-HCl, pH 7.4, 150 mM NaCl, 1 mM EDTA, 1% Triton X-100, and protease inhibitors. The lysate was centrifuged at 10,000 ***g*** for 15 minutes at 4°C and the supernatant solution was incubated with goat polyclonal IgG against Beclin (2 hours at 4°C), followed by 1 hour incubation with protein A Sepharose beads. The beads were washed three times with IP buffer, twice with phosphate-buffered saline (PBS), and the immune complexes were eluted from the beads and subjected to SDS-PAGE and immunoblot analysis as described previously (Wilson et al., 1996). Primary antibodies used for immunoblot analysis included mouse monoclonal antibody against Beclin (BD Biosciences), rabbit polyclonal antibody against hVps34 (Zymed Laboratories), mouse monoclonal antibody against Bcl-2, and rabbit polyclonal antibody against Bcl-X_L (Santa Cruz Biotechnology). For the converse immunoprecipitation, Bcl-2 was pulled-down with a rabbit polyclonal antibody (Santa Cruz Biotechnology) and the immunoprecipitates were immunoblotted with the monoclonal antibodies against Bcl-2 or Beclin. The antibody against hVps34 did not work for immunoprecipitation.

Immunofluorescence microscopy

Organelle morphology was assessed in control and Beclin KD cells grown on laminin-coated glass coverslips for 24 hours. For detection of EEA1, cells were fixed with 3% paraformaldehyde and permeabilized with 0.05% saponin in PBS. For LAMP1 or GM130, cells were fixed with ice-cold methanol for 10 minutes. All cells were blocked with 10% goat serum in PBS for 30 minutes and the following monoclonal antibodies were applied for 1 hour in PBS with 10% goat serum: anti-LAMP1 antibody (University of Iowa Developmental Studies Hybridoma Bank, Iowa City, IA), anti-GM130 and anti-EEA1 (BD Biosciences). Cells were then washed three times with 10% goat serum in PBS and incubated for 1 hour with Alexa Fluor 568 goat anti-mouse IgG (Molecular Probes). Photomicrographs were taken with a Nikon Eclipse 800 fluorescence microscope equipped with a digital camera. Images were acquired and processed using ImagePro software (Media Cybernetics).

Induction of macroautophagy

Macroautophagy was induced by nutrient starvation or exposure to C2-ceramide (N-acetyl D-erythro-sphingosine; Calbiochem). For starvation, cells were washed with HBSS three times and then incubated in HBSS for 4 hours. For C2-ceramide treatment, cells were incubated with 10 μM or 20 μM C2-ceramide in DMEM + 0.1% FBS for 24 hours. Ceramide was dissolved in dimethlysulfoxide (DMSO), and control cultures contained equal amounts of vehicle. To monitor the induction of macroautophagy, the relative amounts of endogenous LC3 in the unmodified form (LC3-I) and the phosphatidylethanolamine (PE)-conjugated form (LC3-II) were determined by immunoblot analysis of whole-cell lysate, using a rabbit polyclonal antibody against LC3 (Kabeya et al., 2000) kindly provided by Tamotsu Yoshimori (National Institute for Basic Biology, Okazaki, Japan). The chemiluminescent signals from the immunoblot were quantified with a Kodak 440CF image station. For cells starved in HBSS, macroautophagy was also monitored by sequestration of the cytosolic enzyme lactate dehydrogenase (LDH) into membrane-bound components prepared by centrifugation of cell lysate over a metrizamide/sucrose cushion as described (Kopitz et al., 1990; Stromhaug et al., 1998). Aliquots of the whole-cell lysate and the pelleted material were subjected to SDS-PAGE and immunoblot analysis with a mouse monoclonal antibody against LDH (Sigma).

Detection and quantification of acidic vesicular organelles with acridine orange (AO)

Vital staining of cells with AO (Molecular Probes) was performed essentially as described (Paglin et al., 2001). Cells were grown on laminin-coated coverslips (for fluorescence microscopy) or in 96-well plates (for quantification of red fluorescence) and treated with C2-ceramide or vehicle (DMSO) for the indicated time. AO was added for 15 minutes at a final concentration of 1 μg/ml, and the cells were then washed three times with PBS. Unfixed cells were examined immediately by fluorescence microscopy using a Nikon Eclipse 800 microscope with the red filter set (G-2E/C; excitation 528-553, emission 600-660). Red fluorescence was quantified with a microplate fluorimeter (Molecular Devices) with excitation and emission wavelengths set at 488 nm and 655 nm, respectively. To normalize the measurements to the number of cells present in each well, a solution of ethidium bromide (EB) was added to a final concentration of 0.2 μM and the fluorescence emitted from the DNA complexes was measured at 530 nm (excitation), 590 nm (emission). The AO red fluorescence was expressed as a ratio to the EB fluorescence.

Cathepsin D processing

Steady-state levels of intracellular cathepsin D were measured in whole-cell lysates by SDS-PAGE and immunoblot analysis, using goat anti-cathepsin D antibody from Santa Cruz Biotechnology. To measure the kinetics of cathepsin D processing, U-251 cells were pulse-labeled for 30 minutes in methionine-free DMEM containing 10% FBS and 100 μCi/ml [^{35}S]methionine (Easy Tag express labeling mix; 1175 Ci/mmol, Perkin Elmer), then chased for 4 hours in DMEM containing 10% FBS, 200 μM methionine and 200 μM cysteine. Cells were washed three times with PBS, harvested using a cell scraper, homogenized and solublized in 50 mM Tris-HCl, pH 7.4, 150 mM NaCl, 1% Nonidet P40, 0.5% sodium deoxycholate, 0.1% SDS, 5 mM EDTA. Insoluble material was removed by centrifugation at 100,000 ***g*** for 45 minutes at 4°C and the lysates were precleared with protein A Sepharose. Samples were then incubated for 2 hours with a polyclonal antibody against cathepsin D (Biodesign International). Immune complexes were then collected on protein A Sepharose and subjected to SDS-PAGE, fluorography and Phosphorimager analysis as described previously (Wilson et al., 1996).

Endocytosis of HRP

Cells grown to approximately 80% confluence were washed with DMEM and then incubated at 37°C with HRP (2 mg/ml) in DMEM containing 1% bovine serum albumin (BSA) for the time periods indicated in the figure. Cells were placed on ice, washed three times with ice-cold PBS containing 1% BSA and one time with PBS. Cells were then scraped into PBS and collected by centrifugation at 390 ***g*** for 4 minutes at 4°C. Cell pellets were washed once with PBS and lysed in PBS containing 0.5% Triton X-100. Lysates were cleared by centrifugation at 10,000 ***g*** for 10 minutes at 4°C, and equal aliquots were removed for peroxidase assay, using the One-Step Turbo TMB enzyme-linked immunosorbent assay kit (Pierce Chemical). After addition of sulfuric acid stop solution, absorbance at 450 nm was measured and the enzyme activity was normalized to total protein, determined using a colorimetric assay (Bio-Rad).

EGFR internalization and degradation

Parallel cultures of control or Beclin KD cells were seeded at 200,000 cells per dish on laminin-coated cover slips in 60 mm dishes and grown for 48 hours. The cells were then washed with PBS and maintained in serum-free DMEM overnight to

allow the EGFR to accumulate on the cell surface. EGFR internalization was stimulated by incubating the cells with 200 ng/ml EGF (Upstate Biotechnology) in HBSS containing 20 mM HEPES and 0.2% BSA for 30 minutes or 70 minutes at room temperature. Immunofluorescence localization of the EGFR was performed using anti-EGFR monoclonal antibody (Upstate Biotechnology), as described earlier for other organelle markers. In a separate study, the cells were harvested in SDS sample buffer at 30 minutes or 70 minutes after stimulation with EGF, and aliquots containing equal amounts of total cell protein were subjected to SDS-PAGE and immunoblot analysis using antibodies that recognize total EGFR or phosphorylated EGFR (Tyr1068; Cell Signaling Technology). Total EGFR or ratios of phospho-EGFR to total EGFR were determined by scanning the blots with a Kodak 440CF Image Station.

Cell growth

For growth curves, cells were seeded in 60 mm dishes at 200,000 cells per dish. At daily intervals, cells were harvested from three parallel dishes and counted with a Coulter Z1 particle counter. For measurement of colony formation in soft agar, 1500 cells were suspended in DMEM containing 10% FBS, 1 μg/ml puromycin and 0.3% w/v SeaPlaque agar (FMC Bioproducts) and layered over the same medium with 0.6% agar in three parallel dishes. On the 14th day after plating, colonies were stained by incubation with 5 mg/ml 3-[4,5-dimethylthiazol-2-yl]-2,5-diphenyltetrazolium bromide at 37°C for 25 minutes. Colonies were counted manually after obtaining digital images of the plates with an EPSON expression 800 scanner. Visual inspection of the colonies formed in plates containing control or Beclin KD cells did not reveal any obvious differences in their size or morphology.

We thank Jane Ding for technical assistance and Tamotsu Yoshimori for providing the antibody against LC3. This work was supported by a US Department of Defense Breast Cancer Research Program Grant, W81XWH-04-1-0493 to W.A.M.

References

Aita, V. M., Liang, X. H., Murty, V. V., Pincus, D. L., Yu, W., Cayanis, E., Kalachikov, S., Gilliam, T. C. and Levine, B. (1999). Cloning and genomic organization of beclin 1, a candidate tumor suppressor gene on chromosome 17q21. *Genomics* **59**, 59-65.

Aki, T., Yamaguchi, K., Fujimiya, T. and Mizukami, Y. (2003). Phosphoinositide 3-kinase accelerates autophagic cell death during glucose deprivation in the rat cardiomyocyte-derived cell line H9c2. *Oncogene* **22**, 8529-8535.

Boya, P., Gonzalez-Polo, R. A., Casares, N., Perfettini, J. L., Dessen, P., Larochette, N., Metivier, D., Meley, D., Souquere, S., Yoshimori, T. et al. (2005). Inhibition of macroautophagy triggers apoptosis. *Mol. Cell. Biol.* **25**, 1025-1040.

Brown, W. J., DeWald, D. B., Emr, S. D., Plutner, H. and Balch, W. E. (1995). Role for phosphatidylinositol 3-kinase in the sorting and transport of newly synthesized lysosomal enzymes in mammalian cells. *J. Cell Biol.* **130**, 781-796.

Brummelkamp, T. R., Bernards, R. and Agami, R. (2002). A system for stable expression of short interfering RNAs in mammalian cells. *Science* **296**, 550-553.

Bursch, W., Ellinger, E., Kienzl, H., Torok, L., Pandey, S., Sikorska, M., Walker, R. and Hermann, R. S. (1996). Active cell death induced by the anti-estrogens tamoxifen and ICI 164 384 in human mammary carcioma cells (MCF-7) in culture: the role of autophagy. *Carcinogenesis* **17**, 1595-1607.

Cheever, M. L., Sato, T. K., de Beer, T., Kutateladze, T. G., Emr, S. D. and Overduin, M. (2001). Phox domain interaction with PtdIns(3)P targets the Vam7 t-SNARE to vacuole membranes. *Nat. Cell Biol.* **3**, 613-618.

Corvera, S. (2001). Phosphatidylinositol 3-Kinase and the control of endosome dynamics: New players defined by structural motifs. *Traffic* **2**, 859-866.

Corvera, S., D'Arrigo, A. and Stenmark, H. (1999). Phosphoinositides in membrane traffic. *Curr. Opin. Cell Biol.* **11**, 460-465.

Davidson, H. W. (1995). Wortmannin causes mistargeting of procathepsin D. evidence for the involvement of a phosphatidylinositol 3-kinase in vesicular transport to lysosomes. *J. Cell Biol.* **130**, 797-805.

De Renzis, S., Sonnichsen, B. and Zerial, M. (2002). Divalent Rab effectors regulate the sub-compartmental organization and sorting of early endosomes. *Nat. Cell Biol.* **4**, 124-133.

Delbruck, R., Desel, C., von Figura, K. and Hille-Rehfeld, A. (1994). Proteolytic processing of cathepsin D in prelysosomal organelles. *Eur. J. Cell Biol.* **64**, 7-14.

Deneka, M. and van Der, S. P. (2002). 'Rab'ing up endosomal membrane transport. *Nat. Cell Biol.* **4**, E33-E35.

Dunn, W. A., Jr (1990a). Studies on the mechanisms of autophagy: Formation of the autophagic vacuole. *J. Cell Biol.* **110**, 1923-1933.

Dunn, W. A., Jr (1990b). Studies on the mechanisms of autophagy: Maturation of the autophagic vacuole. *J. Cell Biol.* **110**, 1935-1945.

Dunn, W. A., Jr (1994). Autophagy and related mechanisms of lysosome-mediated protein degradation. *Trends Cell Biol.* **4**, 139-143.

Eskelinen, E. L., Prescott, A. R., Cooper, J., Brachmann, S. M., Wang, L., Tang, X., Backer, J. M. and Lucocq, J. M. (2002). Inhibition of autophagy in mitotic animal cells. *Traffic* **3**, 878-893.

Fernandez-Borja, M., Wubbolts, R., Calafat, J., Janssen, H., Divecha, N., Dusseljee, S. and Neefjes, J. (1999). Multivesicular body morphogenesis requires phosphatidylinositol 3-kinase activity. *Curr. Biol.* **9**, 55-58.

Fruman, D. A., Rameh, L. E. and Cantley, L. C. (1999). Phosphoinositide binding domains: embracing 3-phosphate. *Cell* **97**, 817-820.

Furuya, N., Yu, J., Byfield, M., Pattingre, S. and Levine, B. (2005). The evolutionarily conserved domain of Beclin 1 is required for Vps34 binding, autophagy and tumor suppression. *Autophagy* **1**, 46-52.

Futter, C. E., Collinson, L. M., Backer, J. M. and Hopkins, C. R. (2001). Human VPS34 is required for internal vesicle formation within multivesicular endosomes. *J. Cell Biol.* **155**, 1251-1264.

Gordon, P. and Seglen, P. O. (1988). Prelysosomal convergence of autophagic and endocytic pathways. *Biochem. Biophys. Res. Commun.* **151**, 40-47.

Ikonomov, O. C., Sbrissa, D., Foti, M., Carpentier, J. L. and Shisheva, A. (2003). PIKfyve controls fluid phase endocytosis but not recycling/degradation of endocytosed receptors or sorting of procathepsin D by regulating multivesicular body morphogenesis. *Mol. Biol. Cell* **14**, 4581-4591.

Kabeya, Y., Mizushima, N., Ueno, T., Yamamoto, A., Kirisako, T., Noda, T., Kominami, E., Ohsumi, Y. and Yoshimori, T. (2000). LC3, a mammalian homologue of yeast apg8p, is localized in autophagosome membranes after processing. *EMBO J.* **19**, 5720-5728.

Kametaka, S., Okano, T., Ohsumi, M. and Ohsumi, Y. (1998). Apg14p and Apg6/Vps30p form a protein complex essential for autophagy in the yeast, Saccharomyces cerevisiae. *J. Biol. Chem.* **273**, 22284-22291.

Kanai, F., Liu, H., Field, S. J., Akbary, H., Matsuo, T., Brown, G. E., Cantley, L. C. and Yaffe, M. B. (2001). The PX domains of p47phox and p40phox bind to lipid products of PI(3)K. *Nat. Cell Biol.* **3**, 675-678.

Kanzawa, T., Kondo, Y., Ito, H., Kondo, S. and Germano, I. (2003). Induction of autophagic cell death in malignant glioma cells by arsenic trioxide. *Cancer Res.* **63**, 2103-2108.

Kanzawa, T., Germano, I. M., Komata, T., Ito, H., Kondo, Y. and Kondo, S. (2004). Role of autophagy in temozolomide-induced cytotoxicity for malignant glioma cells. *Cell Death Differ.* **11**, 448-457.

Katzmann, D. J., Odorizzi, G. and Emr, S. D. (2002). Receptor downregulation and multivesicular-body sorting. *Nat. Rev. Mol. Cell. Biol.* **3**, 893-905.

Kegel, K. B., Kim, M., Sapp, E., McIntyre, C., Castano, J. G., Aronin, N. and DiFiglia, M. (2000). Huntingtin expression stimulates endosomal-lysosomal activity, endosome tubulation, and autophagy. *J. Neurosci.* **20**, 7268-7278.

Kihara, A., Kabeya, Y., Ohsumi, Y. and Yoshimori, T. (2001a). Beclin-phosphatidylinositol 3-kinase complex functions at the trans- Golgi network. *EMBO Rep.* **2**, 330-335.

Kihara, A., Noda, T., Ishihara, N. and Ohsumi, Y. (2001b). Two Distinct Vps34 Phosphatidylinositol 3-kinase complexes function in autophagy and carboxypeptidase Y sorting in Saccharomyces cerevisiae. *J. Cell Biol.* **152**, 519-530.

Kirkegaard, K., Taylor, M. P. and Jackson, W. T. (2004). Cellular autophagy: surrender, avoidance and subversion by microorganisms. *Nat. Rev. Microbiol.* **2**, 301-314.

Klionsky, D. J. (2005). The molecular machinery of autophagy: unanswered questions. *J. Cell Sci.* **118**, 7-18.

Klionsky, D. J. and Emr, S. D. (2000). Autophagy as a regulated pathway of cellular degradation. *Science* **290**, 1717-1721.

Klionsky, D. J., Herman, P. K. and Emr, S. D. (1990). The fungal vacuole: composition, function, and biogenesis. *Microbiol. Rev.* **54**, 266-292.

Komata, T., Kanzawa, T., Nashimoto, T., Aoki, H., Endo, S., Nameta, M., Takahashi, H., Yamamoto, T., Kondo, S. and Tanaka, R. (2004). Mild heat shock induces autophagic growth arrest, but not apoptosis in U251-MG and U87-MG human malignant glioma cells. *J. Neurooncol.* **68**, 101-111.

Kopitz, J., Kisen, G. O., Gordon, P. B., Bohley, P. and Seglen, P. O. (1990). Nonselective autophagy of cytosolic enzymes by isolated rat hepatocytes. *J. Cell Biol.* **111**, 941-953.

Larsen, K. E. and Sulzer, D. (2002). Autophagy in neurons: a review. *Histol. Histopathol.* **17**, 897-908.

Lawrence, B. and Brown, W. (1992). Autophagic vacuoles rapidly fuse with pre-existing lysosomes in cultured hepatocytes. *J. Cell Sci.* **102**, 515-526.

Levine, B. and Klionsky, D. J. (2004). Development by self-digestion: molecular mechanisms and biological functions of autophagy. *Dev. Cell* **6**, 463-477.

Liang, X. H., Kleeman, L. K., Jiang, H. H., Gordon, G., Goldman, J. E., Berry, G., Herman, B. and Levine, B. (1998). Protection against fatal Sindbis virus encephalitis by beclin, a novel Bcl-2-interacting protein. *J. Virol.* **72**, 8586-8596.

Liang, X. H., Jackson, S., Seaman, M., Brown, K., Kempkes, B., Hibshoosh, H. and Levine, B. (1999). Induction of autophagy and inhibition of tumorigenesis by beclin 1. *Nature* **402**, 672-676.

Lockshin, R. A. and Zakeri, Z. (2004). Apoptosis, autophagy, and more. *Int. J. Biochem. Cell Biol.* **36**, 2405-2419.

Marino, G. and Lopez-Otin, C. (2004). Autophagy: molecular mechanisms, physiological functions and relevance in human pathology. *Cell Mol. Life Sci.* **61**, 1439-1454.

Melendez, A., Talloczy, Z., Seaman, M., Eskelinen, E. L., Hall, D. H. and Levine, B. (2003). Autophagy genes are essential for dauer development and life-span extension in C. elegans. *Science* **301**, 1387-1391.

Mizushima, N. (2004). Methods for monitoring autophagy. *Int. J. Biochem. Cell Biol.* **36**, 2491-2502.

Mizushima, N., Yamamoto, A., Hatano, M., Kobayashi, Y., Kabeya, Y., Suzuki, K., Tokuhisa, T., Ohsumi, Y. and Yoshimori, T. (2001). Dissection of autophagosome formation using Apg5-deficient mouse embryonic stem cells. *J. Cell Biol.* **152**, 657-668.

Munafo, D. B. and Colombo, M. I. (2002). Induction of autophagy causes dramatic changes in the subcellular distribution of GFP-Rab24. *Traffic* **3**, 472-482.
Murray, J. T., Panaretou, C., Stenmark, H., Miaczynska, M. and Backer, J. M. (2002). Role of Rab5 in the recruitment of hVps34/p150 to the early endosome. *Traffic* **3**, 416-427.
Ory, D. S., Neugeboren, B. A. and Mulligan, R. C. (1996). A stable human-derived packaging cell line for production of high titer retrovirus/vesicular stomatitis virus G pseudotypes. *Proc. Natl. Acad. Sci. USA* **93**, 11400-11406.
Paglin, S., Hollister, T., Delohery, T., Hackett, N., McMahill, M., Sphicas, E., Domingo, D. and Yahalom, J. (2001). A novel response of cancer cells to radiation involves autophagy and formation of acidic vesicles. *Cancer Res.* **61**, 439-444.
Panaretou, C., Domin, J., Cockcroft, S. and Waterfield, M. D. (1997). Characterization of p150, an adaptor protein for the human phosphatidylinositol (PtdIns) 3-kinase. Substrate presentation by phosphatidylinositol transfer protein to the p150.Ptdins 3-kinase complex. *J. Biol. Chem.* **272**, 2477-2485.
Pattingre, S., Tassa, A., Qu, X., Garuti, R., Liang, X. H., Mizushima, N., Packer, M., Schneider, M. D. and Levine, B. (2005). Bcl-2 antiapoptotic proteins inhibit beclin1-dependent autophagy. *Cell* **122**, 927-939.
Petiot, A., Ogier-Denis, E., Blommaart, E. F., Meijer, A. J. and Codogno, P. (2000). Distinct classes of phosphatidylinositol 3-kinases are involved in signaling pathways that control macroautophagy in HT-29 cells. *J. Biol. Chem.* **275**, 992-998.
Petiot, A., Faure, J., Stenmark, H. and Gruenberg, J. (2003). PI(3)P signaling regulates receptor sorting but not transport in the endosomal pathway. *J. Cell Biol.* **162**, 971-979.
Qu, X., Yu, J., Bhagat, G., Furuya, N., Hibshoosh, H., Troxel, A., Rosen, J., Eskelinen, E. L., Mizushima, N., Ohsumi, Y. et al. (2003). Promotion of tumorigenesis by heterozygous disruption of the beclin 1 autophagy gene. *J. Clin. Invest.* **112**, 1809-1820.
Reaves, B. J., Bright, N. A., Mullock, B. M. and Luzio, J. P. (1996). The effect of wortmannin on the localisation of lysosomal type I integral membrane glycoproteins suggests a role for phosphoinositide 3-kinase activity in regulating membrane traffic late in the endocytic pathway. *J. Cell Sci.* **109**, 749-762.
Rijnboutt, S., Stoorvogel, W., Geuze, H. J. and Strous, G. J. (1992). Identification of subcellular compartments involved in biosynthetic processing of cathepsin D. *J. Biol. Chem.* **267**, 15665-15672.
Row, P. E., Reaves, B. J., Domin, J., Luzio, J. P. and Davidson, H. W. (2001). Overexpression of a rat kinase-deficient phosphoinositide 3-kinase, Vps34p, inhibits cathepsin D maturation. *Biochem. J.* **353**, 655-661.
Scarlatti, F., Bauvy, C., Ventruti, A., Sala, G., Cluzeaud, F., Vandewalle, A., Ghidoni, R. and Codogno, P. (2004). Ceramide-mediated macroautophagy involves inhibition of protein kinase B and upregulation of Beclin 1. *J. Biol. Chem.* **279**, 18384-18391.
Seaman, M. N., Marcusson, E. G., Cereghino, J. L. and Emr, S. D. (1997). Endosome to Golgi retrieval of the vacuolar protein sorting receptor, Vps10p, requires the function of the VPS29, VPS30, and VPS35 gene products. *J. Cell Biol.* **137**, 79-92.
Shimizu, S., Kanaseki, T., Mizushima, N., Mizuta, T., Arakawa-Kobayashi, S., Thompson, C. B. and Tsujimoto, Y. (2004). Role of Bcl-2 family proteins in a non-apoptotic programmed cell death dependent on autophagy genes. *Nat. Cell Biol.* **6**, 1221-1228.
Siddhanta, U., McIlroy, J., Shah, A., Zhang, Y. and Backer, J. M. (1998). Distinct roles for the p110alpha and hVPS34 phosphatidylinositol 3′-kinases in vesicular trafficking, regulation of the actin cytoskeleton, and mitogenesis. *J. Cell Biol.* **143**, 1647-1659.
Simonsen, A., Lippe, R., Christoforidis, S., Gaullier, J. M., Brech, A., Callaghan, J., Toh, B. H., Murphy, C., Zerial, M. and Stenmark, H. (1998). EEA1 links PI(3)K function to Rab5 regulation of endosome fusion. *Nature* **394**, 494-498.
Simonsen, A., Wurmser, A. E., Emr, S. D. and Stenmark, H. (2001). The role of phosphoinositides in membrane transport. *Curr. Opin. Cell Biol.* **13**, 485-492.
Simonsen, A., Birkeland, H. C., Gillooly, D. J., Mizushima, N., Kuma, A., Yoshimori, T., Slagsvold, T., Brech, A. and Stenmark, H. (2004). Alfy, a novel FYVE-domain-containing protein associated with protein granules and autophagic membranes. *J. Cell Sci.* **117**, 4239-4251.
Song, X., Xu, W., Zhang, A., Huang, G., Liang, X., Virbasius, J. V., Czech, M. P. and Zhou, G. W. (2001). Phox homology domains specifically bind phosphatidylinositol phosphates. *Biochemistry* **40**, 8940-8944.
Stein, M. P., Feng, Y., Cooper, K. L., Welford, A. M. and Wandinger-Ness, A. (2003). Human VPS34 and p150 are Rab7 interacting partners. *Traffic* **4**, 754-771.
Stenmark, H., Aasland, R. and Driscoll, P. C. (2002). The phosphatidylinositol 3-phosphate-binding FYVE finger. *FEBS Lett.* **513**, 77-84.
Stromhaug, P. E., Berg, T. O., Fengsrud, M. and Seglen, P. O. (1998). Purification and characterization of autophagosomes from rat hepatocytes. *Biochem. J.* **335**, 217-224.
Sui, G., Soohoo, C., Affar, e. B., Gay, F., Shi, Y., Forrester, W. C. and Shi, Y. (2002). A DNA vector-based RNAi technology to suppress gene expression in mammalian cells. *Proc. Natl. Acad. Sci. USA* **99**, 5515-5520.
Takeuchi, H., Kondo, Y., Fujiwara, K., Kanzawa, T., Aoki, H., Mills, G. B. and Kondo, S. (2005). Synergistic augmentation of rapamycin-induced autophagy in malignant glioma cells by phosphatidylinositol 3-kinase/protein kinase B inhibitors. *Cancer Res.* **65**, 3336-3346.
Tanida, I., Tanida-Miyake, E., Komatsu, M., Ueno, T. and Kominami, E. (2002). Human Apg3p/Aut1p homologue is an authentic E2 enzyme for multiple substrates, GATE-16, GABARAP, and MAP-LC3, and facilitates the conjugation of hApg12p to hApg5p. *J. Biol. Chem.* **277**, 13739-13744.
Tanida, I., Ueno, T. and Kominami, E. (2004). LC3 conjugation system in mammalian autophagy. *Int. J. Biochem. Cell Biol.* **36**, 2503-2518.
Traganos, F. and Darzynkiewicz, Z. (1994). Lysosomal proton pump activity: supravital cell staining with acridine orange differentiates leukocyte subpopulations. *Methods Cell Biol.* **41**, 185-194.
Tuma, P. L., Nyasae, L. K., Backer, J. M. and Hubbard, A. L. (2001). Vps34p differentially regulates endocytosis from the apical and basolateral domains in polarized hepatic cells. *J. Cell Biol.* **154**, 1197-1208.
Vazquez, F. and Sellers, W. R. (2000). The PTEN tumor suppressor protein: an antagonist of phosphoinositide 3-kinase signaling. *Biochim. Biophys. Acta* **1470**, M21-M35.
Volinia, S., Dhand, R., Vanhaesebroeck, B., MacDougall, L. K., Stein, R., Zvelebil, M. J., Domin, J., Panaretou, C. and Waterfield, M. D. (1995). A human phosphatidylinositol 3-kinase complex related to the yeast Vps34p-Vps15p protein sorting system. *EMBO J.* **14**, 3339-3348.
Wilson, A. L., Erdman, R. A. and Maltese, W. A. (1996). Association of Rab1B with GDP-dissociation inhibitor (GDI) is required for recycling but not initial membrane targeting of the Rab protein. *J. Biol. Chem.* **271**, 10932-10940.
Wurmser, A. E., Gary, J. D. and Emr, S. D. (1999). Phosphoinositide 3-kinases and their FYVE domain-containing effectors as regulators of vacuolar/lysosomal membrane trafficking pathways. *J. Biol. Chem.* **274**, 9129-9132.
Xu, Y., Hortsman, H., Seet, L., Wong, S. H. and Hong, W. (2001). SNX3 regulates endosomal function through its PX-domain-mediated interaction with PtdIns(3)P. *Nat. Cell Biol.* **3**, 658-666.
Yoshimori, T. (2004). Autophagy: a regulated bulk degradation process inside cells. *Biochem. Biophys. Res. Commun.* **313**, 453-458.
Yu, L., Alva, A., Su, H., Dutt, P., Freundt, E., Welsh, S., Baehrecke, E. H. and Lenardo, M. J. (2004). Regulation of an ATG7-beclin 1 program of autophagic cell death by caspase-8. *Science* **304**, 1500-1502.
Yue, Z., Jin, S., Yang, C., Levine, A. J. and Heintz, N. (2003). Beclin 1, an autophagy gene essential for early embryonic development, is a haploinsufficient tumor suppressor. *Proc. Nat. Acad. Sci. USA* **100**, 15077-15082.
Zakeri, Z., Bursch, W., Tenniswood, M. and Lockshin, R. A. (1995). Cell death:programmed, apoptosis,necrosis or other? *Cell Death Differ.* **2**, 87-96.

Gene silencing reveals a specific function of hVps34 phosphatidylinositol 3-kinase in late versus early endosomes

Erin E. Johnson, Jean H. Overmeyer, William T. Gunning and William A. Maltese*

Department of Biochemistry and Cancer Biology, Medical University of Ohio, Toledo, OH 43614, USA

*Author for correspondence (e-mail: wmaltese@meduohio.edu)

Accepted 9 December 2005
Journal of Cell Science 119, 1219-1232 Published by The Company of Biologists 2006
doi:10.1242/jcs.02833

Summary

The human type III phosphatidylinositol 3-kinase, hVps34, converts phosphatidylinositol (PtdIns) to phosphatidylinositol 3-phosphate [PtdIns(3)*P*]. Studies using inhibitors of phosphatidylinositide 3-kinases have indicated that production of PtdIns(3)*P* is important for a variety of vesicle-mediated trafficking events, including endocytosis, sorting of receptors in multivesicular endosomes, and transport of lysosomal enzymes from the trans-Golgi network (TGN) to the endosomes and lysosomes. This study utilizes small interfering (si)RNA-mediated gene silencing to define the specific trafficking pathways in which hVps34 functions in human U-251 glioblastoma cells. Suppression of hVps34 expression reduced the cellular growth rate and caused a striking accumulation of large acidic phase-lucent vacuoles that contain lysosomal membrane proteins LAMP1 and LGP85. Analysis of these structures by electron microscopy suggests that they represent swollen late endosomes that have lost the capacity for inward vesiculation but retain the capacity to fuse with lysosomes. Morphological perturbation of the late endosome compartment was accompanied by a reduced rate of processing of the endosomal intermediate form of cathepsin D to the mature lysosomal form. There was also a reduction in the rate of epidermal growth factor receptor (EGFR) dephosphorylation and degradation following ligand stimulation, consistent with the retention of the EGFR on the limiting membranes of the enlarged late endosomes. By contrast, the suppression of hVps34 expression did not block trafficking of cathepsin D between the TGN and late endosomes, or endocytic uptake of fluid-phase markers, or association of a PtdIns(3)*P*-binding protein, EEA1, with early endosomes. LAMP1-positive vacuoles were depleted of PtdIns(3)*P* in the hVps34-knockdown cells, as judged by their inability to bind the PtdIns(3)*P* probe GFP-2xFYVE. By contrast, LAMP1-negative vesicles continued to bind GFP-2xFYVE in the knockdown cells.

Overall, these findings indicate that hVps34 plays a major role in generating PtdIns(3)*P* for internal vesicle formation in multivesicular/late endosomes. The findings also unexpectedly suggest that other wortmannin-sensitive kinases and/or polyphosphoinositide phosphatases may be able to compensate for the loss of hVps34 and maintain PtdIns(3)*P* levels required for vesicular trafficking in the early endocytic pathway or the TGN.

Key words: Endosome, Vps34, Phosphatidylinositol 3-kinase, Trafficking, Golgi, Lysosome

Introduction

Mammalian cells contain three distinct types of phosphoinositide 3-OH kinase (PI 3-kinase) (Fruman et al., 1998; Vanhaesebroeck et al., 2001). Type III PI 3-kinase catalyzes the phosphorylation of phosphatidylinositol at the D-3 position of the inositol ring, generating phosphatidylinositol 3-phosphate [PtdIns(3)*P*] (Odorizzi et al., 2000). The prototype for this type of enzyme, Vps34, was first identified in *Saccharomyces cerevisiae*, where it is one of several gene products required for delivery of soluble proteins to the vacuole (Schu et al., 1993; Herman et al., 1992) and for autophagic sequestration of cytoplasmic proteins during starvation (Kihara et al., 2001b; Wurmser and Emr, 2002). Under both circumstances, association of Vps34 with cellular membranes depends on a myristoylated regulatory subunit, Vps15 (Kihara et al., 2001b; Stack et al., 1995). In mammalian cells, Vps34 interacts with p150, a regulatory subunit similar to Vps15 (Panaretou et al., 1997).

PtdIns(3)*P* is required for membrane recruitment of several proteins implicated in the regulation of vesicular transport and intracellular protein sorting (Corvera, 2001; Simonsen et al., 2001). Some of these proteins (e.g. sorting nexins) contain a PX phosphoinositide-binding domain (Song et al., 2001; Cheever et al., 2001; Kanai et al., 2001; Xu et al., 2001), whereas others contain a structural motif termed the FYVE domain that binds to PtdIns(3)*P* with high affinity (Corvera et al., 1999; Fruman et al., 1999; Wurmser et al., 1999). Specific FYVE-domain proteins [early endosomal antigen 1 (EEA1), Rabenosyn-5, Rabip4] interact with Rab GTPases that control vesicle docking and fusion in the early endocytic pathway (Nielsen et al., 2000; Simonsen et al., 1998; Cormont et al., 2001; Kauppi et al., 2002). Interestingly, some Rabs that function in the early (Rab5) and late (Rab7) steps of the endocytic pathway also interact with the p150 subunit of the mammalian Vps34 complex, suggesting that the synthesis of PtdIns(3)*P* and the recruitment of FYVE-domain proteins

might be coordinately regulated (Murray et al., 2002; Stein et al., 2003).

Early evidence that PI 3-kinase activity is important for protein trafficking in mammalian cells came from studies in which inhibitors of PI 3-kinase (wortmannin and LY294002) were found to impair targeting of procathepsin D from the trans-Golgi network (TGN) to the lysosomal compartment (Davidson, 1995; Brown et al., 1995). Subsequent work using a kinase-deficient dominant-negative form of mammalian Vps34 suggested that the block in cathepsin D maturation was indeed related to a requirement for the type III PI 3-kinase (Row et al., 2001). Separate lines of evidence have suggested that mammalian Vps34 might also be required for receptor sorting in the early endocytic pathway. For example, Siddhanta et al. reported that microinjection of an inhibitory antibody against Vps34 interfered with ligand-stimulated translocation of the platelet-derived growth factor (PDGF) receptor between peripheral early endosomes and perinuclear late endosomal compartments (Siddhanta et al., 1998). Further investigations using inhibitory antibodies or wortmannin have suggested that Vps34 might play an essential role in the formation of internal vesicles within multivesicular endosomes (MVEs) (Futter et al., 2001), which are a key sorting compartment between early endosomes and lysosomes (reviewed by Gruenberg and Maxfield, 1995). Finally, in accord with studies in yeast, the mammalian Vps34 appears to play an important role in the process of macroautophagy in human cells subjected to nutrient deprivation (Petiot et al., 2000).

Although the aforementioned experimental approaches have provided important insights into the functions of Vps34 in mammalian cells, each has particular limitations. For example, wortmannin can simultaneously inhibit multiple types of PI 3-kinase (Vanhaesebroeck et al., 2001) and at least one type of phosphatidylinositol 4-kinase (Meyers and Cantley, 1997), making it difficult to attribute physiological effects to a specific enzyme. Likewise, overexpression of interfering Vps34 mutants may tie up key effectors or docking proteins that normally interact with more than one distinct kinase. Finally, antibody microinjection studies, although precise, can be applied only to small populations of cells, precluding most biochemical analyses of protein trafficking pathways. In recent years, the rapid development of methods for stable gene silencing by RNA interference (RNAi) has provided a powerful new option for defining the functions of specific proteins in mammalian cells (Sui et al., 2002; Paul et al., 2002; Brummelkamp et al., 2002).

In the present study, we have applied siRNA technology to pinpoint the function of human Vps34 (hVps34) in cultured U-251 glioblastoma cells. Suppression of hVps34 caused extreme swelling of late endosomes, consistent with defective membrane internalization into MVEs without concomitant reduction of incoming membrane traffic from the TGN and early endosomes. However, in contrast to some earlier findings based on PI 3-kinase inhibitors, specific silencing of hVps34 expression did not impair: (1) the exit of procathepsin D from the TGN; (2) the endocytic internalization of cell-surface receptors and fluid-phase markers; or (3) the association of a FYVE-domain protein (EEA1) with early endosomes. These studies indicate that the role of hVps34 in producing PtdIns(3)*P* for membrane trafficking is limited mainly to the multivesicular late endosome compartments, and that other mechanisms might exist to produce PtdIns(3)*P* required for vesicular trafficking in the early endosomes and TGN.

Results

Reduction of hVps34 expression by siRNA-mediated gene silencing causes accumulation of cytoplasmic vacuoles

To obtain a cell population in which expression of hVps34 was specifically and uniformly suppressed, we utilized a replication-deficient retroviral vector that drives the expression of RNAi sequences and confers puromycin resistance on infected cells (Brummelkamp et al., 2002). Vectors were engineered to contain either a sequence matching a unique

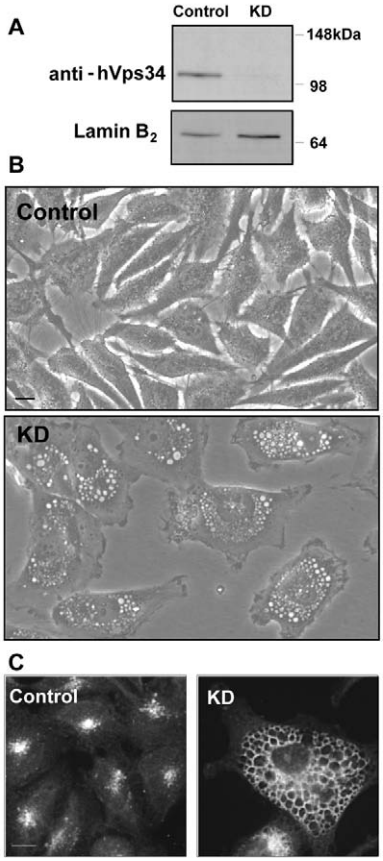

Fig. 1. siRNA-mediated suppression of hVps34 expression in U-251 glioma cells induces accumulation of LAMP1-positive cytoplasmic vacuoles. (A) U-251 cells infected with retrovirus carrying the control or hVps34 KD siRNA sequences surviving after 5 days of puromycin selection were subjected to immunoblot analysis with a polyclonal anti-hVps34 IgG as described in the Materials and Methods. Nuclear lamin B_2 served as one of several controls for nonspecific effects of the siRNA. (B) Phase contrast images of the live control and hVps34 KD cells. Bar, 10 μm. Based on counting 100 cells in multiple phase micrographs, 73% of the hVps34 KD cells exhibited the vacuolar phenotype, defined as multiple small-sized to intermediate-sized vacuoles (0.5-1.0 μ), with at least two vacuoles per cell exceeding a diameter of 2 μ. (C) Control and hVps34 KD cells were seeded at 100,000 cells/dish in 35 mm dishes. 24 hours later, cells were examined by immunofluorescence microscopy using a primary antibody against the lysosomal and late endosomal membrane protein LAMP1. Bar, 10 μm.

region of the hVPS34 mRNA, or a 'control' sequence that did not match any known GenBank entry. In preliminary tests with several cell lines infected with a green fluorescent protein (GFP) reporter construct, the human U-251 glioblastoma line showed high initial infection efficiency with the retroviral vector. Therefore, we chose to use this cell line for studies of hVps34. As illustrated by the immunoblots in Fig. 1A, expression of hVps34 was almost undetectable in puromycin-resistant cells that received the hVps34-'knockdown' vector (hVps34 KD cells), compared with cells that were infected with the control vector. In all of the experiments described in this paper, similar immunoblot results were obtained, verifying that expression of hVps34 was decreased by at least 90% relative to the parallel control cultures. Expression levels of unrelated proteins such as lamin B_2 (Fig. 1A), calreticulin and lactate dehydrogenase (LDH) (not shown) were comparable in the control and KD cells. The latter findings indicate that the loss of hVps34 expression was not due to a general effect of the siRNA on protein synthesis.

Examination of the cultures by phase contrast microscopy revealed striking morphological differences between the hVps34 KD cells and the matched controls (Fig. 1B). Specifically, more than 70% of the KD cells were filled with numerous phase-lucent spherical cytoplasmic vacuoles ranging 0.5-4.0 μ in diameter. To begin to assess the origin of the vacuoles in the hVps34 KD cells, we performed indirect immunofluorescence microscopy using an antibody against LAMP1, a glycoprotein localized in membranes surrounding lysosomes and late endosomes (Gough et al., 1999). As shown in Fig. 1C, the limiting membranes of the vacuoles in the KD cells were clearly outlined by antibodies against LAMP1.

To rule out the possibility that the striking accumulation of LAMP1-positive vacuoles induced by the siRNA targeted against hVps34 might be a result of off-target effects, we performed a similar study using a second retroviral construct containing an RNAi sequence matching a different non-overlapping portion of the hVPS34 mRNA. This construct, designated KD2, was similar to the original KD construct in being able to reduce the expression of hVps34 (Fig. 2A). Moreover, the phenotype of the cells expressing KD2 was similar to that described with the original KD construct, with accumulation of large LAMP1-positive vacuoles as a predominant feature (Fig. 2B). Therefore, for the remainder of the studies described in this report, we used the original KD construct with the understanding that its morphological and physiological effects were attributable to selective knockdown of hVps34 expression.

Electron microscopy revealed that the vacuoles in the hVps34 KD cells were generally electron lucent (Fig. 3A). Some contained sparsely distributed electron-dense material along with a few internal vesicles or membrane whorls (Fig. 3B). The vacuoles were always circumscribed by a single membrane, indicating that they did not represent enlarged autophagosomes (Fig. 3B).

Vacuoles in hVps34 KD cells are derived from late endosomes

Previous reports have suggested that hVps34 is associated with Golgi membranes (Kihara et al., 2001a) and endosomes (Murray et al., 2002) in mammalian cells. The immunofluorescent localization of LAMP1 to the vacuole membranes (Figs 1 and 2) is most consistent with a late endosomal origin for these structures. To explore this possibility further, we performed indirect immunofluorescence microscopy using several additional antibodies against proteins localized in specific organelles (Fig. 4). The limiting membranes of the vacuoles were clearly outlined by an antibody against another lysosomal/late endosomal membrane glycoprotein, LGP85 (Kuronita et al., 2002). An antibody

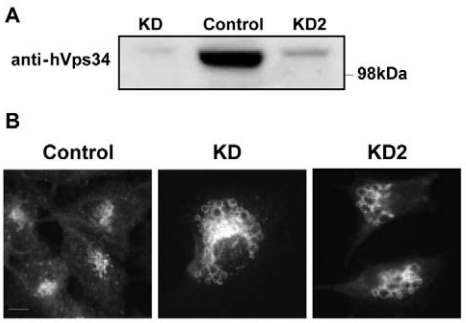

Fig. 2. Accumulation of LAMP1-positive vacuoles is specific to suppression of hVps34 expression. (A) U-251 cells infected with retrovirus harboring the control or two different hVps34-specific RNAi sequences (KD and KD2) were subjected to immunoblot analysis as described previously. (B) Control, hVps34 KD and hVps34 KD2 cells were seeded at 100,000 cells/dish in 35 mm dishes. 48 hours later, cells were examined by immunofluorescence microscopy using an antibody against LAMP1. Bar, 10 μm.

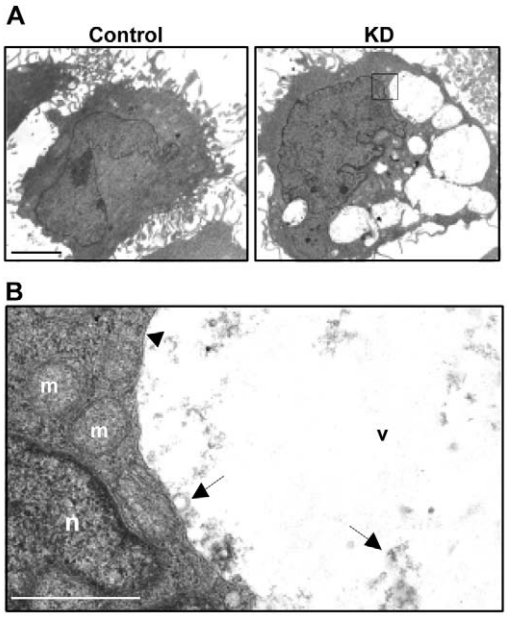

Fig. 3. Vacuoles in the hVps34 KD cells are membrane-bound structures with occasional internal vesicles and electron-dense material. Control and hVps34 KD cells were examined by electron microscopy. (A) Control and KD cells magnified 3,900×. Bar, 5 μm. (B) Highlighted region of KD cell from panel A at 21,000×. Bar, 1 μm. Labeled structures: m, mitochondria; n, nucleus; v, vacuole. The arrowhead points to a single membrane surrounding the vacuole. Arrows point to occasional small internal vesicles and electron-dense material.

against lysobisphosphatidic acid (LBPA), a phospholipid that is normally concentrated in the internal membranes of MVEs and late endosomes (Kobayashi et al., 1998), did not stain the interior of the vacuoles and reacted with the peripheral membranes with less uniformity than the LAMP1 and LGP85 antibodies. In the control cells, LAMP1, LGP85 and LBPA were all localized to clusters of punctuate structures adjacent to the nucleus, typical of the late endosome and/or lysosome distribution of these markers seen in many types of cells.

Immunofluorescent staining for proteins associated with membranes of the Golgi apparatus or endoplasmic reticulum suggested that the vacuoles did not arise directly from these compartments in the hVps34 KD cells (Fig. 4). The Golgi marker GM130 exhibited a compact juxtanuclear distribution typical of Golgi localization. The cation-independent mannose-6-phosphate receptor (M6PR) did not accumulate in the limiting membranes of the vacuoles. Instead, M6PR was detected mainly in a compact region adjacent to the nucleus, similar to the GM130 Golgi marker. The M6PR is involved in the delivery of newly synthesized lysosomal hydrolases from the TGN to MVEs (Le Borgne and Hoflack, 1998; Ghosh et al., 2003; Press et al., 1998). The distribution of M6PR in the control and hVps34 KD cells is consistent with previous reports indicating that, at steady state, most of the M6PR is localized in the TGN (Hirst et al., 1998; Kobayashi et al., 1998). Calreticulin exhibited a diffuse web-like pattern that appeared to be concentrated in regions of the cytoplasmic compartment displaced by the vacuoles. Although this gives the appearance that the vacuoles are surrounded by calreticulin, we do not believe that calreticulin is actually in the limiting

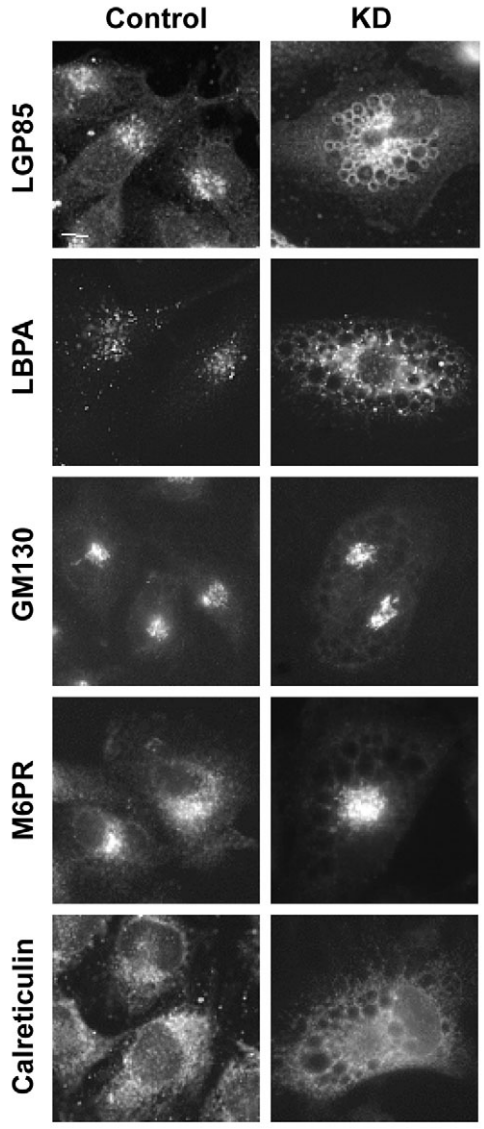

Fig. 4. Vacuoles in the hVps34 KD cells exhibit characteristics of late endosomes or lysosomes. Control and hVps34 KD cells were seeded at 100,000 cells/dish in 35 mm dishes. 24 hours later, cells were examined by immunofluorescence microscopy using the primary antibodies indicated at the left of the figure. Bar, 10 μm.

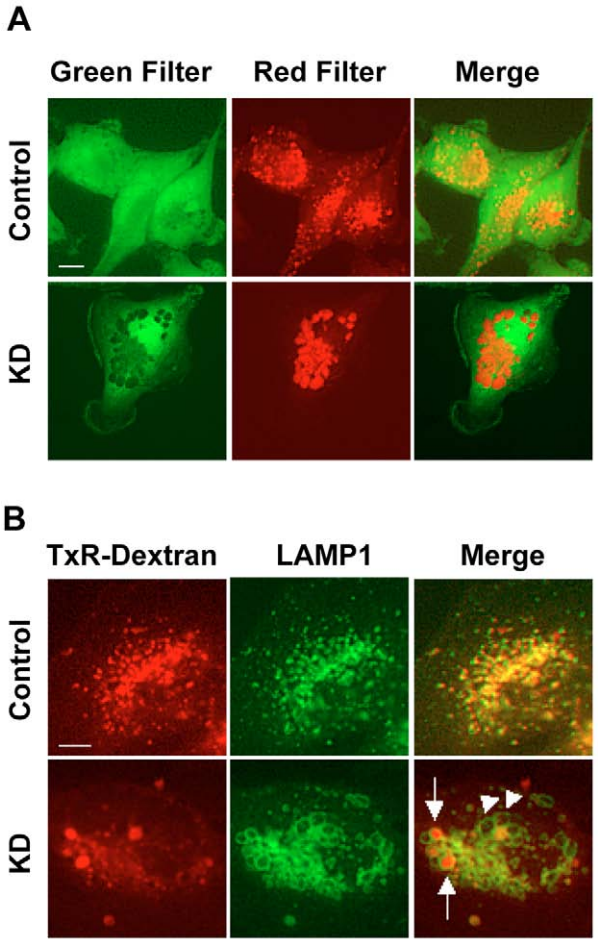

Fig. 5. Vacuoles in the hVps34 KD cells are acidic and receive traffic from the endocytic compartment. (A) Control and hVps34 KD cells were incubated with 2.5 μg/ml Acridine Orange (AO) for 30 minutes. The cells were then examined by fluorescence microscopy using green (excitation wavelength: 465-495 nm; emission wavelength: 515-555 nm) and red (excitation wavelength: 528-553 nm; emission wavelength 600-660 nm) filters. Red fluorescence emanates from AO in acidic compartments. Bar, 10 μm. (B) Control and KD cells were incubated with 500 μg/ml Texas Red (TxR)-dextran for 16 hours. Following incubation for 2 hours, cells were fixed and co-stained with a monoclonal antibody against LAMP1. Arrows indicate vacuoles containing both LAMP1 and TxR-dextran. Arrowheads point to vacuoles lacking TxR-dextran. Bar, 10 μm.

membrane, based on a comparison with the more obvious membrane staining of LAMP1 and LGP85. Nevertheless, at the level of resolution afforded by light microscopy, we cannot definitively rule out some association of calreticulin with the vacuoles.

To characterize the cytoplasmic vacuoles further, we performed supravital staining of the cells with the lysosomotropic agent Acridine Orange (AO) (Fig. 5A). The non-protonated monomeric form of AO emits green fluorescence in the cytoplasm. However, when the dye enters an acidic compartment (e.g. lysosomes or late endosomes), the protonated form becomes trapped in aggregates that fluoresce bright red or orange (Traganos and Darzynkiewicz, 1994; Paglin et al., 2001; Kanzawa et al., 2003). The images in Fig. 5A demonstrate that the numerous vacuoles observed in the hVps34 KD cells are acidic vesicular organelles that sequester AO.

On the basis of the presence of lysosomal membrane markers and their ability to sequester AO, we hypothesized that the vacuoles in the hVps34 KD cells were derived from late endosomes or lysosomes. To test this hypothesis further, we labeled the endosomal system by adding a fluid phase tracer, Texas Red (TxR)-dextran, to the culture medium for 16 hours (Fig. 5B). The distribution of TxR-dextran was compared with that of LAMP1. In the control cells, the TxR-dextran was concentrated in a cluster of small vesicles adjacent to the nucleus. Consistent with the expected uptake of TxR-dextran into endosomes and lysosomes, the tracer showed extensive colocalization with LAMP1-positive compartments (Fig. 5B). Examination of the hVps34 KD cells revealed that the fluid phase tracer was incorporated into some of the large LAMP1-positive cytoplasmic vacuoles (arrows) as well as numerous smaller vesicular structures (Fig. 5B). However, the persistence of some LAMP1-positive vacuoles that did not incorporate TxR-dextran after prolonged incubation (arrowheads) suggests that a subpopulation of these structures might be functionally disengaged from the fluid-phase endocytic pathway.

Suppression of hVps34 expression does not disrupt the PtdIns(3)*P*-dependent localization of the early endosome protein EEA1

To assess the morphology of the early endosomes, we examined the subcellular distribution of EEA1, a FYVE-domain protein that is known to be recruited to the early endosome membrane in a PtdIns(3)*P*- and Rab5-dependent manner (Christoforidis et al., 1999; Simonsen et al., 1998). There was no clear association of EEA1 with the membranes of the numerous large vacuoles in the hVps34 KD cells (Fig. 6A). Instead, the protein was detected predominantly in a population of smaller vesicles with a pattern similar to the control cells. We occasionally observed ring-like structures that could represent swollen early endosomes in the KD cells. However, these structures were not numerous and were distinct from the much larger phase-lucent vacuoles. In contrast to the bright punctate fluorescence pattern of EEA1 in the control and hVps34 KD cells, control cells treated with 1 μM wortmannin showed only a diffuse reticular staining pattern. The loss of punctate EEA1 distribution is consistent with the release of EEA1 from endosomal membranes reported to occur in other cell lines treated with PI 3-kinase inhibitors (Simonsen et al., 1998; Petiot et al., 2003). At 1 μM, wortmannin generally

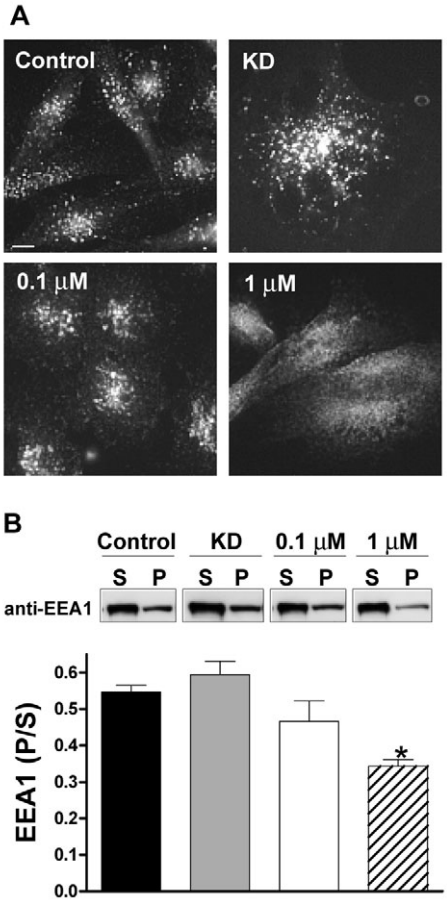

Fig. 6. Suppression of hVps34 expression does not prevent membrane association of the early endosome marker EEA1. (A) Control and hVps34 KD cells were seeded at 100,000 cells/dish in 35 mm dishes. 24 hours later, cells were examined by immunofluorescence microscopy using an anti-EEA1 antibody. Control cells treated with 0.1 μM or 1 μM wortmannin for 1 hour are also shown. (B) Cytosol (S) and particulate (P) fractions were prepared from control cells, hVps34 KD cells, or control cells treated for 1 hour with the indicated concentrations of wortmannin (0.1 μM or 1 μM), as described in the Materials and Methods. Immunoblot analysis was performed with an antibody against EEA1 and the relative amount of EEA1 recovered in the P fraction is expressed as a ratio to the amount in the S fraction. The results are means (±s.e.m.) of three determinations performed on separate cultures. The asterisk indicates that the decrease relative to the control and KD cells was significant at $P< 0.05$ (Student's *t* test). Essentially the same results were obtained when the amount of EEA1 recovered in the P fraction was normalized to the amount of a membrane marker (calreticulin) recovered in the same fraction (not shown).

inhibits all types of PI 3-kinase (Vanhaesebroeck et al., 2001). Interestingly, a lower concentration of wortmannin (0.1 μM), which is reported to inhibit type I and type III PI 3-kinases but not the type II PI 3-kinase isoform C2α (Virbasius et al., 1996; Prior and Clague, 1999), did not disrupt EEA1 localization in the U-251 cells (Fig. 6A).

To examine the subcellular distribution of EEA1 further, control and hVps34 KD cells were fractionated into cytosolic and particulate components, and the partitioning of EEA1 between these components was determined by immunoblot

analysis (Fig. 6B). The proportion of EEA1 in the particulate versus soluble fraction in the KD cells was not significantly different from the controls. When considered together with the immunofluorescence studies in Fig. 6A, these results indicate that EEA1 is able to associate with endosomal membranes in U-251 cells under conditions where expression of hVps34 is almost completely suppressed. Short-term treatment of the cells with 1 μM wortmannin resulted in a significant ($P<0.05$) decline in the proportion of EEA1 in the particulate fraction compared with either the control or KD cells (Fig. 6B). This decrease paralleled the elimination of punctate EEA1 fluorescence in Fig. 6A, suggesting that it corresponds to the loss of EEA1 from endosomal membranes. By contrast, 0.1 μM wortmannin produced only a slight and statistically insignificant decline in the ratio of particulate to soluble EEA1 (Fig. 6B), in accord with the persistence of punctate EEA1 staining at the lower wortmannin concentration (Fig. 6A). The latter observation suggests that the lack of an effect of hVps34 knockdown on EEA1 membrane localization could be related in part to a type II PI 3-kinase contributing to the maintenance of the PtdIns(3)*P* pool in the early endosomes.

LAMP1-positive vacuoles are depleted of PtdIns(3)*P*, as measured by a GFP-2xFYVE probe

The preceding observations predict that LAMP1-positive late endosome compartments are depleted of PtdIns(3)*P* in the hVps34 KD cells, whereas early endosome compartments are at least partially spared. To test this hypothesis, we transfected control and hVps34 KD cells with a vector that expresses a GFP-2xFYVE probe previously shown to bind specifically to PtdIns(3)*P* in cellular membranes (Gillooly et al., 2003; Gillooly et al., 2000; Petiot et al., 2003). GFP-2xFYVE was localized in numerous cytoplasmic vesicles in the control cells (Fig. 7, upper panels). Some of these were positive for LAMP1, whereas others were not, consistent with the presence of PtdIns(3)*P* in both early and late endosomes. Most of the vesicles labeled with GFP-2xFYVE in the control cells (Fig. 7) appeared swollen when compared with normal endosomes (e.g. Fig. 6A control). This was expected, given earlier reports

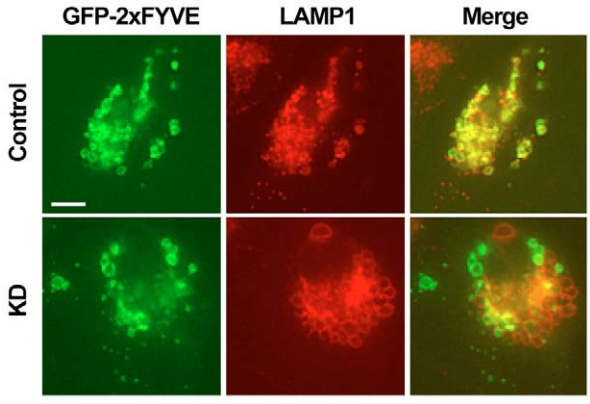

Fig. 7. LAMP1-positive vacuoles formed in hVps34 KD cells are depleted of PtdIns(3)*P*, as measured by localization of a GFP-2xFYVE probe. Control or hVps34 KD cells were transfected with a vector encoding GFP-2xFYVE. After 16 hours, the cells were processed for immunofluorescence, using primary antibodies against GFP and LAMP1. Bar, 10 μm.

that overexpression of 2xFYVE probes can disrupt early endosome fusion (Gillooly et al., 2000) and sorting in MVEs (Petiot et al., 2003). The presence of PtdIns(3)*P* in LAMP1-positive compartments might seem surprising in light of the aforementioned evidence that PtdIns(3)*P* is localized predominantly in early endosomes. However, some studies have also shown that the GFP-2xFYVE probe localizes extensively on Rab7-positive late endosomes (Stein et al., 2003), which are typically positive for LAMP1 (Bucci et al., 2000). In contrast to the control cells, a very different picture emerged when the hVps34 KD cells were examined by the same technique (Fig. 7, lower panels). Here, the numerous large LAMP1-positive vesicles did not bind the GFP-2xFYVE probe, suggesting that they are indeed derived from late endosomes depleted of PtdIns(3)*P*. However, the hVps34 KD cells continued to exhibit GFP-2xFYVE labeling of a distinct population of LAMP1-negative vesicles (Fig. 7). We presume that these vesicles are early endosomes that are not completely depleted of PtdIns(3)*P*, although we are unable to confirm this directly by EEA1 localization because the 2xFYVE probe releases EEA1 from membranes (Petiot et al., 2003).

Endocytosis is not disrupted in hVps34 KD cells

The earlier observation that a fluid-phase tracer, TxR-dextran, was incorporated into LAMP1-positive compartments in the hVps34 KD cells (Fig. 5B) suggested that production of PtdIns(3)*P* by hVps34 was not essential for delivery of early endosome cargo to late endosomes in U-251 cells. Previous studies have shown that, when vesicular transport from early endosomes to late endosomes is inhibited, there is a reduction in cellular uptake of the soluble endocytic tracer horseradish peroxidase (HRP) (Li and Stahl, 1993; Mayran et al., 2003). Thus, to explore the integrity of the early endocytic pathway in the hVps34 KD cells, we determined the kinetics of HRP uptake. As shown in Fig. 8A, the rate of HRP uptake was not reduced in the KD cells. On the contrary, HRP uptake was increased compared with the controls. One possible explanation for this observation might be an increased intracellular sequestration of HRP due to a defect in endosome recycling in the hVps34 KD cells. To address this possibility, cells were pre-loaded with biotinylated transferrin and the amount of ligand released into the medium was measured during a chase with unlabeled transferrin. As shown in Fig. 8B (inset), an increased amount of biotinylated transferrin was taken up into the hVps34 KD cells compared with the controls during the initial 30 minute pre-loading period, consistent with the increased HRP uptake observed in Fig. 8A. However, the percentages of intracellular biotinylated transferrin subsequently released into the medium were essentially identical for the control and KD cells (Fig. 8B). These results indicate that endosome recycling is not disrupted in the hVps34 KD cells. It remains to be determined what factors may contribute to the apparent increase in endocytic uptake of the fluid-phase marker and transferrin in the hVps34 KD cells.

As a means to evaluate growth factor receptor trafficking in the endocytic pathway, we examined the fate of activated epidermal growth factor receptor (EGFR). In serum-deprived cells grown in the absence of EGF, degradation of EGFR is minimal and receptors accumulate on the cell surface. However, upon addition of EGF, the receptors are rapidly activated by tyrosine phosphorylation in the C-terminal

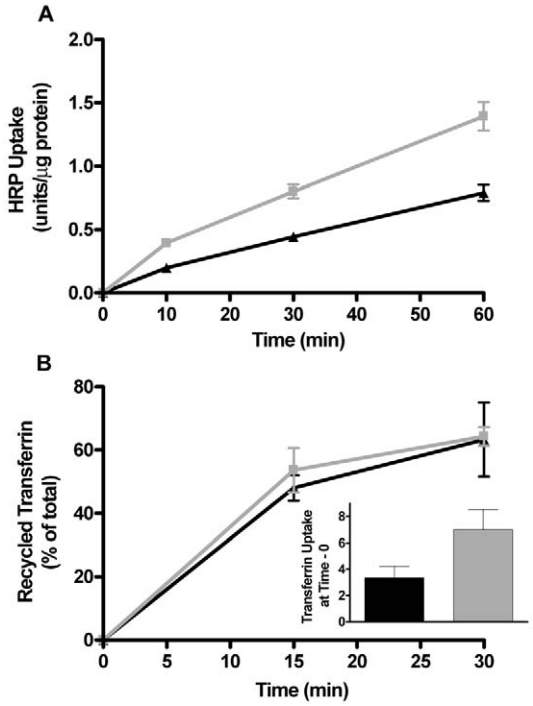

Fig. 8. (A) Suppression of hVps34 expression does not interfere with the endocytosis of a fluid phase marker, horseradish peroxidase (HRP). (A) Control (black) and hVps34 KD (gray) cells were incubated for the indicated periods of time with 2 mg/ml HRP in DMEM + 1% BSA. Washed cells were lysed and HRP activity was determined as described in the Materials and Methods. Each point represents the mean±s.e.m. from triplicate dishes of each cell line. (B) Suppression of hVps34 expression does not impair recycling of transferrin. Control (black) and hVps34 KD (gray) cells were allowed to internalize biotinylated transferrin for 30 minutes, then were chased with an excess of unlabeled transferrin for 15 or 30 minutes. The amounts of biotinylated transferrin in the cells and medium were determined as described in the Materials and Methods. The recycled transferrin (released into the medium) is expressed as percentage of total biotinylated transferrin. The bar graph in the inset shows the relative amount of biotinylated transferrin (normalized to calreticulin) taken up by the control (black bar) and KD (gray bar) cells after the 30 minutes pre-loading period. Each point represents the mean±s.e.m. from triplicate dishes of each cell line.

cytoplasmic domain and the EGF-EGFR complexes are internalized into clathrin-coated early endosomes. Downregulation of activated receptors depends upon their delivery to MVEs, where receptor complexes are sorted into internal vesicles that are ultimately degraded when late endosomes fuse with lysosomes (Katzmann et al., 2002). When EGFR was localized by immunofluorescence, 30 minutes after addition of EGF to hVps34 KD cells, most of the receptors were found in small internal vesicles that were distinct from the large vacuoles labeled by the late endosome/lysosome marker LGP85 (Fig. 9A). However, after 60 minutes, some EGFR could be detected in the limiting membranes surrounding the large LGP85-positive vacuoles (Fig. 9A, arrows). This suggested that delivery of EGFR from early endosomes to the surface membranes of the enlarged late endosomal structures was not impaired in the hVps34 KD cells.

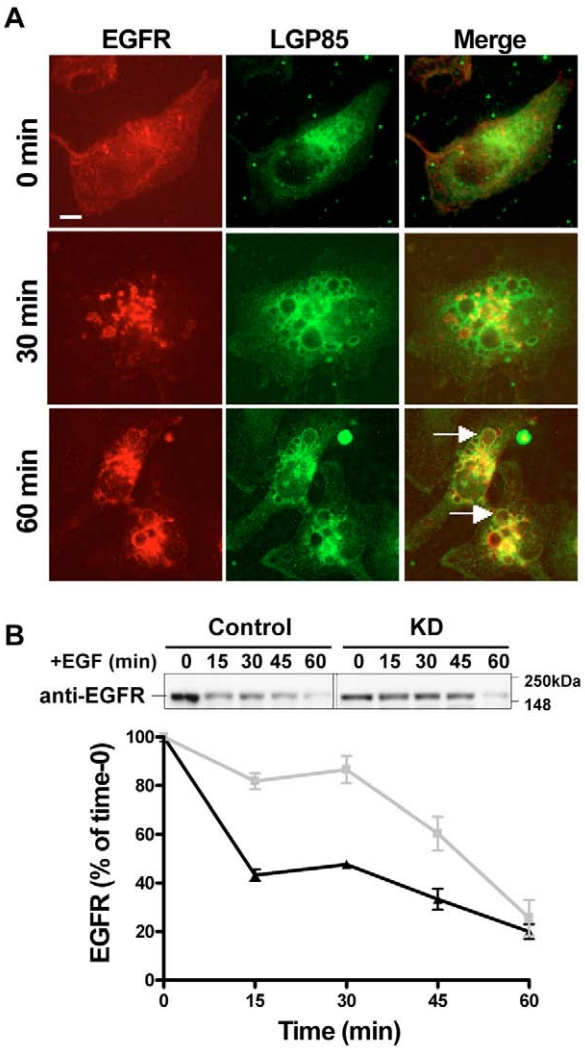

Fig. 9. Suppression of hVps34 expression does not impede internalization of the EGFR, but slows initial receptor degradation. Control and hVps34 KD cells were stimulated with EGF after overnight incubation with serum-free medium. (A) KD cells were fixed and co-stained with EGFR and LGP85 antibodies before addition of EGF (0 min) and at different time points (30 min, 60 min) after addition of EGF. Arrows indicate vacuoles positive for both the EGFR and LGP85. The brightness of the EGFR image at 60 minutes was enhanced by approximately 50% to compensate for its weaker EGFR immunofluorescence compared with the brightness of the image at 30 minutes. Bar, 10 μm. (B) To measure EGFR degradation, triplicate cultures of control and KD cells were harvested at the indicated times after the addition of EGF and subjected to immunoblot analysis for total EGFR. The graph illustrates the data (mean±s.e.m.) generated from densitometer scans of ECL signals on film.

Knockdown of hVps34 impairs degradation of the EGFR

To examine degradation of the EGFR, immunoblot analysis of total EGFR was performed at intervals after addition of EGF. The results indicate that the initial rate of degradation of the receptor was substantially slowed in the hVps34 KD cells compared with the controls (Fig. 9B); however, between 45-60 minutes, the receptor eventually underwent degradation to an extent similar to the controls. Although the portion of the blot

shown in the figure focuses on the full-length receptor, examination of the lower portion of the blot did not reveal any evidence for accumulation of unique partially degraded EGFR fragments in the KD cells.

To assess the amount of activated EGFR at intervals after EGF stimulation, blots were probed with an antibody that specifically recognizes phosphorylated residue Tyr1068 in the C-terminal domain of the receptor, then re-probed to quantify total EGFR. The C-terminal domain faces the cytoplasm when EGFR is in the limiting membrane of the endosome, but it is incorporated into the lumen of vesicles that invaginate to the interior of the MVE (Katzmann et al., 2002). As shown in Fig. 10A, nearly all of the EGFR was in the non-phosphorylated state at the starting point; but, within 30 minutes of adding EGF, both control and hVps34 KD cells exhibited a dramatic increase in the proportion of phospho-EGFR relative to total receptor. However, in the hVps34 KD cells, the ratio of phospho-EGFR to total EGFR was approximately double that observed in the control cells. Thus, it appears that, prior to being exposed to lysosomal proteases, a higher percentage of the EGFR remains phosphorylated in the hVps34 KD cells. In agreement with this concept, activation of the ERK (p44/42 MAP kinase) signaling pathway, as measured by the ratio of phospho-ERK1/2 to total ERK1/2, was augmented in the hVps34 KD cells compared with the controls (Fig. 10B).

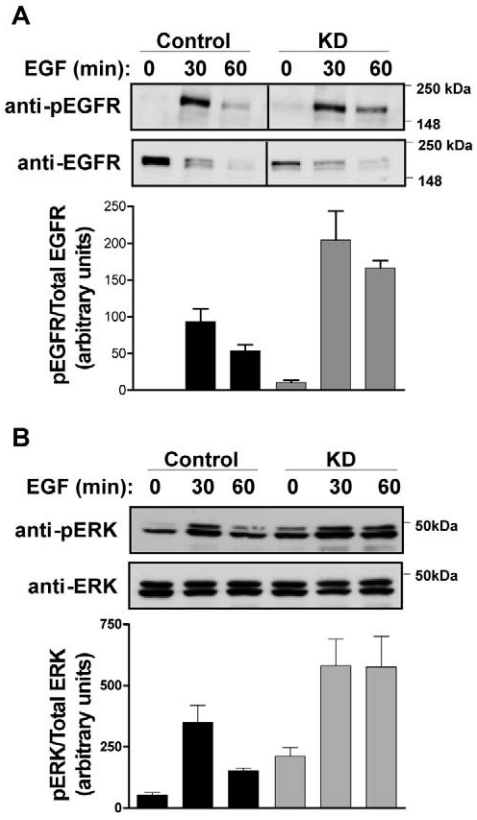

Fig. 10. Suppression of hVps34 expression potentiates EGFR signaling. To measure EGFR phosphorylation and signaling, the control and KD cells were harvested at the indicated times after the addition of EGF and subjected to immunoblot analysis for (A) phospho-EGFR (pEGFR) and total EGFR, or (B) phospho-ERK1/2 (pERK) and total ERK1/2. The bar graphs illustrate the data generated from Kodak Imager scans of blots from triplicate cultures of each cell line.

Knockdown of hVps34 does not impair transport of procathepsin D from the TGN to endosomes, but slows cathesin D processing in lysosomes

To determine if the enlarged endosomal structures in the hVps34 KD cells were capable of accepting cargo normally delivered to late endosomes from the TGN, we focused on the lysosomal enzyme cathepsin D (Pohlmann et al., 1995). Newly synthesized procathepsin D (51-53 kDa) associates with the cation-independent M6PR in the TGN and is delivered to the endosomal compartment, where it is activated by removal of the propeptide to generate an intermediate that migrates at 46-48 kDa on SDS gels. The final step in cathepsin D processing is completed in the lysosomes, where the intermediate is cleaved to the mature form, which contains two non-covalently linked chains of 31 kDa and 14 kDa (Rijnboutt et al., 1992; Delbruck et al., 1994).

To evaluate the processing of newly synthesized procathepsin D, we performed a pulse-chase analysis (Fig. 11A). When [^{35}S]methionine-labeled cathepsin D was immunoprecipitated after a 30 minute pulse, nearly all of the radiolabeled protein was in the 53 kDa form in both control and KD cells. After a 4 hour chase, the control cells converted most of the procathepsin D to the mature form, with some intermediate form still detected. There was no residual radiolabeled procathepsin D in the hVps34 KD cells after the 4 hour chase, suggesting that delivery of procathepsin D from the TGN to the late endosome compartment was not substantially altered in the absence of hVps34 (Fig. 11A). However, compared with the control, there was a 50% decrease in the relative amount of the mature 31 kDa cathepsin D and a corresponding increase in the 47 kDa intermediate form in the KD cells (Fig. 11A). By contrast, a complete block of cathepsin D maturation instituted by raising the endosomal and lysosomal pH with NH_4Cl, is manifested by the absence of any radiolabeled 31 kDa cathepsin D after a 4 hour chase (Fig. 11A). These results are indicative of a kinetic block at the late endosome to lysosome transition in the hVps34 KD cells, resulting in slower lysosomal processing of the cathepsin D intermediate, but not a complete obstruction of its delivery to lysosomes.

This interpretation is reinforced by the immunoblot depicted in Fig. 11B, which shows that the steady-state level of the 47 kDa cathepsin D intermediate was markedly elevated in the hVps34 KD cells. In agreement with the pulse-chase study, there was no accumulation of the 53 kDa procathepsin D that could indicate a problem with trafficking from the TGN. Likewise, immunoblot analysis of procathepsin D released into the medium showed no indication that an increased amount of procathepsin D was being diverted into the secretory pathway in the hVps34 KD cultures (not shown). The similar levels of mature 31 kDa cathepsin D in the immunoblots of control and KD cells might seem puzzling at first, given the slower intermediate processing observed in Fig. 11A. However, this is most probably related to the fact that lysosomal enzymes have long half-lifes compared with their precursors (Hentze et al., 1984; Reilly, et al., 1989; Nissler et al., 1999); thus, over time, a reduced rate of intermediate processing might have an

imperceptible impact on the accumulated pool of end product detected by immunoblot assay.

Vacuoles in the hVps34 KD cells can merge with pre-existing lysosomes

The finding that final proteolytic processing of the 47 kDa cathepsin D intermediate was slowed but not completely blocked in the hVps34 KD cells strongly suggests that the enlarged endosome-derived vacuoles are able to acquire lysosomal characteristics by limited fusion with pre-existing lysosomes. This could also explain how EGFR is ultimately degraded in the hVps34 KD cells (Fig. 9B). Further support for this interpretation comes from an examination of the hVps34 KD cells by immunogold electron microscopy, using a primary antibody against cathepsin D to identify lysosomes (Fig. 11C). With this method, we frequently noted smaller electron-dense lysosomes, heavily labeled with gold particles, in close proximity to the larger electron-lucent vacuoles (Fig. 11C, arrow). In some cases, it appeared that cathepsin D was being delivered to the lumen of the vacuole after fusion with the structure (Fig. 11C, black arrowhead). When taken together with the results of the cathepsin D processing studies (Fig. 11A,B) and the EGFR degradation experiment (Fig. 9B), these morphological observations indicate that the enlarged endosome-derived vacuoles in the hVps34 KD cells retain a limited capacity to fuse with lysosomal compartments.

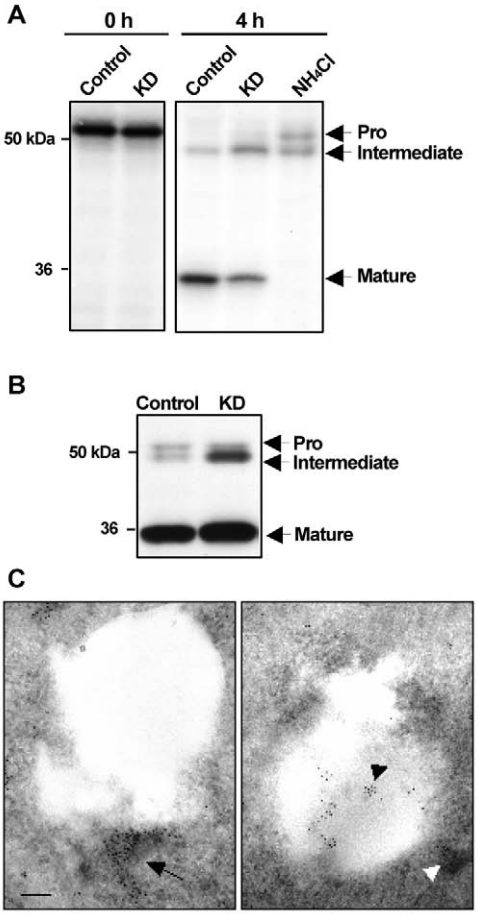

Fig. 11. The late endosomal intermediate form of cathepsin D accumulates in the absence of hVps34, but there is no inhibition of the early step of procathepsin D processing. (A) Control and hVps34 KD cells were seeded at 350,000 cells/dish in 10 cm dishes. Cells were labeled with 100 μCi/ml [^{35}S]methionine, then harvested after 30 minutes or chased in medium with unlabeled methionine for 4 hours. A separate control culture was incubated with 15 mM NH_4Cl during the 4 hour chase. Cathepsin D was immunoprecipitated and subjected to SDS-PAGE and fluorography. Pro, newly synthesized 51-53 kDa procathepsin D containing a propeptide; Intermediate, cathepsin D after removal of the propeptide to generate an intermediate form that migrates at 46-48 kDa; Mature, cathepsin D after cleavage to generate the mature form that contains two non-covalently linked chains of 31 kDa and 14 kDa. (B) Immunoblot analysis of endogenous cathepsin D in whole cell lysates from control and hVps34 KD cells. (C) The hVps34 KD cells were subjected to immunogold labeling with an antibody against cathepsin D. The left panel shows a lysosome heavily labeled for cathepsin D (arrow) adjacent to a larger electron-lucent vacuole. The right panel shows cathepsin D delivered to the lumen of an enlarged vacuole (black arrowhead), with a lysosome adjacent to the vacuole (white arrowhead). Bar, 0.5 μm.

Suppression of hVps34 expression inhibits cell proliferation

The cells in the hVps34 KD cultures were approximately 2-3 times larger than those in the control cultures, and they did not reach a comparable density when maintained for several days after the initial puromycin selection. This prompted us to ask whether suppressing the expression of hVps34 might affect the growth of the U-251 cells. As shown in Fig. 12A, the growth rate of the KD cells was markedly reduced compared with the matched control cell line. A decreased rate of cell proliferation was confirmed by comparing the incorporation of [methyl-^{3}H]thymidine into DNA in control versus KD cells at points where the control cells were at low density (day 2) or near confluence (day 6) (Fig. 12B). Apoptotic cell death, measured by annexin staining, was not a major factor in reducing the density of hVps34 KD cells, even though U-251 cells were capable of a robust apoptotic response when treated with tumor necrosis factor α (TNF-α) (Fig. 12C).

Discussion

In the present study, we used the highly specific method of siRNA-mediated gene silencing to explore the function of the human type III PI 3-kinase hVps34. Our observations indicate that silencing of hVps34 expression mainly affects membrane-sorting events within the multivesicular and late endosome compartments, with surprisingly little effect on vesicular trafficking through the early part of the endocytic pathway or the export of proteins from the TGN to endosomes. The acidic characteristics of the vacuoles in the hVps34 KD cells, coupled with the dearth of internal structures and the presence of LAMP1 and LGP85 in their limiting membranes, indicates that they represent enlarged late endosomes. Interestingly, despite their distorted size, these structures seem to retain a substantial capacity to merge with primary lysosomes, allowing for eventual degradation of the EGFR and only partial impairment of the processing of the intermediate form of cathepsin D to the mature form.

One of the novel findings emerging from the present studies is the absence of any effect of blocking hVps34 expression on the first step in procathepsin D processing, which depends on transport of the proenzyme from the TGN to the late

endosomes (Rijnboutt et al., 1992; Delbruck et al., 1994). Previous reports have indicated that hVps34 is localized predominantly in Golgi membranes (Kihara et al., 2001a) and that inhibition of PI 3-kinase activity with wortmannin causes intracellular accumulation of unprocessed procathepsin D, which then enters the secretory pathway (Davidson, 1995). Follow-up studies by Row et al. implicated Vps34 as the probable wortmannin target by showing that overexpression of a kinase-deficient form of rat Vps34 produced a similar impairment in procathepsin D conversion to the 47-48 kDa endosomal intermediate (Row et al., 2001). The discrepancy between these earlier results and the present findings based on siRNA-mediated silencing of hVps34 could be related to differences in the mechanisms used for interference with hVps34 function. For instance, siRNA is expected to eliminate endogenous hVps34 and deplete PtdIns(3)*P* at specific subcellular sites where the enzyme normally catalyzes the production of this phospholipid. By contrast, overexpression of a kinase-deficient form of Vps34 might act by competing with endogenous hVps34 for binding to the p150 adaptor (Panaretou et al., 1997) or other interacting proteins such as Rab5 (Murray et al., 2002) and Rab7 (Stein et al., 2003). This might cause perturbations of protein trafficking pathways as a result of titration of Vps34 partners, but not necessarily due to loss of PtdIns(3)*P* production by endogenous hVps34.

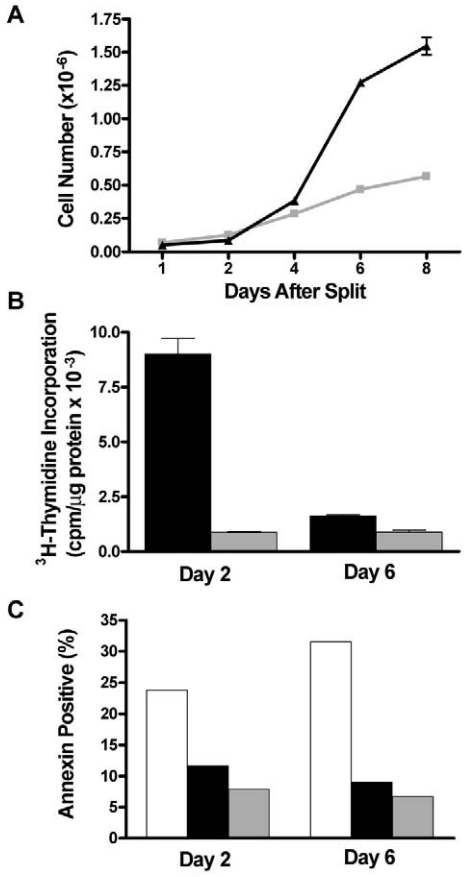

Fig. 12. hVps34 KD cells exhibit a marked reduction in growth rate. (A) Following 2 days of selection, control (black) and hVps34 KD (gray) cells were seeded in 35 mm dishes at an equal density of 50,000 cells/dish. At the indicated time points, triplicate dishes from each cell line were harvested and counted with a Coulter Z1 particle counter (mean±s.e.m.). (B) Control (black) and KD (gray) cells were seeded in 25 cm^2 flasks at 150,000 cells/flask. On the indicated days, triplicate flasks of each cell line were incubated with [^{3}H]thymidine (1.0 μCi/ml) for 5 hours. Radioactivity incorporated into TCA-precipitable material was counted and normalized to total cellular protein (mean±s.e.m.). (C) Control (black) and KD (gray) cells were seeded in 60 mm dishes at 200,000 cells/dish. On the indicated days, duplicate dishes from each cell line were harvested and stained with annexin-V. Annexin-positive cells were counted using a Guava personal cytometer. Cells treated overnight with TNF-α (white) served as a positive control for apoptosis.

If hVps34 is not specifically responsible for producing PtdIns(3)*P* needed for vesicular trafficking of cathepsin D out of the TGN, it is conceivable that other closely related PI 3-kinases might fulfill this role. In this regard, it is worth mentioning two novel PI 3-kinase activities that could serve as potential alternate sources of PtdIns(3)*P* in the Golgi compartment. Both appear to be required for genesis of constitutive transport vesicles in the TGN. The first is associated with TGN38 and a regulatory complex termed p62^{cplx} (Jones et al., 1998). The second was found to associate with TGN46 (Hickinson et al., 1997). Neither of these PI 3-kinases has yet been characterized in sufficient detail to indicate how closely they might be related to Vps34 or if they might be required for endosome- and lysosome-directed trafficking of proenzymes associated with the M6PR.

Our finding that hVps34 knockdown had little or no effect on EEA1 localization or early endocytic trafficking, yet severely affected late endosome morphology and function, was quite unexpected. Previous studies using FYVE-domain probes have demonstrated that PtdIns(3)*P* is concentrated in microdomains in the membranes surrounding early endosomes, as well as in the internal vesicles of MVEs (Gillooly et al., 2003; Gillooly et al., 2000). Therefore, the most obvious implication of our findings is that knockdown of hVps34 results in a more extreme depletion of PtdIns(3)*P* in the late endosomes than in the early endosomes. We did not attempt to perform direct phospholipid analyses on early and late endosome fractions because of the difficulty of accumulating large numbers of hVps34 KD cells. However, our studies with the GFP-2xFYVE probe support the notion that PtdIns(3)*P* depletion is more severe in LAMP1-positive compartments than in LAMP1-negative vesicles (Fig. 7). One possible explanation for this observation is that the small amount of residual hVps34 remaining in the KD cells is selectively directed to early endosomes where it can preserve the PtdIns(3)*P* pool. Although we cannot rule this out, we believe that a more likely possibility is that early endosomes have alternative pathways for producing PtdIns(3)*P*, whereas late endosomes are more dependent on hVps34.

One alternative pathway that could produce sufficient PtdIns(3)*P* to maintain early endosome function might include a type I PI 3-kinase, working in tandem with phosphoinositide 4- and 5-phosphatases. Type I PI 3-kinases are heterodimers composed of p110 catalytic subunits and p85 or p55 regulatory subunits (Vanhaesebroeck et al., 2001). The large increase in cellular phosphatidylinositol (3,4,5)-trisphosphate [PtdIns(3,4,5)P_3] typically observed upon stimulation of type I enzymes suggests that phosphatidylinositol (4,5)-bisphosphate [PtdIns(4,5)P_2] is the preferred substrate in vivo (Fruman et al.,

1998; Leevers et al., 1999). The potential exists for PtdIns(3)*P* to be generated from PtdIns(3,4,5)P_3 through the sequential actions of inositol-polyphosphate 5-phosphatase (Kisseleva et al., 2000) and inositol-polyphosphate 4-phosphatase (Norris et al., 1995; Norris et al., 1997), which are capable of removing the 5′-phosphate and the 4′-phosphate from PtdIns(3,4,5)P_3 and PtdIns(3,4)P_2, respectively. Indeed, in a recent study utilizing function-blocking antibodies, Shin et al. demonstrated that a Rab5-regulated enzyme cascade consisting of PI 3-kinase β (p110β-p85α) and two phosphatases (PI 5- and PI 4-phosphatases) might generate as much as 30% of the PtdIns(3)*P* in early endosomal fractions (Shin et al., 2005). Furthermore, by silencing the expression of the PI 4-phosphatase, they demonstrated that this pathway is functionally important for endocytosis and maintenance of PtdIns(3)*P* levels in Hela cells. Finally, in astrocytes from *weeble* mice that carry a loss-of-function mutation in the gene for the PI 4-phosphatase, intracellular PtdIns(3)*P* levels were reduced by 27% compared with wild-type cells. The studies with *weeble* mice raise the intriguing possibility that a similar type I PI 3-kinase β kinase and/or phosphatase enzyme cascade could contribute to maintaining the pool of PtdIns(3)*P* needed for EEA1 localization and vesicular trafficking in the early endosome compartment of tumor cells of astrocytic origin. Such an alternative pathway could be particularly important in tumors where PTEN mutations frequently occur. For example, in the absence of an active PTEN phosphoinositide 3-phosphatase, the pool of PtdIns(3,4,5)P_3 available to generate PtdIns(3)*P* through the PI 4-phosphatase and PI 5-phosphatase cascade could be substantially increased.

Another alternative mechanism to generate PtdIns(3)*P* could involve a type II PI 3-kinase (e.g. PI 3-kinase C2α). The type II PI 3-kinases remain poorly understood, but there is some evidence that they are localized in the TGN and clathrin-coated vesicles (Prior and Clague, 1999). Indeed, it is quite likely that type II PI 3-kinase can produce PtdIns(3)*P* in mammalian cells, since these enzymes preferentially phosphorylate phosphatidylinositol over PtdIns(4)*P* and PtdIns(4,5)P_3 in vitro (Arcaro et al., 1998; Fruman et al., 1998). The type II PI 3-kinases are less sensitive to wortmannin than hVps34 and type I PI 3-kinases. Thus, our observation that EEA1 localization is sensitive to 1 μM wortmannin but not 0.1 μM wortmannin (Fig. 6) is consistent with the possibility that a type II PI 3-kinase contributes to maintaining the PtdIns(3)*P* pool in early endosomes in the hVps34 KD cells. Ultimately, siRNA knockdown studies of individual type I and type II PI 3-kinases and associated phosphatases may have to be combined with the knockdown of hVps34 to dissect the specific alternative source of PtdIns(3)*P* in the early endosome compartment of mammalian cells. These studies are likely to be quite challenging, in light of the apparent requirement for a minimal level of PtdIns(3)*P* to maintain cell growth (discussed below).

There have been conflicting reports regarding the importance of PI 3-kinase for post-endocytic sorting of activated receptors that enter the cell through clathrin-coated pits. In one study, wortmannin inhibited the formation of internal vesicles in the MVE compartments of HEp2 cells, but the EGFR was still able to reach the perimeter membrane of lysosomes, exposing the N-terminal ligand-binding domain to a degradative environment (Futter et al., 2001). However, in another study with BHK-21 cells (Petiot et al., 2003), wortmannin treatment prevented the translocation of ligand-stimulated EGFR from early endosomes to late endosomes. Our results (Fig. 9A) support the conclusion that hVps34 is not absolutely essential for translocation of activated EGFR to late endosomes in U-251 cells. Degradation of EGFR ultimately occurs in the absence of hVps34 (Fig. 9B), apparently because the enlarged vacuoles retain the capacity for fusion with pre-existing lysosomes. However, the failure of inward vesiculation appears to slow the initial rate of EGFR delivery to lysosomes. Interestingly, prior to degradation, a much higher proportion of the EGFR pool in the hVps34 KD cells remains in a phosphorylated state capable of activating the ERK pathway (Fig. 10). One mechanism for dephosphorylation of EGFR involves protein tyrosine phosphatase 1B on the surface of the endoplasmic reticulum (Haj et al., 2002). However, the possibility that tyrosine dephosphorylation might occur in conjunction with internalization of the EGFR into the MVEs has also been suggested (Gill, 2002). Since the phosphorylated C-terminal domain of the EGFR on the surface of endosomes is capable of interacting with cytoplasmic adaptors and signaling to the ERK pathway (Burke et al., 2001; Wiley and Burke, 2001), we conclude that, in the absence of PtdIns(3)*P* generated by hVps34, an increased proportion of the EGFR is retained on the surface of the enlarged endosomes in an active phosphorylated state prior to eventual degradation of the N-terminal domain by lysosomal proteases.

The morphological phenotype of the hVps34 KD cells resembles the ‘class E’ vacuolar phenotype that can be triggered in mammalian cells by interfering with the assembly of the ESCRT-III complex on MVEs (Babst et al., 1998; Bishop and Woodman, 2000). This suggests a molecular mechanism whereby suppression of hVps34 might cause a failure of inward vesiculation of MVEs. Specifically, PtdIns(3,5)P_2 has been identified as an important phospholipid for membrane recruitment of hVps24, a key component of ESCRT-III (Whitley et al., 2003). Since the kinase responsible for generating PtdIns(3,5)P_3 is in fact a PtdIns(3)*P*-binding FYVE-domain protein termed PIKfyve (Sbrissa et al., 1999; Ikonomov et al., 2003), reduced expression of hVps34 and localized depletion of PtdIns(3)*P* might prevent membrane recruitment of PIKfyve and the subsequent PtdIns(3,5)P_3-dependent assembly of ESCRT-III. Further investigation of this possibility will have to await the development of antibodies that can reliably detect endogenous PIKfyve by immunofluorescence.

In addition to the striking morphological changes affecting the late endosome compartment, we noted a markedly reduced growth rate in the hVps34 KD cells (Fig. 12). This observation is consistent with studies in *Caenorhabditis elegans*, where loss-of-function mutations in the gene encoding the hVps34 ortholog LET-512/Vps34 are associated with an embryonic lethal phenotype (Roggo et al., 2002). A recent report has implicated Vps34 in the nutrient-sensitive regulation of p70 S6-kinase (Byfield et al., 2005). Thus, disruption of the regulation of translation could be one mechanism underlying the growth inhibitory effects of Vps34 knockdown. In an earlier study, Siddhanta et al. found that a neutralizing antibody against hVps34 could block the insulin-stimulated increase in DNA synthesis in GRC-LR+73 cells only when it was microinjected during a defined temporal window of the G1 phase of the cell cycle (Siddhanta et al., 1998). This raises the

intriguing possibility that, in addition to its roles in membrane sorting in MVEs and the regulation of p70 S6-kinase, hVps34 might play a specific role in the control of DNA replication and/or transcription. Although this possibility remains to be explored in mammalian cells, studies using plant cells have found that Vps34 is associated with discrete nuclear and nucleolar transcription sites (Drobak et al., 1995; Bunney et al., 2000). In light of these observations, the prospect of a role for hVp34 in the nucleus of mammalian cells promises to be an important topic for future study.

Materials and Methods

hVps34 gene silencing

U-251 human glioblastoma cells were obtained from the DCT Tumor Repository (National Cancer Institute) and were maintained in Dulbecco's modified Eagle medium (DMEM), supplemented with 10% fetal bovine serum (FBS). The pSUPER.retro.puro vector was obtained from OligoEngine. Two short hairpin RNAs were designed to target 19 bp sequences specific to human Vps34 mRNA. The oligonucleotide sequences used for siRNA interference with hVps34 expression corresponded to $5'\text{-}_{675}$GTGTGATGATAAGGAATAT$_{693}$-$3'$ (KD) and $5'\text{-}_{135}$GTTCTCAGGACTATATCAA$_{153}$-$3'$ (KD2) of the human *VPS34* cDNA sequence (GenBank: BC033004), followed by a 9-nucleotide non-complimentary spacer (TTCAAGAGA) and the reverse compliment of the initial 19-nucleotide sequence. The control siRNA target sequence, $5'\text{-}_{395}$AATACGGCATGTCTCGCCA$_{413}$-$3'$, contained a single base mismatch (underlined) at position 407 from the *hVPS34* sequence and it did not match any other known sequences in the GenBank database. Retrovirus was produced in HEK293 GPG packaging cells (Ory et al., 1996) maintained in DMEM + 10% heat-inactivated FBS with 1 μg/ml puromycin, 300 μg/ml G418 and 2 μg/ml doxycycline. For transfection, the HEK293 GPG cells were seeded at 1.2×10^7 cells/dish on 100 mm dishes in DMEM containing 10% heat-inactivated FBS. 24 hours later, the cells were transfected with pSUPER.retro.puro constructs using Lipofectamine-Plus reagent (Invitrogen). 48 and 72 hours after transfection, the virus-enriched medium was collected and passed through a 0.22 μm filter. Infections of the U-251 cells were performed on three sequential days in the presence of 4.0 μg/ml hexadimethrine bromide (Sigma). Cells were then trypsinized and re-plated in selection medium containing 1 μg/ml puromycin.

For each experiment, control and hVps34-knockdown (KD) cell lines were harvested in order to verify the decrease in hVps34 expression. Briefly, equal amounts of protein were subjected to SDS-PAGE and immunoblot analysis using a polyclonal antibody against hVps34 (Zymed Laboratories), followed by horseradish peroxidase (HRP)-conjugated goat anti-rabbit IgG and enhanced chemiluminescent (ECL) detection reagent (Amersham-Pharmacia Biotech) (Wilson et al., 1996). Antibodies against unrelated proteins such as lamin B_2 (Zymed Laboratories), lactate dehydrogenase (LDH) (Sigma) and calreticulin (Stressgen) were used to check for nonspecific effects of the siRNA. Immunoblot signals were quantified using a Kodak 440CF Image Station.

Characterization of vacuoles by immunofluorescence microscopy

Phase contrast images of control and hVps34 KD cells were obtained using an Olympus IX70 inverted microscope equipped with a digital camera, using SPOT imaging software (Diagnostic Instruments). For immunofluorescence studies, cells were seeded on laminin-coated glass coverslips in 35 mm dishes at 100,000 cells per dish. 24 hours later, cells were washed with PBS, fixed with ice-cold methanol for 10 minutes, and blocked with 10% goat serum in PBS for 30 minutes. The following primary antibodies were applied for 1 hour in PBS with 10% goat serum: anti-LAMP1 (University of Iowa Developmental Studies Hybridoma Bank), anti-LGP85 (gift from Y. Tanaka, Kyushu University, Fukuoka, Japan), anti-M6PR and anti-calreticulin (Affinity Bioreagents), anti-GM130 (BD Biosciences), and anti-LBPA (gift from T. Kobayashi, RIKEN Frontier Research System, Saitama, Japan). Cells were washed three times with 10% goat serum in PBS, then incubated for 1 hour with Alexa Fluor 568 goat anti-mouse (1:800; Molecular Probes) or Alexa Fluor 488 goat anti-rabbit IgG (1:500; Molecular Probes) in PBS with 10% goat serum. After washing three times with PBS, the coverslips containing the cells were mounted with DAKO fluorescent mounting medium and photomicrographs were taken with a Nikon Eclipse 800 fluorescence microscope equipped with a Sensys digital camera and ImagePro software (Media Cybernetics).

To visualize acidic intracellular compartments, cells were incubated with Acridine Orange (2.5 μg/ml; Molecular Probes) in serum-free, Phenol Red-free DMEM for 30 minutes at 37°C. Cells were then washed twice and the coverslips were immediately inverted onto a drop of serum-free DMEM containing 20% glycerol and examined by fluorescence microscopy.

To highlight the endosomal and lysosomal compartments, cells were incubated with a fluid-phase tracer, Texas Red-dextran (10,000 M_r, 500 μg/ml; Molecular Probes) in Phenol Red-free DMEM with 10% FBS for 16 hours at 37°C. Following incubation for 2 hours in dextran-free DMEM, cells were washed with PBS, fixed with ice-cold methanol, and stained with anti-LAMP1 followed by FITC-conjugated goat anti-mouse IgG (Sigma).

Electron microscopy

For transmission electron microscopy (EM), cell pellets fixed with 3% glutaraldehyde for 1 hour were washed three times for 10 minutes with 0.2 M sodium cacodylate, post-fixed for 2 hours with 1% OsO_4 followed by 1 hour with saturated uranyl acetate. Dehydration was carried out by a graded series of chilled ethanol solutions (30-100%) and a final dehydration with 100% acetone. Cells were infiltrated overnight in Spurr's resin (Electron Microscope Sciences) and ultrathin sections were obtained and collected on copper 300-mesh support grids. Sections were stained with uranyl acetate and lead citrate, and examined using a Philips CM 10 transmission electron microscope.

For immunogold staining of cathepsin D, cell pellets were fixed with 1% glutaraldehyde and washed sequentially with cacodylate buffer and 50 mM ammonium chloride. Following dehydration with ethanol only, the cells were infiltrated and embedded in LR White® embedding media (London Resin). Sections were collected with gold support grids and blocked with a solution of 10% fish gelatin in PBS for 1 hour and incubated for 2 hours with goat anti-cathepsin D antibody (Santa Cruz Biotechnology) (1:40 dilution in PBS) followed by 1 hour with donkey anti-goat IgG conjugated with 6 nm colloidal gold (Jackson ImmunoResearch Labs). The samples were post-fixed with 1% glutaraldehyde, washed, and stained with uranyl acetate and lead citrate.

Metabolic labeling and immunoprecipitation of cathepsin D

Cells were seeded in 100 mm dishes at 350,000 cells per dish in medium containing 1 μg/ml puromycin. After 24 hours, the cells were washed and incubated for 30 minutes in methionine-free DMEM containing 10% FBS. The cultures were labeled for 30 minutes in the same medium containing 100 μCi/ml [^{35}S]methionine/cysteine (Easy Tag™ EXPRESS, 1.18 μCi/mmol; NEN/PerkinElmer), washed once with PBS, and then chased in complete medium supplemented with 200 μM methionine and 200 μM cysteine for 4 hours. At the end of the chase, cells were washed twice, scraped into ice-cold PBS, and collected by centrifugation for 5 minutes at 400 ***g***. Cell lysates were prepared in 200 μl RIPA buffer (100 mM Tris-HCl, pH 7.4, 2 mM EDTA, 0.5% Nonidet P-40, 0.1% SDS, 0.5% sodium deoxycholate) supplemented with complete mini protease inhibitors (Roche). Insoluble material was removed by centrifugation at 100,000 ***g*** for 1 hour at 4°C and the soluble fractions were pre-cleared by incubation with protein A sepharose beads for 30 minutes at 4°C. After removal of the beads, immunoprecipitation was performed essentially as previously described (Dugan et al., 1995), using a polyclonal antibody against cathepsin D (Biodesign International). SDS-PAGE and fluorographic analysis of the immunoprecipitated proteins was performed by standard methods (Wilson et al., 1998). Immunoblotting for total cellular cathepsin D was performed as described earlier, using a goat polyclonal antibody against cathepsin D (Santa Cruz Biotechnology).

Endocytosis of HRP

Cells were washed with DMEM and incubated with 2 mg/ml HRP (Sigma) in DMEM containing 1% BSA at 37°C. At designated time points, cells were placed on ice, washed three times with ice-cold PBS containing 1% BSA and one time with PBS alone. Cells were scraped from the dish into PBS, pelleted by centrifugation, washed once more with PBS and then disrupted in PBS containing 0.5% Triton X-100. Cell lysates were clarified by centrifugation at 10,000 ***g*** for 5 minutes at 4°C, and HRP activity in the supernatant was determined using a Turbo TMB enzyme-linked immunosorbent assay kit (Pierce Chemical). Results were normalized to protein, measured with a BCA protein assay kit (Pierce Chemical).

Transferrin receptor recycling

Cells were pre-incubated in serum-free DMEM for 1 hour, then incubated for 30 minutes at 37°C with 50 μg/ml biotinylated holo-transferrin (Sigma) in serum-free medium. The cultures were placed on ice, washed twice with ice-cold DMEM, and then stripped in 10 mM acetic acid, 150 mM NaCl (pH 3.5) for 1 minute to remove residual surface-bound transferrin. Cells were chased for the indicated time periods in medium containing 0.5 mg/ml unlabeled holo-transferrin and 0.1 mM deferoxamine mesylate. At each time point, the medium was collected and the cells were lysed in 50 mM HEPES, pH 7.4, 150 mM NaCl, 10 mM EDTA, 2 mM EGTA, 1% Triton X-100 and 0.1% SDS. Samples of medium and cell lysate were mixed with 5× concentrated SDS sample buffer and subjected to SDS-PAGE. Proteins were transferred to polyvinylidene fluoride (PVDF) membranes and the biotinylated transferrin was detected by ECL following incubation with streptavidin-HRP. ECL signals were quantified with the Kodak 440 CF Image Station.

EGFR internalization and degradation

Cells infected with the hVps34 KD or control vectors were selected for 5 days and seeded at equal density in 60 mm dishes. On the following day, the cells were switched to serum-free medium and maintained for 16 hours to allow the EGFR to

accumulate on the cell surface. Receptor internalization and degradation were then stimulated by addition of EGF (100 ng/ml; Upstate Biotechnology). At designated intervals after addition of EGF, cells were washed twice with ice-cold PBS and harvested in SDS-PAGE sample buffer. Equal amounts of protein were then subjected to SDS-PAGE and immunoblot analysis, using antibodies against total EGFR (BD Biosciences), phospho-EGFR (Cell Signaling Technology), phospho-ERK and total ERK (Cell Signaling Technology). ECL signals were quantified directly with the Kodak Image Station, as described above, or by densitometry after film exposure. In a separate study, cells were fixed in methanol at intervals after EGF stimulation, and localization of the receptor was determined by immunofluorescence analysis as described earlier, using the antibody against total EGFR.

Subcellular distribution of EEA1

Cells were trypsinized and collected by centrifugation at 400 ***g*** for 5 minutes at 4°C. Cell pellets were washed three times with ice-cold PBS and allowed to swell for 15 minutes at 4°C in hypotonic buffer (10 mM HEPES, pH 7.5, 1.5 mM $MgCl_2$, 10 mM KCl, 1 mM DTT and protease inhibitors). The cells were disrupted with 15 strokes of a Teflon homogenizer and sucrose was added to a final concentration of 0.25 M. Soluble and particulate fractions were obtained by centrifugation at 100,000 ***g*** for 1 hour at 4°C. Equal percentages of the soluble and particulate fractions were subjected to SDS-PAGE and immunoblot analysis using an antibody against EEA1 (BD Biosciences). ECL signals were quantified by densitometry, using the Kodak 440CF Image Station. For immunofluorescent localization of EEA1, cells were fixed with 3% paraformaldehyde for 15 minutes at room temperature, quenched with 50 mM NH_4Cl in PBS (5 minutes), permeabilized with 50 μg/ml digitonin in PBS (5 minutes), and blocked with 10% goat serum in PBS for 30 minutes. Anti-EEA1 was then applied for 1 hour followed by Alexa Fluor 568 goat anti-mouse IgG.

Localization of PtdIns(3)*P* with a GFP-FYVE probe

After 4 days of selection, cells infected with the hVps34 knockdown and control vectors were seeded on laminin-coated glass coverslips in 35 mm dishes at 100,000 cells per dish. 24 hours later, cells were transfected with pEGFP-2xFYVE (Petiot et al., 2003) (provided by H. Stenmark, Norwegian Radium Hospital, Oslo, Norway) using Lipofectamine-Plus reagent. 16 hours later, the coverslips were fixed in methanol and processed for immunofluorescence as described earlier, using Living Colors® anti-GFP (BD Biosciences) to detect the GFP-2xFYVE probe, and anti-LAMP1 antibody to detect late endosome and lysosome compartments.

Cell growth and survival

To assess cell growth, hVps34 KD or control cells that had been selected for two days were seeded in 35 mm dishes at 50,000 cells per dish. On specified days, the cells were trypsinized and counted using a Coulter Z-series particle counter (Beckman-Coulter Corporation). To measure DNA synthesis, cells were seeded in 25 cm^2 flasks at 150,000 cells per flask. On days 2 and 6, cells were incubated for 5 hours in medium containing 1 μCi/ml [methyl-^{3}H]thymidine (5 Ci/mmol; Amersham Biosciences). Incorporation of radioactivity into TCA-precipitable material was determined as described previously (Maltese et al., 1981).

For assessment of apoptotic cell death, cells were seeded in 60 mm dishes at 200,000 cells per dish. On days 2 and 6, floating and adherent cells were harvested and stained with annexin-V and 7-amino-actinomycin D as described in the protocol for the Guava Nexin™ kit (Guava Technologies). Staining was quantified using a Guava personal cytometer. Control cells treated for 18 hours with 10 ng/ml TNF-α (Calbiochem) plus 2.5 μg/ml cyclohexamide (Sigma) served as a positive control for apoptosis.

This work was supported in part by grants from the NIH (RO1CA34569) and the U.S. DOD (Idea Award W81XWH-04-1-0493).

References

Arcaro, A., Volinia, S., Zvelebil, M. J., Stein, R., Watton, S. J., Layton, M. J., Gout, I., Ahmadi, K., Downward, J. and Waterfield, M. D. (1998). Human phosphoinositide 3-kinase C2beta, the role of calcium and the C2 domain in enzyme activity. *J. Biol. Chem.* **273**, 33082-33090.

Babst, M., Wendland, B., Estepa, E. J. and Emr, S. D. (1998). The Vps4p AAA ATPase regulates membrane association of a Vps protein complex required for normal endosome function. *EMBO J.* **17**, 2982-2993.

Bishop, N. and Woodman, P. (2000). ATPase-defective mammalian VPS4 localizes to aberrant endosomes and impairs cholesterol trafficking. *Mol. Biol. Cell* **11**, 227-239.

Brown, W. J., DeWald, D. B., Emr, S. D., Plutner, H. and Balch, W. E. (1995). Role for phosphatidylinositol 3-kinase in the sorting and transport of newly synthesized lysosomal enzymes in mammalian cells. *J. Cell Biol.* **130**, 781-796.

Brummelkamp, T. R., Bernards, R. and Agami, R. (2002). A system for stable expression of short interfering RNAs in mammalian cells. *Science* **296**, 550-553.

Bucci, C., Thomsen, P., Nicoziani, P., McCarthy, J. and van Deurs, B. (2000). Rab7: a key to lysosome biogenesis. *Mol. Biol. Cell* **11**, 467-480.

Bunney, T. D., Watkins, P. A., Beven, A. F., Shaw, P. J., Hernandez, L. E., Lomonossoff, G. P., Shanks, M., Peart, J. and Drobak, B. K. (2000). Association of phosphatidylinositol 3-kinase with nuclear transcription sites in higher plants. *Plant Cell* **12**, 1679-1688.

Burke, P., Schooler, K. and Wiley, H. S. (2001). Regulation of epidermal growth factor receptor signaling by endocytosis and intracellular trafficking. *Mol. Biol. Cell* **12**, 1897-1910.

Byfield, M. P., Murray, J. T. and Backer, J. M. (2005). hVps34 is a nutrient-regulated lipid kinase required for activation of p70 S6 kinase. *J. Biol. Chem.* **280**, 33076-33082.

Cheever, M. L., Sato, T. K., de Beer, T., Kutateladze, T. G., Emr, S. D. and Overduin, M. (2001). Phox domain interaction with PtdIns(3)P targets the Vam7 t-SNARE to vacuole membranes. *Nat. Cell Biol.* **3**, 613-618.

Christoforidis, S., McBride, H. M., Burgoyne, R. D. and Zerial, M. (1999). The Rab5 effector EEA1 is a core component of endosome docking. *Nature* **397**, 621-625.

Cormont, M., Mari, M., Galmiche, A., Hofman, P. and Marchand-Brustel, Y. (2001). A FYVE-finger-containing protein, Rabip4, is a Rab4 effector involved in early endosomal traffic. *Proc. Natl. Acad. Sci. USA* **98**, 1637-1642.

Corvera, S. (2001). Phosphatidylinositol 3-kinase and the control of endosome dynamics: new players defined by structural motifs. *Traffic* **2**, 859-866.

Corvera, S., D'Arrigo, A. and Stenmark, H. (1999). Phosphoinositides in membrane traffic. *Curr. Opin. Cell Biol.* **11**, 460-465.

Davidson, H. W. (1995). Wortmannin causes mistargeting of procathepsin D. evidence for the involvement of a phosphatidylinositol 3-kinase in vesicular transport to lysosomes. *J. Cell Biol.* **130**, 797-805.

Delbruck, R., Desel, C., von Figura, K. and Hille-Rehfeld, A. (1994). Proteolytic processing of cathepsin D in prelysosomal organelles. *Eur. J. Cell Biol.* **64**, 7-14.

Drobak, B. K., Watkins, P. A., Bunney, T. D., Dove, S. K., Shaw, P. J., White, I. R. and Millner, P. A. (1995). Association of multiple GTP-binding proteins with the plant cytoskeleton and nuclear matrix. *Biochem. Biophys. Res. Commun.* **210**, 7-13.

Dugan, J. M., deWit, C., McConlogue, L. and Maltese, W. A. (1995). The ras-related GTP binding protein, Rab1B, regulates early steps in exocytic transport and processing of β-amyloid precursor protein. *J. Biol. Chem.* **270**, 10982-10989.

Fruman, D. A., Meyers, R. E. and Cantley, L. C. (1998). Phosphoinositide kinases. *Annu. Rev. Biochem.* **67**, 481-507.

Fruman, D. A., Rameh, L. E. and Cantley, L. C. (1999). Phosphoinositide binding domains: embracing 3-phosphate. *Cell* **97**, 817-820.

Futter, C. E., Collinson, L. M., Backer, J. M. and Hopkins, C. R. (2001). Human VPS34 is required for internal vesicle formation within multivesicular endosomes. *J. Cell Biol.* **155**, 1251-1264.

Ghosh, P., Dahms, N. M. and Kornfeld, S. (2003). Mannose 6-phosphate receptors: new twists in the tale. *Nat. Rev. Mol. Cell. Biol.* **4**, 202-212.

Gill, G. N. (2002). A pit stop at the ER. *Science* **295**, 1654-1655.

Gillooly, D. J., Morrow, I. C., Lindsay, M., Gould, R., Bryant, N. J., Gaullier, J. M., Parton, R. G. and Stenmark, H. (2000). Localization of phosphatidylinositol 3-phosphate in yeast and mammalian cells. *EMBO J.* **19**, 4577-4588.

Gillooly, D. J., Raiborg, C. and Stenmark, H. (2003). Phosphatidylinositol 3-phosphate is found in microdomains of early endosomes. *Histochem. Cell Biol.* **120**, 445-453.

Gough, N. R., Zweifel, M. E., Martinez-Augustin, O., Aguilar, R. C., Bonifacino, J. S. and Fambrough, D. M. (1999). Utilization of the indirect lysosome targeting pathway by lysosome-associated membrane proteins (LAMPs) is influenced largely by the C-terminal residue of their GYXXphi targeting signals. *J. Cell Sci.* **112**, 4257-4269.

Gruenberg, J. and Maxfield, F. R. (1995). Membrane transport in the endocytic pathway. *Curr. Opin. Cell Biol.* **7**, 552-563.

Haj, F. G., Verveer, P. J., Squire, A., Neel, B. G. and Bastiaens, P. I. H. (2002). Imaging sites of receptor dephosphorylation by PTP1B on the surface of the endoplasmic reticulum. *Science* **295**, 1708-1711.

Hentze, M., Hasilik, A. and von Figura, K. (1984). Enhanced degradation of cathepsin D synthesized in the presence of the threonine analog beta-hydroxynorvaline. *Arch. Biochem. Biophys.* **230**, 375-382.

Herman, P. K., Stack, J. H. and Emr, S. D. (1992). An essential role for a protein and lipid kinase complex in secretory protein sorting. *Trends Cell Biol.* **2**, 363-368.

Hickinson, D. M., Lucocq, J. M., Towler, M. C., Clough, S., James, J., James, S. R., Downes, C. P. and Ponnambalam, S. (1997). Association of a phosphatidylinositol-specific 3-kinase with a human trans-Golgi network resident protein. *Curr. Biol.* **7**, 987-990.

Hirst, J., Futter, C. E. and Hopkins, C. R. (1998). The kinetics of mannose 6-phosphate receptor trafficking in the endocytic pathway in HEp-2 cells: the receptor enters and rapidly leaves multivesicular endosomes without accumulating in a prelysosomal compartment. *Mol. Biol. Cell* **9**, 809-816.

Ikonomov, O. C., Sbrissa, D., Foti, M., Carpentier, J. L. and Shisheva, A. (2003). PIKfyve controls fluid phase endocytosis but not recycling/degradation of endocytosed receptors or sorting of procathepsin D by regulating multivesicular body morphogenesis. *Mol. Biol. Cell* **14**, 4581-4591.

Jones, S. M., Alb, J. G., Jr, Phillips, S. E., Bankaitis, V. A. and Howell, K. E. (1998). A phosphatidylinositol 3-kinase and phosphatidylinositol transfer protein act synergistically in formation of constitutive transport vesicles from the trans-Golgi network. *J. Biol. Chem.* **273**, 10349-10354.

Kanai, F., Liu, H., Field, S. J., Akbary, H., Matsuo, T., Brown, G. E., Cantley, L. C. and Yaffe, M. B. (2001). The PX domains of p47phox and p40phox bind to lipid products of PI(3)K. *Nat. Cell Biol.* **3**, 675-678.

Kanzawa, T., Kondo, Y., Ito, H., Kondo, S. and Germano, I. (2003). Induction of autophagic cell death in malignant glioma cells by arsenic trioxide. *Cancer Res.* **63**, 2103-2108.

Katzmann, D. J., Odorizzi, G. and Emr, S. D. (2002). Receptor downregulation and multivesicular-body sorting. *Nat. Rev. Mol. Cell. Biol.* **3**, 893-905.

Kauppi, M., Simonsen, A., Bremnes, B., Vieira, A., Callaghan, J., Stenmark, H. and Olkkonen, V. M. (2002). The small GTPase Rab22 interacts with EEA1 and controls endosomal membrane trafficking. *J. Cell Sci.* **115**, 899-911.

Kihara, A., Kabeya, Y., Ohsumi, Y. and Yoshimori, T. (2001a). Beclin-phosphatidylinositol 3-kinase complex functions at the trans- Golgi network. *EMBO Rep.* **2**, 330-335.

Kihara, A., Noda, T., Ishihara, N. and Ohsumi, Y. (2001b). Two distinct Vps34 phosphatidylinositol 3-kinase complexes function in autophagy and carboxypeptidase Y sorting in Saccharomyces cerevisiae. *J. Cell Biol.* **152**, 519-530.

Kisseleva, M. V., Wilson, M. P. and Majerus, P. W. (2000). The isolation and characterization of a cDNA encoding phospholipid-specific inositol polyphosphate 5-phosphatase. *J. Biol. Chem.* **275**, 20110-20116.

Kobayashi, T., Stang, E., Fang, K. S., de Moerloose, P., Parton, R. G. and Gruenberg, J. (1998). A lipid associated with the antiphospholipid syndrome regulates endosome structure and function. *Nature* **392**, 193-197.

Kuronita, T., Eskelinen, E. L., Fujita, H., Saftig, P., Himeno, M. and Tanaka, Y. (2002). A role for the lysosomal membrane protein LGP85 in the biogenesis and maintenance of endosomal and lysosomal morphology. *J. Cell Sci.* **115**, 4117-4131.

Le Borgne, R. and Hoflack, B. (1998). Protein transport from the secretory to the endocytic pathway in mammalian cells. *Biochim. Biophys. Acta* **1404**, 195-209.

Leevers, S. J., Vanhaesebroeck, B. and Waterfield, M. D. (1999). Signalling through phosphoinositide 3-kinases: the lipids take centre stage. *Curr. Opin. Cell Biol.* **11**, 219-225.

Li, G. and Stahl, P. D. (1993). Structure-function relationship of the small GTPase rab5. *J. Biol. Chem.* **268**, 24475-24480.

Maltese, W. A., Reitz, B. A. and Volpe, J. J. (1981). Effects of isoleucine deprivation on synthesis of sterols and fatty acids in LM-cells. *J. Biol. Chem.* **256**, 2185-2193.

Mayran, N., Parton, R. G. and Gruenberg, J. (2003). Annexin II regulates multivesicular endosome biogenesis in the degradation pathway of animal cells. *EMBO J.* **22**, 3242-3253.

Meyers, R. and Cantley, L. C. (1997). Cloning and characterization of a wortmannin-sensitive human phosphatidylinositol 4-kinase. *J. Biol. Chem.* **272**, 4384-4390.

Murray, J. T., Panaretou, C., Stenmark, H., Miaczynska, M. and Backer, J. M. (2002). Role of Rab5 in the recruitment of hVps34/p150 to the early endosome. *Traffic* **3**, 416-427.

Nielsen, E., Christoforidis, S., Uttenweiler-Joseph, S., Miaczynska, M., Dewitte, F., Wilm, M., Hoflack, B. and Zerial, M. (2000). Rabenosyn-5, a novel Rab5 effector, is complexed with hVPS45 and recruited to endosomes through a FYVE finger domain. *J. Cell Biol.* **151**, 601-612.

Nissler, K., Strubel, W., Kreusch, S., Rommerskirch, W., Weber, E. and Wiederanders, B. (1999). The half-life of human procathepsin S. *Eur. J. Biochem.* **263**, 717-725.

Norris, F. A., Auethavekiat, V. and Majerus, P. W. (1995). The isolation and characterization of cDNA encoding human and rat brain inositol polyphosphate 4-phosphatase. *J. Biol. Chem.* **270**, 16128-16133.

Norris, F. A., Atkins, R. C. and Majerus, P. W. (1997). The cDNA cloning and characterization of inositol polyphosphate 4-phosphatase type II. Evidence for conserved alternative splicing in the 4-phosphatase family. *J. Biol. Chem.* **272**, 23859-23864.

Odorizzi, G., Babst, M. and Emr, S. D. (2000). Phosphoinositide signaling and the regulation of membrane trafficking in yeast. *Trends Biochem. Sci.* **25**, 229-235.

Ory, D. S., Neugeboren, B. A. and Mulligan, R. C. (1996). A stable human-derived packaging cell line for production of high titer retrovirus/vesicular stomatitis virus G pseudotypes. *Proc. Natl. Acad. Sci USA* **93**, 11400-11406.

Paglin, S., Hollister, T., Delohery, T., Hackett, N., McMahill, M., Sphicas, E., Domingo, D. and Yahalom, J. (2001). A novel response of cancer cells to radiation involves autophagy and formation of acidic vesicles. *Cancer Res.* **61**, 439-444.

Panaretou, C., Domin, J., Cockcroft, S. and Waterfield, M. D. (1997). Characterization of p150, an adaptor protein for the human phosphatidylinositol (PtdIns) 3-kinase. Substrate presentation by phosphatidylinositol transfer protein to the p150.Ptdins 3-kinase complex. *J. Biol. Chem.* **272**, 2477-2485.

Paul, C. P., Good, P. D., Winer, I. and Engelke, D. R. (2002). Effective expression of small interfering RNA in human cells. *Nat. Biotechnol.* **20**, 505-508.

Petiot, A., Ogier-Denis, E., Blommaart, E. F., Meijer, A. J. and Codogno, P. (2000). Distinct classes of phosphatidylinositol 3′-kinases are involved in signaling pathways that control macroautophagy in HT-29 cells. *J. Biol. Chem.* **275**, 992-998.

Petiot, A., Faure, J., Stenmark, H. and Gruenberg, J. (2003). PI3P signaling regulates receptor sorting but not transport in the endosomal pathway. *J. Cell Biol.* **162**, 971-979.

Pohlmann, R., Boeker, M. W. and von Figura, K. (1995). The two mannose 6-phosphate receptors transport distinct complements of lysosomal proteins. *J. Biol. Chem.* **270**, 27311-27318.

Press, B., Feng, Y., Hoflack, B. and Wandinger-Ness, A. (1998). Mutant Rab7 causes the accumulation of cathepsin D and cation-independent mannose 6-phosphate receptor in an early endocytic compartment. *J. Cell Biol.* **140**, 1075-1089.

Prior, I. A. and Clague, M. J. (1999). Localization of a class II phosphatidylinositol 3-kinase, PI3KC2alpha, to clathrin-coated vesicles. *Mol. Cell. Biol. Res. Commun.* **1**, 162-166.

Reilly, J. J., Jr, Mason, R. W., Chen, P., Joseph, L. J., Sukhatme, V. P., Yee, R. and Chapman, H. A., Jr (1989). Synthesis and processing of cathepsin L, an elastase, by human alveolar macrophages. *Biochem. J.* **257**, 493-498.

Rijnboutt, S., Stoorvogel, W., Geuze, H. J. and Strous, G. J. (1992). Identification of subcellular compartments involved in biosynthetic processing of cathepsin D. *J. Biol. Chem.* **267**, 15665-15672.

Roggo, L., Bernard, V., Kovacs, A. L., Rose, A. M., Savoy, F., Zetka, M., Wymann, M. P. and Muller, F. (2002). Membrane transport in Caenorhabditis elegans: an essential role for VPS34 at the nuclear membrane. *EMBO J.* **21**, 1673-1683.

Row, P. E., Reaves, B. J., Domin, J., Luzio, J. P. and Davidson, H. W. (2001). Overexpression of a rat kinase-deficient phosphoinositide 3-kinase, Vps34p, inhibits cathepsin D maturation. *Biochem. J.* **353**, 655-661.

Sbrissa, D., Ikonomov, O. C. and Shisheva, A. (1999). PIKfyve, a mammalian ortholog of yeast Fab1p lipid kinase, synthesizes 5-phosphoinositides. Effect of insulin. *J. Biol. Chem.* **274**, 21589-21597.

Schu, P. V., Takegawa, K., Fry, M. J., Stack, J. H., Waterfield, M. D. and Emr, S. D. (1993). Phosphatidylinositol 3-kinase encoded by yeast VPS34 gene essential for protein sorting. *Science* **260**, 88-91.

Shin, H. W., Hayashi, M., Christoforidis, S., Lacas-Gervais, S., Hoepfner, S., Wenk, M. R., Modregger, J., Uttenweiler-Joseph, S., Wilm, M., Nystuen, A. et al. (2005). An enzymatic cascade of Rab5 effectors regulates phosphoinositide turnover in the endocytic pathway. *J. Cell Biol.* **170**, 607-618.

Siddhanta, U., McIlroy, J., Shah, A., Zhang, Y. and Backer, J. M. (1998). Distinct roles for the p110alpha and hVPS34 phosphatidylinositol 3′- kinases in vesicular trafficking, regulation of the actin cytoskeleton, and mitogenesis. *J. Cell Biol.* **143**, 1647-1659.

Simonsen, A., Lippe, R., Christoforidis, S., Gaullier, J. M., Brech, A., Callaghan, J., Toh, B. H., Murphy, C., Zerial, M. and Stenmark, H. (1998). EEA1 links PI(3)K function to Rab5 regulation of endosome fusion. *Nature* **394**, 494-498.

Simonsen, A., Wurmser, A. E., Emr, S. D. and Stenmark, H. (2001). The role of phosphoinositides in membrane transport. *Curr. Opin. Cell Biol.* **13**, 485-492.

Song, X., Xu, W., Zhang, A., Huang, G., Liang, X., Virbasius, J. V., Czech, M. P. and Zhou, G. W. (2001). Phox homology domains specifically bind phosphatidylinositol phosphates. *Biochemistry* **40**, 8940-8944.

Stack, J. H., DeWald, D. B., Takegawa, K. and Emr, S. D. (1995). Vesicle-mediated protein transport: regulatory interactions between the Vps15 protein kinase and the Vps34 PtdIns 3-kinase essential for protein sorting to the vacuole in yeast. *J. Cell Biol.* **129**, 321-334.

Stein, M. P., Feng, Y., Cooper, K. L., Welford, A. M. and Wandinger-Ness, A. (2003). Human VPS34 and p150 are Rab7 interacting partners. *Traffic* **4**, 754-771.

Sui, G., Soohoo, C., Affar, e. B., Gay, F., Shi, Y., Forrester, W. C. and Shi, Y. (2002). A DNA vector-based RNAi technology to suppress gene expression in mammalian cells. *Proc. Natl. Acad. Sci. USA* **99**, 5515-5520.

Traganos, F. and Darzynkiewicz, Z. (1994). Lysosomal proton pump activity: supravital cell staining with acridine orange differentiates leukocyte subpopulations. *Methods Cell Biol.* **41**, 185-194.

Vanhaesebroeck, B., Leevers, S. J., Ahmadi, K., Timms, J., Katso, R., Driscoll, P. C., Woscholski, R., Parker, P. J. and Waterfield, M. D. (2001). Synthesis and function of 3-phosphorylated inositol lipids. *Annu. Rev. Biochem.* **70**, 535-602.

Virbasius, J. V., Guilherme, A. and Czech, M. P. (1996). Mouse p170 is a novel phosphatidylinositol 3-kinase containing a C2 domain. *J. Biol. Chem.* **271**, 13304-13307.

Whitley, P., Reaves, B. J., Hashimoto, M., Riley, A. M., Potter, B. V. and Holman, G. D. (2003). Identification of mammalian Vps24p as an effector of phosphatidylinositol 3,5-bisphosphate-dependent endosome compartmentalization. *J. Biol. Chem.* **278**, 38786-38795.

Wiley, H. S. and Burke, P. M. (2001). Regulation of receptor tyrosine kinase signaling by endocytic trafficking. *Traffic* **2**, 12-18.

Wilson, A. L., Erdman, R. A. and Maltese, W. A. (1996). Association of Rab1B with GDP-dissociation inhibitor (GDI) is required for recycling but not initial membrane targeting of the Rab protein. *J. Biol. Chem.* **271**, 10932-10940.

Wilson, A. L., Erdman, R. A., Castellano, F. and Maltese, W. A. (1998). Prenylation of Rab8 GTPase by type I and type II geranylgeranyl transferases. *Biochem. J.* **333**, 497-504.

Wurmser, A. E. and Emr, S. D. (2002). Novel PtdIns(3)P-binding protein Etf1 functions as an effector of the Vps34 PtdIns 3-kinase in autophagy. *J. Cell Biol.* **158**, 761-772.

Wurmser, A. E., Gary, J. D. and Emr, S. D. (1999). Phosphoinositide 3-kinases and their FYVE domain-containing effectors as regulators of vacuolar/lysosomal membrane trafficking pathways. *J. Biol. Chem.* **274**, 9129-9132.

Xu, Y., Hortsman, H., Seet, L., Wong, S. H. and Hong, W. (2001). SNX3 regulates endosomal function through its PX-domain-mediated interaction with PtdIns(3)P. *Nat. Cell Biol.* **3**, 658-666.